

# Lateral Dynamic Behaviour of Articulated Commercial Vehicles

M.F.J. Luijten

D&C 2010.044  
DAF 51050/10-207

Master's thesis  
Eindhoven, August, 2010

Coach: ir. R.M.A.F. Verschuren (DAF)

Supervisors: prof. dr. H. Nijmeijer (TU/e)  
dr. ir. I.J.M. Besselink (TU/e)

Committee: prof. dr. H. Nijmeijer (TU/e)  
dr. ir. I.J.M. Besselink (TU/e)  
dr. ir. F.E. Veldpaus (TU/e)  
ir. R.M.A.F. Verschuren (DAF)

Eindhoven University of Technology  
Department Mechanical Engineering  
Dynamics and Control Group

DAF Trucks N.V.  
Vehicle Control Group





---

# Abstract

---

Additional to the conventional tractor-semitrailer, truck-centre axle trailer and truck-full trailer combinations, Ecocombi's (longer and heavier truck combinations) have been introduced pre legislatively as an experiment in the Netherlands. Electronic stability control functions are applied on trucks to enhance safety. The challenge of designing such functions is to guarantee robustness for all truck variations, such as lay-out, length, mass, number of axles and number of articulations. Therefore, fundamental understanding of the effect of these variations on the dynamic yaw behaviour of articulated vehicles is required. Linear single track vehicle models are used in this study to gain this fundamental insight.

Stability analysis reveals that when the cornering stiffness scales linearly with vertical load and when legal axle loads are obeyed, the conventional vehicle combinations hardly become unstable in yaw. The measure stability does not show explicit differences between the vehicle combinations. Therefore, the performance measure rearward amplification is used, which is a measure for the amount of lateral acceleration amplification. A frequency domain approach is applied as the results of this approach are better reproducible than the results of a time domain approach which is often used in literature to calculate rearward amplification.

A smaller value for rearward amplification indicates a better dynamic performance of the combination. This can be achieved in general by decreasing the distance between the centre of gravity of the towing vehicle and the coupling point, by increasing the drawbar length and trailer wheelbase, by applying multiple axles and by placing the axles per group further apart. Furthermore, a semitrailer results in a relatively small rearward amplification value in relation to the other combinations, as its trailer wheelbase is relatively large. For a centre axle trailer, adding inertia results in a larger rearward amplification value of this unit. A full trailer has mainly a kinematic coupling with its towing unit when the steering dolly mass and inertia are assumed to be zero. In this case, the parameters of the trailer have no effect on the dynamics of the towing vehicle. Finally, especially for Ecocombi's it is important to model the amount of axles in relation to the lengths, masses and inertias of the units.

The results presented in this report pertain to optimal driving conditions. It is recommended to investigate the effect of excitations of the truck other than the steering wheel input on the dynamic performance of truck combinations.



---

## Samenvatting

---

Ecocombi's (langere en zwaardere vrachtwagencombinaties) worden toegestaan als proef in Nederland, naast de conventionele tractor-oplegger, bakwagen-middenasaanhanger en bakwagen-molensasaanhanger. Elektronische stabiliteitsregelingen worden toegepast op vrachtwagens om de veiligheid op de weg te verbeteren. De uitdaging voor het ontwerp van zulke functies is het garanderen van robuustheid voor alle variaties, zoals lay-out, massa, lengte, aantal assen en aantal geledingen. Onderwerp van deze studie is het verkrijgen van een fundamenteel inzicht in de dynamische gierstabiliteit van gelede voertuigen, zodat de invloed van variaties beter begrepen wordt. Hiertoe zijn lineaire enkelsporige voertuigmodellen gebruikt.

De conventionele vrachtwagens blijken bijna niet instabiel te krijgen te zijn, wanneer de bandstijfheid lineair schaalst met de last op de band en wanneer aan de toegestane maximale aslasten voldaan wordt. De maat stabiliteit laat geen duidelijk onderscheid zien tussen de voertuigcombinaties. Er is daarom een maat voor de gierdemping toegepast. Een frequentie domein aanpak is gebruikt, omdat de resultaten van deze aanpak beter reproduceerbaar zijn dan de resultaten van een tijd domain aanpak welke vaak in de literatuur gebruikt wordt.

De prestatie van een combinatie wordt beter naarmate de gierdemping toeneemt. In het algemeen moet hiervoor het koppelpunt dicht bij het zwaartepunt van het voorvoertuig geplaatst worden, moeten de dissels en de wielbasis van de trailer lang zijn, moeten meerdere assen toegepast worden en moeten deze assen ver uit elkaar geplaatst worden. Bovendien zorgt een oplegger voor veel gierdemping vergeleken met de andere trailers, omdat de wielbasis van deze aanhanger relatief lang is. De prestatie van een middenasaanhanger neemt af wanneer het traagheidsmoment in de trailer toeneemt. Een molensasaanhanger is voornamelijk kinematisch gekoppeld met zijn voorwagen wanneer de massa en het traagheidsmoment van de stuurdollie verwaarloosd kunnen worden. In dit geval hebben de parameters van de trailer geen invloed op de dynamica van het voorvoertuig. Tenslotte is het vooral voor Ecocombi's belangrijk om het aantal assen in de combinatie te modelleren in relatie tot de lengte van het voertuig, de massa en het traagheidsmoment.

De resultaten van deze studie gelden voor optimale condities. Het wordt aanbevolen om onder andere de invloed van een aanstoting van het voertuig anders dan de stuurwielhoek te onderzoeken.



---

# Notation

---

## Abbreviations

CAT	Truck-centre axle trailer
cog	Centre of gravity
FRF	Frequency response function
FT	Truck-full trailer
lc	lane change
RA	Rearward amplification
Semi	Tractor-semitrailer

## Tyre, axle and vehicle symbols

$\alpha_a$	Tyre slip angle	rad
$\beta, \dot{\beta} = r_1$	Yaw angle of the towing vehicle	rad
$\delta_v$	Steering wheel angle	rad
$\eta_v$	Understeer coefficient	-
$\phi$	Relative angle between the first articulation and the towing vehicle	rad
$\psi$	Relative angle between the second and first articulation	rad
$\rho$	Relative angle between the second articulation and the towing vehicle	rad
$\theta, \dot{\theta} = r_2$	Yaw angle of the first articulation	rad
$\xi, \dot{\xi} = r_3$	Yaw angle of the second articulation	rad
$a_v$	Distance from the front of the articulation to the centre of gravity	m
$a_{y_v}$	Lateral acceleration	m/s <sup>2</sup>
$b_v$	Distance from the centre of gravity to the rear axle	m
$C$	Total cornering stiffness towing vehicle	N/rad
$C_a$	Axle cornering stiffness	N/rad
$C_t$	Total cornering stiffness full trailer	N/rad
$C_{F_\alpha}$	Tyre cornering stiffness	N/rad
$C_{nom}$	Nominal axle cornering stiffness	N/rad
$e_v$	Distance between the rear axle and the coupling point	m
$f_a$	Normalised tyre stiffness coefficient	1/rad
$F_{y_a}$	Lateral tyre / axle force	N
$F_{z_a}$	Vertical tyre / axle force	N

$F_{z_{nom}}$	Nominal vertical force	N
$f_{act}$	Moment contribution factor for multiple axles	-
$h_v$	Distance between the centre of gravity and the coupling point	m
$I_v$	Moment of inertia	kg m <sup>2</sup>
$j$	Half distance between two axles in an axle group	m
$k_v$	Radius of gyration	m
$l_v^*$	Distance between the front of the articulation to the coupling point	m
$l_v$	Wheelbase	m
$m_v$	Mass	kg
$q_v$	Average tyre moment arm	m
$R$	Path radius	m
$S$	Neutral steer point	
$s_v$	Distance from cog or hitch point to neutral steer point	m
$x$	Distance between the centre of gravity and an axle group	m

### Other symbols

$\lambda$	Eigenvalue	
$\omega$	(Natural) frequency	rad/s
$\zeta$	Damping ratio	-
$A_s$	State space system matrix	
$B_s$	State space input matrix	
$c_i$	$i^{th}$ coefficient of the characteristic equation	
$C_s$	State space output matrix	
$D$	Damping matrix	
$D_s$	State space feed through matrix	
$D_c$	Denominator of the critical speed	
$den$	Denominator of a transfer function	
$F$	Input matrix	
$f_r$	Frequency	Hz
$g$	Gravitational acceleration	m/s <sup>2</sup>
$H_i$	$i^{th}$ Hurwitz determinant	
$H_{y,x}(\omega)$	Transfer function; input $x$ , output $y$	
$I$	Unity matrix	
$j$	Complex variable, $j^2 = -1$	
$M$	Mass matrix	
$n$	Maximum number, number of axles in an axle group	
$num$	Nominator of a transfer function	
$Q$	Generalised forces	N
$q$	Generalised coordinate	
$T$	Kinetic energy	J
$U$	Potential energy	J
$V_{char}$	Characteristic speed	m/s
$V_{crit}$	Critical speed	m/s
$x$	State vector	

### Subscripts 'a' reference axles

$a = 1$	Front axle towing vehicle
$a = 2$	Rear axle towing vehicle



$a = 3$	Axle first articulation
$a = 4$	Axle second articulation
$f$	Front axle
$r$	Rear axle

**Subscripts 'v' reference vehicle articulations**

$v = 1$	Towing vehicle
$v = 2$	First articulation
$v = 3$	Second articulation

**Coordinate system**

$r_v$	Yaw velocity	rad/s
$u$	Forward velocity	m/s
$v_v$	Lateral velocity	m/s





---

# Contents

---

<b>Abstract</b>	<b>i</b>
<b>Samenvatting</b>	<b>ii</b>
<b>Notation</b>	<b>vii</b>
<b>1 Introduction</b>	<b>1</b>
1.1 Motivation . . . . .	1
1.2 Objective and scope . . . . .	2
1.3 Organisation of the report . . . . .	3
<b>2 Literature Review on Directional Stability</b>	<b>5</b>
2.1 Stability analysis of single vehicles . . . . .	5
2.2 Stability analysis of vehicles with one articulation . . . . .	7
2.3 Stability analysis of vehicles with two articulations . . . . .	8
2.4 Dynamic performance of Ecocombi's . . . . .	8
2.5 Rearward amplification . . . . .	9
2.6 Concluding remarks . . . . .	12
<b>3 Directional Stability Analysis of Articulated Vehicles</b>	<b>13</b>
3.1 Stability of a single vehicle . . . . .	14
3.1.1 Stability boundaries for a single vehicle . . . . .	15
3.1.2 Cornering stiffness dependency with vertical load . . . . .	16
3.2 Stability of vehicles with one articulation . . . . .	19

3.2.1	Stability boundaries . . . . .	20
3.2.2	Saddle-node bifurcation . . . . .	22
3.2.3	Stability using the normalised cornering stiffness . . . . .	25
3.3	Stability of vehicles with two articulations . . . . .	34
3.4	Concluding remarks . . . . .	39
<b>4</b>	<b>Rearward Amplification</b>	<b>41</b>
4.1	Definitions for rearward amplification . . . . .	41
4.1.1	Differences between frequency domain approach and time domain approach	43
4.1.2	Relation between frequency domain approach and time domain approach	45
4.2	Rearward amplification of a conventional vehicle with two articulations . . . . .	47
4.2.1	Equations for the rearward amplification of a truck-full trailer . . . . .	47
4.2.2	Effect of parameter changes on rearward amplification of a truck-full trailer	52
4.3	Rearward amplification of conventional vehicles with one articulation . . . . .	60
4.4	Comparison of rearward amplification values for all conventional and Ecocombi configurations . . . . .	62
4.5	Concluding remarks . . . . .	66
<b>5</b>	<b>Effect of Multiple Axles on the Dynamic Performance of Articulated Vehicles</b>	<b>69</b>
5.1	Modelling of multiple axles . . . . .	69
5.2	Effect of multiple axles on rearward amplification of all combinations . . . . .	72
5.3	Concluding remarks . . . . .	77
<b>6</b>	<b>Conclusions and Recommendations</b>	<b>79</b>
6.1	Conclusions . . . . .	79
6.2	Recommendations for electronic stability control function tests at DAF . . . . .	81
6.3	Recommendations for further research . . . . .	82
	<b>Bibliography</b>	<b>84</b>
<b>A</b>	<b>Equations of Motion</b>	<b>89</b>
A.1	Assumptions for single track vehicle modelling . . . . .	89
A.2	Equations of motion with single axles . . . . .	89
A.3	Equations of motion with multiple axles . . . . .	92
<b>B</b>	<b>Vehicle and Tyre Parameters</b>	<b>97</b>

---

## Introduction

---

Safety is a common concern for all roads users. It is challenged by the traffic density, which has increased substantially over the past years and is expected to continue to rise in the future. Also the introduction of longer and heavier vehicles, Ecocombi's, challenges road safety. Nevertheless, the number of fatalities in road accidents in the European Union was cut by a quarter between 1990 and 2004. The objective of the EU is to further halve this number by the year 2010.

Langwieder et al. [24] investigated the benefit of electronic stability control functions in real accident situations involving cars and trucks. The purpose of these control functions is to prevent roll-over and yaw instability. He concludes that improving the safety of trucks considerably contributes to road safety as they are involved in 16 % of the fatal accidents; up to 9 % of the serious accidents involving trucks could have been positively influenced or even prevented with electronic stability control functions. Such functions have already been introduced for tractor-semitrailer combinations. They will be mandatory for all new truck types from November 2011 and for all new produced vehicles from November 2014 [4].

### 1.1 Motivation

Figure 1.1 gives an impressions of the truck combinations used on the European roads. The conventional trucks shown in figures 1.1a and b are in the majority. The tractor and truck are single vehicles. Three types of articulated vehicles are used; the tractor-semitrailer and truck-centre axle trailer with one articulation and the truck-full trailer with two articulations. The number of articulations is limited to two by law in the EU. The tractor-semitrailer has a maximum admissible length of 16.5 m, both truck-trailer combinations have a maximum length of 18.75 m. The mass of the combinations is limited to 50 tonnes in the Netherlands and 40 tonnes in most other European countries.

Additionally, Ecocombi's are introduced as a trial in the Netherlands, see figure 1.1c for an overview of the combinations allowed in the Netherlands. In contrast to conventional vehicles, Ecocombi's have a maximum length of 25.25 m and the maximum weight of the combination is 60 tonnes. Some advantages compared to conventional trucks are; reduction in fuel consumption per ton kilometer leading to less emissions, reduced transport costs per ton kilometer due to a reduction in driver costs as the transport volume and payload increases, and road protection due to reduced

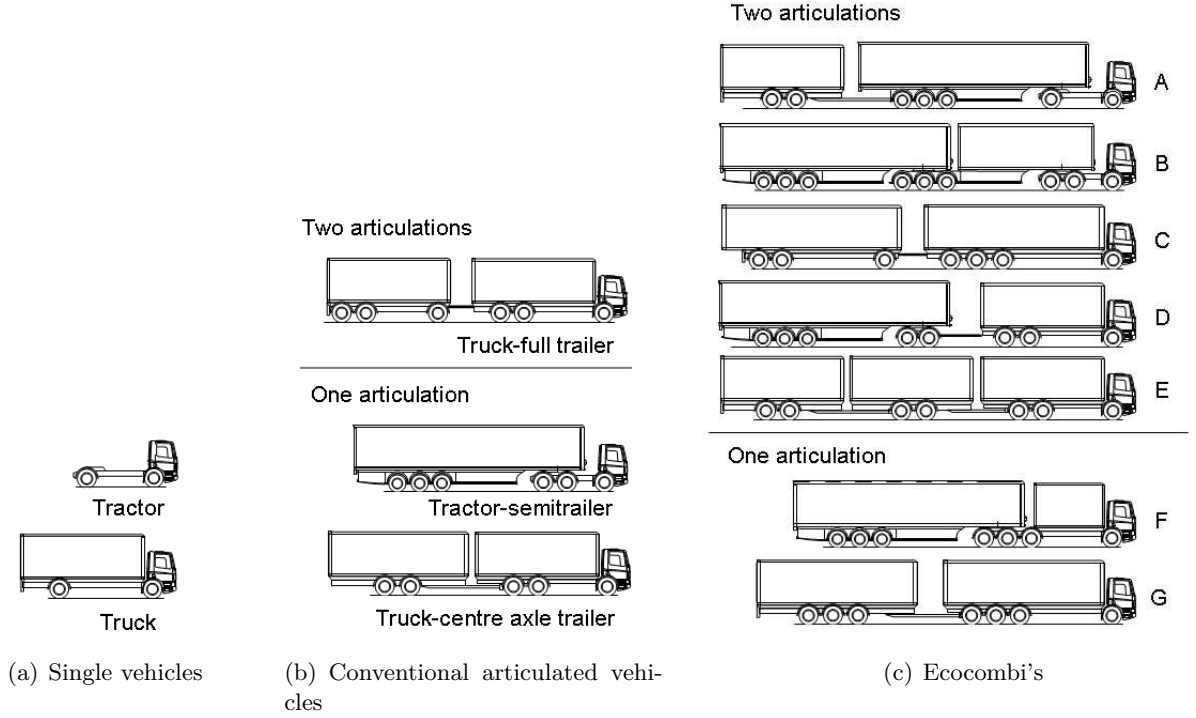


Figure 1.1: Truck combinations

axle loads. Opponents claim for example a decrease in road safety, a modal shift of transportation via rail to the road and extra costs for the infrastructure. Except for the trials mentioned above, Ecocombi's have not been permitted officially in most European countries yet, except for Sweden and Finland. Longer and heavier vehicles are allowed for many years outside Europe, for example in Australia, South Africa, Mexico, Canada and the USA, [21], [32], [27], [3], [30].

A wide range of truck combinations exists, as the vehicle combinations have many different purposes. Some applications are illustrated in figure 1.2. As a result, there are large variations in for instance truck combination, axle configuration, coupling type, number of articulations, load variations, and auxiliaries. The design challenge for the application of electronic stability control functions for all articulated vehicles is to guarantee robustness for all these vehicle configurations [18].

## 1.2 Objective and scope

A fundamental understanding on the stability of articulated vehicles is required in order to comprehend the effects of the various lay-outs and parameters. This knowledge can be used to quickly assess risks, critical situations and critical vehicle configurations when evaluating new stability control functions.

This study focuses on yaw stability of trucks as roll-over has been studied repeatedly in for instance [21], [25], [31] and [36]. Linear single track vehicle models are used to gain insight in the

## World of applications



Figure 1.2: DAFs 'World of Applications' [2]

important phenomena causing the instability and reduced damping of the system. This assumption means that the results are limited to small articulation angles and tyre slip angles. The entire range of vehicles used on the European roads is addressed, which includes conventional trucks and Ecocombi's, as illustrated in figure 1.1. Steered axles other than the towing vehicles front axle are not considered.

Summarising, the goal of this thesis is:

*To gain a fundamental understanding on yaw stability of vehicles with one and two articulations using linear analytical models.*

### 1.3 Organisation of the report

The organisation of this report is as follows: A literature review on the state of the art of yaw stability research of articulated trucks is presented in chapter 2. Methods to investigate the dynamic yaw behaviour of articulated vehicles are developed in chapters 3 and 4. The application to various vehicle combinations and the effect of multiple axles is presented in chapter 5. Finally, chapter 6 gives the conclusions and recommendations.





---

## Literature Review on Directional Stability

---

The range of trucks used on the European roads has been introduced in the previous chapter. A review of yaw stability studies on these vehicles types is presented in this chapter. This review directs the investigation of yaw stability presented in this thesis.

### 2.1 Stability analysis of single vehicles

The stability of single vehicles has thoroughly been investigated, amongst others by Pacejka [28], Besselink [7], Mitschke [26] and Pauwelussen [29]. A lot of work has been performed, both numerically and analytically, to quantify stability boundaries. This section gives a brief overview of single vehicle stability, as these results are well known for many years and the focus of this thesis is on articulated vehicles in particular.

Lateral tyre forces,  $F_y$ , are required to negotiate a curve. They result in tyre slip angles,  $\alpha$ , as illustrated in figure 2.1. This tyre characteristic is linear for small slip angles. The gradient of the curve in the linear regime is the tyre cornering stiffness,  $C_{F_\alpha}$ .

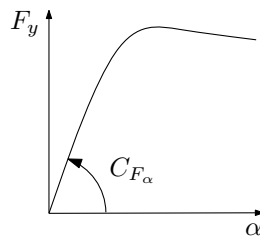


Figure 2.1: Lateral tyre slip characteristic

The same characteristic can be observed for an axle. For an axle  $C_i$  is introduced, with  $i$  denoting the axles;  $i = 1$  for the front axle,  $i = 2$  for the rear axle. Figure 2.2 shows a free body diagram of a one track single vehicle with front and rear axle forces and slip angles.

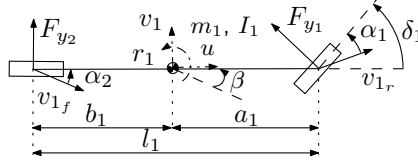


Figure 2.2: Free body diagram single vehicle

The steering characteristics of a single vehicle is expressed in terms of understeer, neutral steer or oversteer. Its nature depends on the relation between the front ( $\alpha_1$ ) and rear ( $\alpha_2$ ) tyre slip angles. When driving in a steady-state curve, the following relations hold:

$$\begin{aligned}\alpha_1 > \alpha_2 &\Rightarrow \text{understeer} \\ \alpha_1 = \alpha_2 &\Rightarrow \text{neutral steer} \\ \alpha_1 < \alpha_2 &\Rightarrow \text{oversteer.}\end{aligned}\tag{2.1}$$

Figure 2.3a shows the steering wheel angle,  $\delta_1$ , required to negotiate a steady-state circle with a fixed radius  $R$  when driving with forward velocity  $u$ . When driving very slowly, the steering wheel angle equals the Ackermann angle,  $\delta_1 = \frac{l_1}{R}$ , with  $l_1$  the wheelbase of the vehicle. The steering wheel angle increases when forward speed is increased for understeered vehicles in order to maintain driving on the radius  $R$ . It remains constant for neutrally steered vehicles and decreases for oversteered vehicles. The steering wheel angle and side slip angle relate as follows for steady-state cornering:

$$\delta_1 = \frac{l_1}{R} + \alpha_1 - \alpha_2.\tag{2.2}$$

For an understeered vehicle the characteristic speed,  $V_{char}$ , is defined as the speed where the steering wheel angle is twice the Ackermann angle. For an oversteered vehicle, the critical speed,  $V_{crit}$ , is the speed where the steering wheel angle is zero. The driver has to counter steer the vehicle when increasing the speed further. Furthermore, the vehicle itself is unstable beyond  $V_{crit}$ .

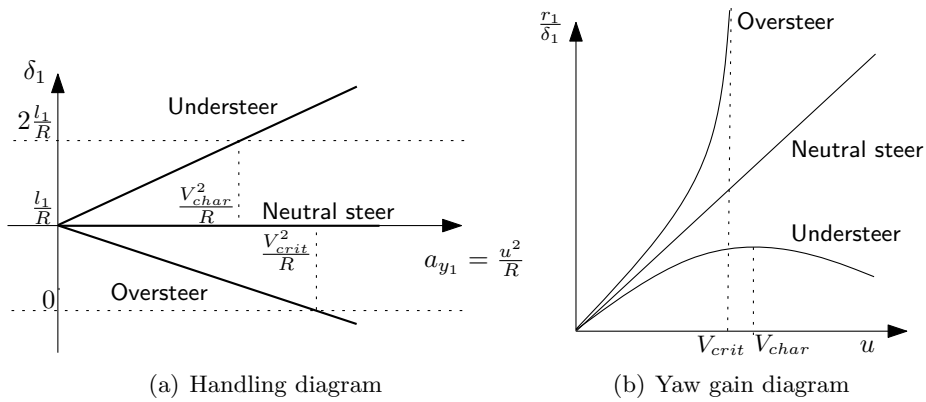


Figure 2.3: Steady-state cornering characteristics

Figure 2.3b shows the yaw velocity gain diagram,  $\frac{r_1}{\delta_1}$ , as function of speed. The yaw rate  $r_1$  is the rotation about the vertical axis of the vehicle. The yaw velocity gain of an understeered vehicle is limited and reaches its maximum at the characteristic speed. Hence, an understeered vehicle is directionally stable at any speed. The yaw velocity gain of a neutrally steered vehicle increases linearly with speed. Finally, the yaw velocity gain of an oversteered vehicle goes to infinity at the critical speed as it is unstable beyond this velocity.

## 2.2 Stability analysis of vehicles with one articulation

Pacejka [28], Andrzejewski et al. [5], Ellis [10], Pauwelussen [29] et al., Hac et al. [17], and Troger et al. [34], studied the stability of vehicles with one articulation, such as tractor-semitrailers, truck-centre axle trailers and car-caravan combinations. Numerical analyses were used by Pacejka and Andrzejewski to find the bifurcations and investigate the effect of parameter changes on stability. Ellis and Pauwelussen derived an algebraic equation for the stability boundary as function of the vehicle parameters.

In general, the following types of instability may occur [28], [34], [10]:

1. Divergent instability. The mass of the trailer is partly supported by the towing vehicle in the coupling point. The vehicle combination makes a monotonically unstable motion when the vertical force of the trailer on the towing vehicle becomes too large.
2. An unstable oscillatory motion. The snaking oscillation amplitude is unlimited, also in the non-linear case. The slip angle increases with increasing amplitudes which lowers the average cornering stiffness as a consequence of the digressive non-linear tyre cornering force characteristic. This will make the situation increasingly worse.

Trailer swing is also often seen as a yaw instability, although the combination may be stable in a mathematical sense. The following two types of trailer swing can be distinguished [10]. They are illustrated in figure 2.4.

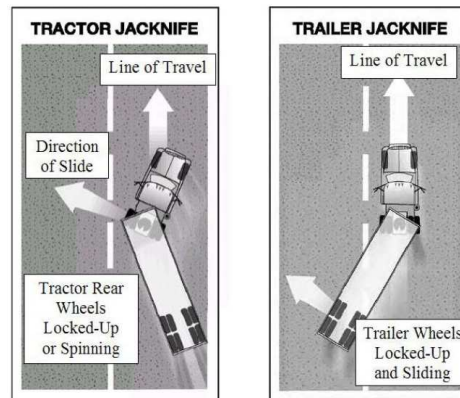


Figure 2.4: Two jack-knife possibilities of a tractor-semitrailer [25]

1. The tractor may jack-knife either under power or when braking, in particular when the rear wheels of the tractor lose grip or traction.
2. Trailer swing may occur when the trailer axle wheels are locked during braking.

## 2.3 Stability analysis of vehicles with two articulations

Ellis [10] and Fancher et al. [13] studied the dynamic stability of a truck-full trailer, which has two articulations. In contrast to a tractor-semitrailer combination, there is no weight transfer between the units of a truck-full trailer. Only a kinematic coupling exists when the following assumptions are made; (1) the steering dolly (front axle of the full trailer) is massless, (2) the articulation angles are small, and (3) no moments about the z-axis of the trailer are applied on the trailer, due to for instance braking or rutting. For small articulation angles, the pintle hitch effectively decouples the towing vehicle and full trailer with respect to the lateral dynamics, as a pintle hitch transmits no moments or side forces. In contrast, a fifth wheel used in a tractor-semitrailer combination transmits both roll moments and side forces. Changes in the mechanical properties of a full trailer will have a negligible effect on handling of the towing vehicle. Consequently, the combination behaves as a linked pair of two single vehicles.

The following types of loss of control and situations which may lead to instability have been found by Ellis based on numerical analysis. Loss of control is often seen as instability; the driver-vehicle closed-loop system can be unstable, or the travelled path can be undesired. However, the vehicle system alone might not be (mathematically) unstable in these situations.

1. A truck jack-knife occurs when the truck drive wheels spin up under traction or lock up during braking; the towing vehicle is oversteered.
2. A trailer jack-knife occurs when the full trailer rear axle experiences a brake lock up; the full trailer is oversteered.
3. The vehicle travels in a straight line when the front towing vehicle axle locks up. This is a stable motion, but the driver loses control; the towing vehicle is understeered.
4. The full trailer attempts to move on a straight path when the front trailer wheels lock up. This results in a large articulation angle at the steering dolly; the trailer is understeered. In this case, only a kinematic coupling between the units cannot be assumed anymore.

The first two types were also found for a vehicle with one articulation. Other types of instability have not been found in literature.

This overview shows that several types of instability can occur for articulated vehicles. In contrast to the single vehicle analysis, few algebraic equations have been found in literature to describe the stability boundaries. The conclusions presented here are mainly based on numerical analysis.

## 2.4 Dynamic performance of Ecocombi's

Recently, many studies have been performed to analyse the effect of Ecocombi's on road safety, as stability is one of the concerns for the legislation of these longer and heavier vehicles. The

conclusions are often based on mathematical models, questionnaires and results from the application of these vehicles in Sweden and Finland and trials in the Netherlands. It is however difficult to extrapolate from one part of Europe to another. The trial in the Netherlands is rather small and the infrastructure as well as the traffic density in the Scandinavian countries is very different compared to other European countries [9], [8].

Performance measures are often used to analyse the performance of articulated vehicles. They can be classified as follows [9], [23], [16]:

- Manoeuvrability and required space determine if a combination fits within the existing infrastructure. Performance measures are for instance; swept-path, high and low speed off-tracking, and out-swing.
- Directional stability and roll-over are important to evaluate dynamic vehicle behaviour. Performance measures are for instance; static roll-over threshold, dynamic load transfer ratio, yaw damping ratio and rearward amplification.

Rearward amplification appears to be the dominant performance property distinguishing the yaw response of multi-articulated vehicles from that of other commercial vehicles. It is used in many studies to quantify dynamic behaviour of articulated vehicles. During transient turning manoeuvres, the lateral acceleration of each trailing unit exceeds that of its preceding unit. As a result, the last trailer in a vehicle train has the tendency to swing out excessively which can lead to roll-over. This performance measure is of special interest for this study and investigated in more detail in the next section.

## 2.5 Rearward amplification

Rearward amplification, abbreviated as *RA*, is a performance measure which quantifies the dynamic lateral acceleration amplification using simulations or full scale road tests. Two definitions have been found in literature. In the first definition, rearward amplification is calculated using time histories of the lateral accelerations. A single or double lane change is often used as input, see figure 2.5a. Rearward amplification is then defined as [21], [31], [6], [23], [16], [9]:

$$RA_t = \frac{\max(\text{abs}(a_{y_{trailer}}))}{\max(\text{abs}(a_{y_{towing}}))}. \quad (2.3)$$

Either the lateral accelerations at the steer and last trailer axle or at the centre of gravities of the towing and last trailing unit are used.

Fancher, Ervin and Winkler et al [13], [15], [11], [36] defined rearward amplification in the frequency domain as the ratio between the lateral acceleration gain of the last trailer (the  $n^{th}$  unit) to the towing vehicles front wheel steering angle,  $H_{a_{y_n}, \delta_1}(\omega)$ , and the lateral acceleration gain of the towing vehicle (the  $1^{st}$  unit) to the front wheel steering angle,  $H_{a_{y_1}, \delta_1}(\omega)$ :

$$RA_f = \max \left| \frac{H_{a_{y_n}, \delta_1}(\omega)}{H_{a_{y_1}, \delta_1}(\omega)} \right| = \max |H_{a_{y_n}, a_{y_1}}(\omega)|. \quad (2.4)$$

Figure 2.5b shows that rearward amplification in both definitions is a function of steering input frequency and that the definitions may give a different value for this performance measure. A

high rearward amplification value corresponds to little yaw damping and a poorly damped dynamic behaviour of the vehicle combination.

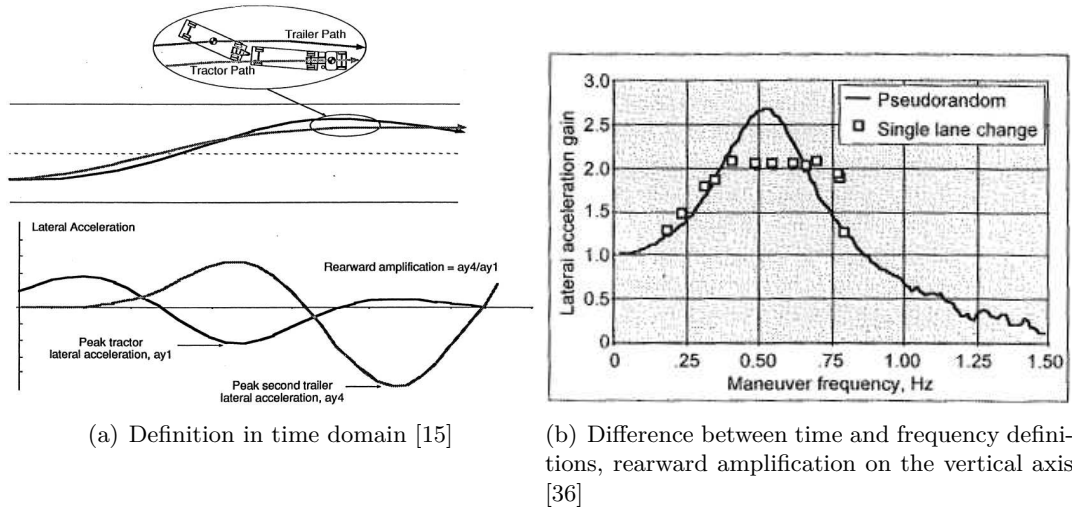


Figure 2.5: Rearward amplification

The next overview lists the effect of various vehicle parameters on rearward amplification and dynamic stability according to [17],[12],[29],[15],[16]:

**Trailer wheelbase:** A short wheelbase of a trailer results in a low trailer yaw damping, which leads to higher rearward amplification values. A centre axle trailer with a tandem axle is an extreme example of a short wheelbase.

**Type of coupling:** A B-type coupling (fifth wheel connection) is favourable for dynamic vehicle behaviour. An A-type coupling (towing hitch with drawbar connection) is not favourable for dynamic stability, but it improves the swept-path of a vehicle compared to a B-type coupling. European vehicles tend to include more A-type couplings than the equivalent vehicles from Australia, South Africa, Mexico, Canada and the United States. This is because the manoeuvrability and required space on the road is very important for European vehicles. In the other countries mentioned, the traffic density is much lower and the available space on the roads is much larger. Therefore, their focus is on reducing rearward amplification.

**Number of articulations:** More articulation joints increase the rearward amplification.

**Coupling rear overhang:** The distance between the coupling point and the trucks rear axle has a large effect on stability. The closer the coupling is to the rear axle, the better the dynamic stability of the vehicle combination.

**Drawbar length:** A longer drawbar reduces rearward amplification.

**Location centre of gravity trailer:** Moving the load rearwards in a combination, e.g. from the towing vehicle to the trailer, increases rearward amplification. Moving the centre of gravity of the trailer rearwards has a similar effect.

**Cornering stiffness:** Increasing the cornering stiffness of the rear axle of the towing vehicle or decreasing the cornering stiffness of the front axle of the towing vehicle increases the tendency to understeer. This is favourable for stability as it was concluded in section 2.1 (page 5) that an understeered vehicle is stable at any speed. Furthermore, increasing the cornering stiffness of the trailer tyres decreases rearward amplification significantly.

Figure 2.6 shows the values for the rearward amplification of some studies analysing conventional vehicles and Ecocombi's. The conditions used for the different studies vary, both in terms of manoeuvres used and loading conditions, making a comparison of results difficult.

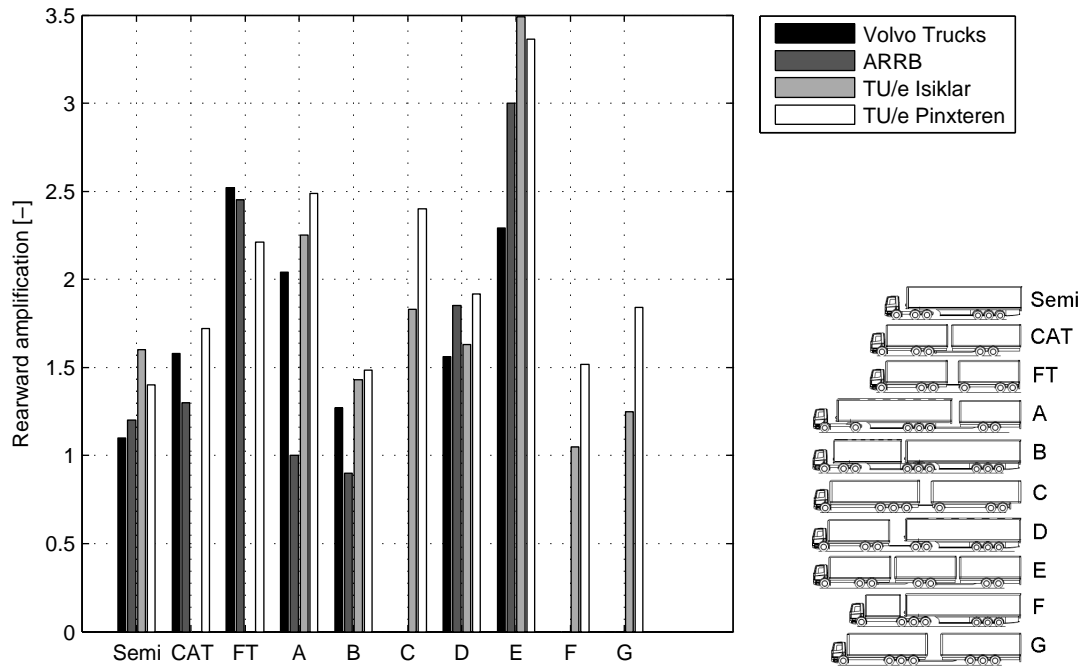


Figure 2.6: Ranking of the vehicle combinations in terms of rearward amplification, Volvo Trucks [6], ARRB [16], TU/e Isiklar [21] and TU/e Pinxteren [31]

Some general conclusions are:

- Conventional trucks are often used as benchmark to quantify the Ecocombi's. The tractor-semitrailer performs very well, the truck-full trailer has a very high rearward amplification and performs poorly.
- From all Ecocombi's, configuration B is the best in terms of rearward amplification. Furthermore, it performs better than both the truck-centre axle trailer and the truck-full trailer.
- The Ecocombi E has a high rearward amplification value in all studies. Reducing the maximum weight improves the dynamic yaw performance. Either the truck-full trailer or this combination performs worst. The studies do not show an clear ranking of these vehicles.
- Ecocombi A has a rather large rearward amplification. The semitrailer is favorable for stability, but the centre axle trailer has little yaw damping.

- Combinations C, D, F and G perform in the mid region.

This overview shows that the Ecocombi's do not show an implicit increase of safety risk in general. Either the truck-full trailer or the E combination performs worst, but the truck-full trailer is already legal in the EU. Nevertheless, it is recommended in many studies to make electronic safety control functions mandatory to reduce safety risks.

The resulting rearward amplification differs per study. The main reasons for these discrepancies are; (1) the vehicle parameters are not the same, (2) some studies use complex multibody models others are based on full scale testing, (3) the input differs per study, and (4) the vehicle speed differs per study.

The results are expected to be better reproducible and more generic when open-loop tests are performed. In simulations this can be overcome quite easily. ISO tests are often used to perform standardised tests to measure rearward amplification. In [1] it is recommended to use a pseudo-random input to determine a maximum value for rearward amplification, as it provides complete information about the frequency dependency of rearward amplification. It is a test method to obtain a frequency response function. However, it is also concluded that a single lane change can be used to determine the performance measure during a realistic manoeuvre. The single lane change may be carried out by applying either a single sine-wave steering input, or by following a path which results in a sine-wave lateral acceleration response. It is concluded that the rearward amplification of the two lane change approaches will differ also, as the frequency content of the two steering wheel inputs differs.

Several test methods for heavy articulated vehicles were analysed by Hoogvelt et al. in [19]. In this study, it was concluded that although it is an open-loop test, a single sine-wave test is still very difficult to perform. It is recommended to use a very skilled and experienced test driver in order to produce a good sinus input, and to use special devices in order to help the driver or a steering robot.

## 2.6 Concluding remarks

In literature, directional stability of single vehicles is studied in a different way compared to stability of articulated vehicles. Due to the complexity of the equations compared to a single vehicle, articulated vehicles are mostly analysed numerically. Sophisticated complex vehicle models or full scale measurements are mostly used. Algebraic expressions for the stability boundaries have been found for only a few vehicle types.

Rearward amplification is a performance measure which is often used to quantify the yaw behaviour of articulated vehicles. A comparison between different studies is difficult, as this performance measure depends on the manoeuvre and conditions.

The use of complex vehicle models makes it difficult to really understand the import phenomena causing dangerous yaw motions of articulated vehicles which may lead to serious accidents. Therefore, to enhance fundamental understanding, a method is developed in the next chapters to assess dynamic behaviour of articulated vehicles. Linear single track vehicle models are used, which only model the most important yaw dynamics of the vehicles. Chapter 3 presents analytical derivations and interpretations of the stability bifurcations. Rearward amplification is studied in detail in chapter 4.



## Directional Stability Analysis of Articulated Vehicles

In this chapter, the directional stability of articulated vehicles is assessed by calculating and analysing the stability boundaries. Algebraic equations of the vehicles are derived to find the bifurcations. For the sake of completeness, single vehicles are discussed as well, though the main focus of this work is on articulated vehicles. To reduce the complexity of the equations, all towing units are considered to have two axles (front and rear) and all trailing units are considered to have one axle. Single tyres are assumed in all cases. The effect of tandem or triple axles is investigated in chapter 5. Only the front axle of the towing vehicle is steered.

Stability of the vehicles is evaluated using the characteristic equation. All roots ( $\lambda$ ) of the characteristic equation of the dynamic system, which describes the yaw dynamics of these vehicles, should have negative real parts for this linear system to be stable. The characteristic equation is given by:

$$c_0\lambda^n + c_1\lambda^{n-1} + \dots c_{n-1}\lambda + c_n = 0, \quad (3.1)$$

where  $c_i$  are the coefficients of the characteristic equation and  $n$  the number of states. Instead of calculating the roots, it is also possible to evaluate the stability of a linear system by considering the coefficients of the characteristic equation only. Klotter [22] found that a necessary, but not sufficient requirement for stability is that all coefficients should be larger than zero;  $c_i > 0$  for  $i = 1 \dots n$ . The requirement for stability is that all Hurwitz determinants should be larger than zero;  $H_i > 0$  for  $i = 1 \dots n$ , with,

$$H_i = \begin{vmatrix} c_1 & c_0 & 0 & 0 & 0 & \dots & 0 \\ c_3 & c_2 & c_1 & c_0 & 0 & \dots & 0 \\ c_5 & c_4 & c_3 & c_2 & c_1 & \dots & 0 \\ \vdots & \vdots & \vdots & \vdots & \vdots & \ddots & \vdots \\ c_{2i-1} & c_{2i-2} & c_{2i-3} & c_{2i-4} & c_{2i-5} & \dots & c_i \end{vmatrix}. \quad (3.2)$$

Klotter simplified this criterion to the following requirements for stability, as it is not necessary to calculate all Hurwitz determinants and all coefficients:

$$\left. \begin{array}{l} c_0, c_1, \dots, c_{n-1}, c_n > 0 \\ H_{n-1}, H_{n-3}, \dots, \begin{cases} c_1 \text{ if } n \text{ is even} \\ H_2 \text{ if } n \text{ is odd} \end{cases} > 0 \end{array} \right\}. \quad (3.3)$$

Two bifurcations can be distinguished. The first one is called as saddle-node bifurcation, see figure 3.1a. In this case one real eigenvalue passes the imaginary axis. For an initially stable system, this occurs due to a parameter variation according to Klotter, when the highest coefficient of the characteristic equation passes zero:

$$c_n = 0. \quad (3.4)$$

In this case an initially stable system becomes monotonically or divergent unstable due to a parameter variation.

The second bifurcation which can occur is the Hopf bifurcation, see figure 3.1b. In this case, a complex conjugate pair of eigenvalues passes the imaginary axis due to a parameter variation. The motion of the system is oscillatory. For an initially stable system, Klotter defined the boundary of stability with an oscillatory behaviour when the highest Hurwitz determinant to be evaluated passes zero:

$$H_{n-1} = 0. \quad (3.5)$$



Figure 3.1: Bifurcations

### 3.1 Stability of a single vehicle

A truck and tractor are of the class single vehicle, see figure 3.2. In this section, the stability boundaries of these vehicles are analysed by deriving the equations of motion and characteristic equation, and by applying the Hurwitz criterion of (3.3).

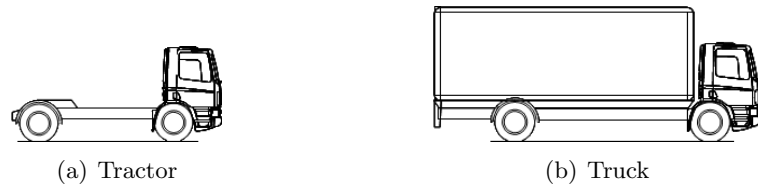


Figure 3.2: Single vehicles

### 3.1.1 Stability boundaries for a single vehicle

Figure 3.3a shows the free body diagram of a single vehicle. It is assumed that the forward velocity  $u$  is positive and constant. The equations of motion read (for a full derivation see appendix A):

$$\begin{bmatrix} m_1 & 0 \\ 0 & I_1 \end{bmatrix} \begin{bmatrix} \dot{v}_1 \\ \dot{r}_1 \end{bmatrix} = -\frac{1}{u} \begin{bmatrix} C & Cs_1 + m_1 u^2 \\ Cs_1 & Cq_1^2 \end{bmatrix} \begin{bmatrix} v_1 \\ r_1 \end{bmatrix} + \begin{bmatrix} C_1 \\ a_1 C_1 \end{bmatrix} \delta_1, \quad (3.6)$$

where the state variables are  $v_1$ , the lateral velocity at the centre of gravity, and  $r_1$ , the yaw velocity with  $r_1 = \dot{\beta}$ . Furthermore, the following abbreviations are used, suggested by Pacejka [28] and illustrated in figure 3.3b:

$$\left. \begin{aligned} C &= C_1 + C_2 \\ Cs_1 &= a_1 C_1 - b_1 C_2 \\ Cq_1^2 &= a_1^2 C_1 + b_1^2 C_2 \\ I_1 &= m_1 k_1^2 \end{aligned} \right\}, \quad (3.7)$$

with,

$C$  : the total cornering stiffness,

$s_1$  : the distance along the longitudinal axis of the vehicle from the center of gravity to the neutral steer point  $S$ . The neutral steer point is the point on the vehicle where an external side force does not impose a yaw angle to the vehicle. This means that  $s_1 = 0$  corresponds to a neutrally steered vehicle,  $s_1 < 0$  to an understeered vehicle and  $s_1 > 0$  to an oversteered vehicle,

$q_1$  : the length which corresponds to an average moment arm,

$k_1$  : the radius of gyration.

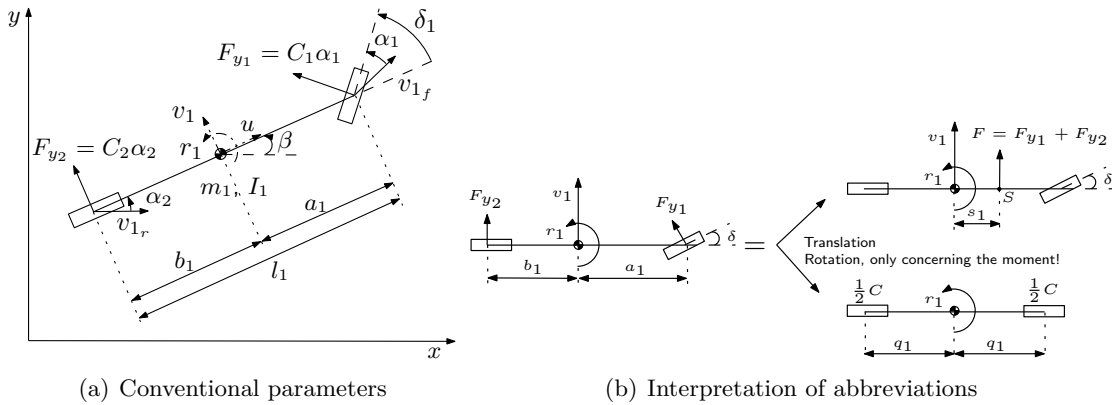


Figure 3.3: Free body diagram

The characteristic equation of a single vehicle is given by:

$$c_0 \lambda^2 + c_1 \lambda + c_2 = 0, \quad (3.8)$$

with,

$$\left. \begin{aligned} c_0 &= 1 \\ c_1 &= C \frac{k_1^2 + q_1^2}{m_1 k_1^2 u} \\ c_2 &= \frac{C}{m_1 k_1^2 u^2} \left( \frac{C(q_1^2 - s_1^2)}{m_1} - s_1 u^2 \right) \end{aligned} \right\}.$$

Physical parameters are assumed, which means that they are all positive except for the neutral steer parameter  $s_1$ . Only forward driving is considered;  $u > 0$ . Furthermore, from (3.7) it follows that:

$$q_1^2 - s_1^2 = l_1^2 \frac{C_1}{C} \frac{C_2}{C}, \quad (3.9)$$

which implies that  $q_1^2 - s_1^2$  is also always positive.

The Hurwitz criterion is applied to study the stability of this vehicle system. According to (3.3) the following should hold for stability ( $H_1 = c_1$ ):

$$\left. \begin{aligned} c_0 &> 0 && : \text{always fulfilled} \\ c_1 &> 0 && : \text{always fulfilled} \\ c_2 &> 0 && : \left\{ \begin{array}{ll} s_1 < 0 & : \text{always fulfilled} \\ s_1 = 0 & : u < \infty \Rightarrow \text{always fulfilled} \\ s_1 > 0 & : u < V_{crit} = \sqrt{\frac{C(q_1^2 - s_1^2)}{m_1 s_1}} \end{array} \right. \\ H_1 &> 0 && : \text{always fulfilled} \end{aligned} \right\}. \quad (3.10)$$

A Hopf bifurcation does not occur for a single vehicle, as the Hurwitz determinant  $H_1$  does not pass zero. All coefficients are larger than zero, so a saddle-node bifurcation occurs when the highest coefficient of the characteristic equation,  $c_2$ , passes zero. In accordance with the conclusions from the handling and yaw velocity gain diagrams presented in the literature review (section 2.1, figure 2.3, page 6) an understeered vehicle ( $s_1 < 0$ ) is always stable. An oversteered vehicle ( $s_1 > 0$ ) is stable if  $u < V_{crit}$ .

From this analysis, it turns out that the location of the neutral steer point is the important parameter to quantify stability of a single vehicle. According to (3.7) this parameter is a function of the location of the centre of gravity and the cornering stiffnesses. In the next section, the effect of scaling the cornering stiffness with vertical load on the neutral steer parameter  $s_1$  is studied.

### 3.1.2 Cornering stiffness dependency with vertical load

The tyre cornering stiffness is not taken as function of vertical force but as a constant parameter in many studies. However, in reality it is a function of the vertical force on the tyre. This relation is investigated by Veldpaus et al. [35] and Houben [20] for truck tyres. Figure 3.4 shows some data points collected from these reports and a second order polynomial fit. Two cases are considered; the characteristic is linear or non-linear.

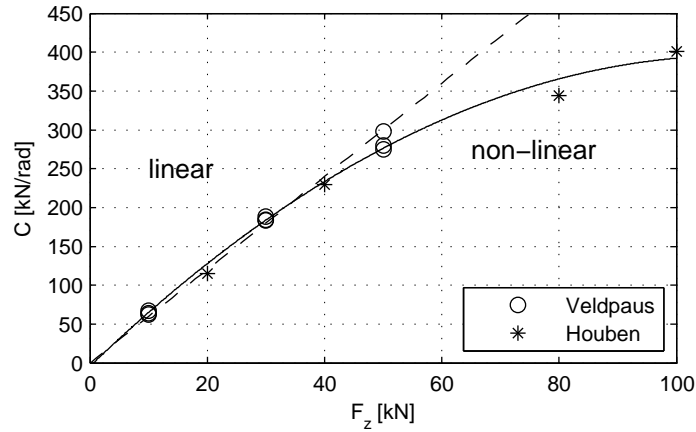


Figure 3.4: Cornering stiffness of a single tyre as function of vertical force [35] [20]

**Linear characteristic:** A normalised cornering stiffness is used to study the effect of scaling the tyre cornering stiffness linearly with vertical load on dynamic stability. It was found in [14] that, in contrast to passenger car tyres, the relation between the tyre cornering stiffness and vertical load is nearly linear for truck tyres. It was also found in [14] that the characteristic shows an even more linear relationship if dual tyres are applied, which is often the case in truck configurations, except for the steered axle. Figure 3.5 shows the cornering stiffness versus vertical load characteristic for a single tyre, and of a dual set composed of two the same type of tyres as the single one. This means that the assumption that the cornering stiffness versus load characteristic is in its linear region is often true for truck tyres. Note that the characteristics in figures 3.4 and 3.5 are for one single tyre, or one set of dual tyres, which means that the axle load should be divided by two.

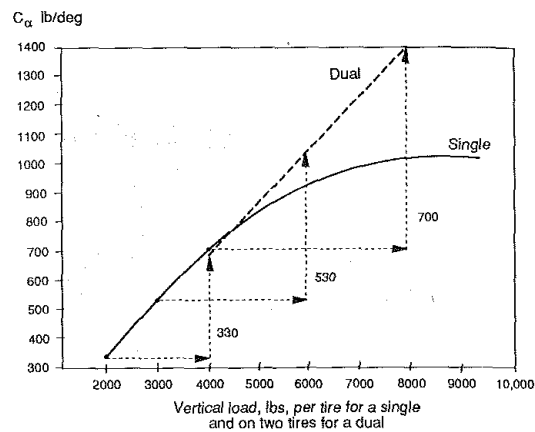


Figure 3.5: Cornering stiffness as function of vertical force, comparison between single and dual tyres [14]

The following relation is used for the linear part of the characteristic:

$$C_i = \frac{F_{z_i}}{F_{z_{nom}}} C_{nom} = f_i F_{z_i}, \quad (3.11)$$

with  $i = 1$  for the front axle,  $i = 2$  for the rear axle, and  $f_i = \frac{C_{nom}}{F_{z_{nom}}}$  the normalised cornering stiffness.

With this expression for the cornering stiffnesses, parameter  $s_1$  defined in (3.7) can be expressed when the normalised cornering stiffness is assumed as:

$$\begin{aligned} s_1 &= a_1 \frac{C_1}{C} - b_1 \frac{C_2}{C} \\ &= a_1 \frac{f_1 F_{z_1}}{f_1 F_{z_1} + f_2 F_{z_2}} - b_1 \frac{f_2 F_{z_2}}{f_1 F_{z_1} + f_2 F_{z_2}} \\ &= \frac{a_1 b_1 (f_1 - f_2)}{f_1 b_1 + f_2 a_1}, \end{aligned} \quad (3.12)$$

with  $F_{z_1} = m_1 g \frac{b_1}{l_1}$  and  $F_{z_2} = m_1 g \frac{a_1}{l_1}$  the vertical axle forces. The tendency to oversteer or understeer is a function of  $f_1$  and  $f_2$ :

$$\left. \begin{aligned} f_1 < f_2 &\Rightarrow \text{understeer, } s_1 < 0, \text{ the vehicle is stable at any speed} \\ f_1 = f_2 &\Rightarrow \text{neutral steer, } s_1 = 0, \text{ the critical speed is infinite} \\ f_1 > f_2 &\Rightarrow \text{oversteer, } s_1 > 0, \text{ the vehicle is stable if } u < V_{crit} = \sqrt{\frac{f_1 f_2 l_1 g}{f_1 - f_2}} \end{aligned} \right\}. \quad (3.13)$$

It was concluded by Houben that the variation in measured cornering stiffness for steer, drive and trailer tyres is fairly small;  $f = f_1 \approx f_2 \approx f_3$ , as illustrated in figure 3.6. Therefore, trucks generally have a nearly neutrally steered character.

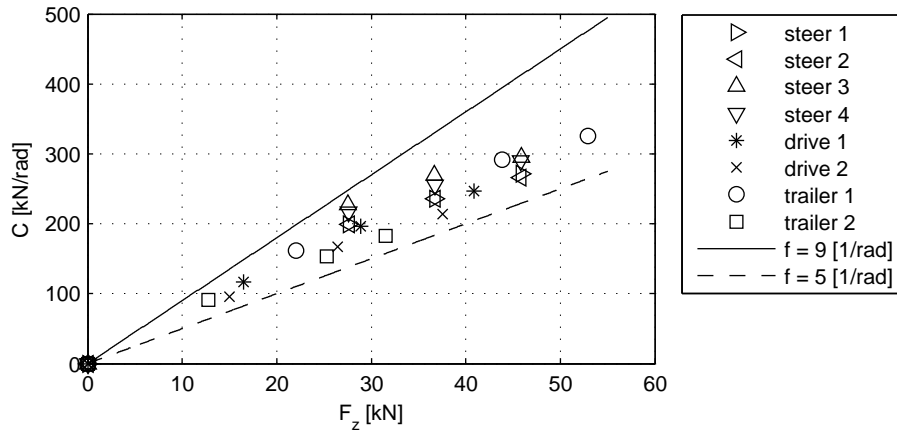


Figure 3.6: Cornering stiffness as function of vertical force, variation between steer, drive and trailer tyres [20]

It can be concluded also, that using the normalised cornering stiffness an initially understeered vehicle will remain understeered, and thus stable at any speed, when changing

vehicle parameters such as mass and dimensions. This is since the criterion in (3.13) for understeered vehicles only depends on the normalised cornering stiffness.

Furthermore, the critical speed for an oversteered vehicle is only determined by the normalised cornering stiffnesses, and the wheelbase of the vehicle. The mass and location of the centre of gravity do not affect stability at all. The critical speed increases when increasing the wheelbase.

**Non-linear characteristic:** The normalised cornering stiffness is used under normal conditions when the characteristics are linear. However, the cornering stiffness dependency is digressive for higher vertical loads. Therefore, a linear relationship cannot be assumed in all cases. Oversteer may for instance occur when a truck is loaded such that the cornering stiffness characteristic of the rear axle gets in the degressive region.

The normalised cornering stiffness is applied throughout this study, as this is a fair representation for the majority of the applications and conditions. Some exceptions are made when necessary.

### 3.2 Stability of vehicles with one articulation

Figure 3.7 shows the tractor-semitrailer and truck-centre axle trailer. They are the conventional vehicle combinations with one articulation used on the European roads. The roll moment coupling between the units is not modelled, as the centre of gravities are assumed to be on the ground in the planar single track modelling approach used in this study. Therefore, the equations of motion as well as the stability boundaries derived in this section apply for all vehicles with one articulation.

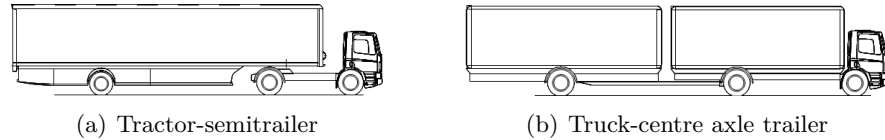
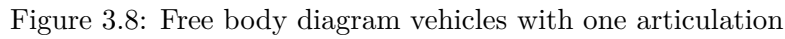


Figure 3.7: Conventional vehicles with one articulation

Figure 3.8 shows the free body diagram for vehicles with one articulation. When neglecting body-roll, the major difference between a truck-centre axle trailer and a tractor-semitrailer is the location of the hitch point. For a tractor-semitrailer, it is located in front of the rear axle of the towing vehicle,  $e_1 < 0$ . For a truck-centre axle trailer it is located behind the rear axle,  $e_1 > 0$ . Furthermore, the centre of gravity of the semitrailer is never behind the trailer rear wheels,  $a_2 < l_2$ ,  $b_2 > 0$ . This in contrast to a truck-centre axle trailer where, at least in theory, the centre of gravity can be located behind the trailer axle.

The stability of these vehicles is analysed in the next sections. First, the equations of motion and characteristic equation are given. Then the Hurwitz criterion is applied.



The equations of motion are derived in appendix A. The state-space description reads:

with the state vector  $(v_1, r_1, \phi, \dot{\phi})$ , with  $v_1$  the lateral velocity at the centre of gravity of the towing vehicle,  $r_1$  the yaw velocity of the towing vehicle with  $r_1 = \dot{\beta}$  and  $\phi$  the relative articulation angle between the trailer and the towing vehicle. The yaw angle of the trailer is given by  $\theta$  with  $\theta = \beta + \phi$ .

$$c_0\lambda^4 + c_1\lambda^3 + c_2\lambda^2 + c_3\lambda + c_4 = 0, \quad (3.15)$$



with,

$$\left. \begin{aligned} c_0 &= m_1 m_2 u [m_1 k_1^2 (k_2^2 + a_2^2) + m_2 k_2^2 (k_1^2 + h_1^2)] \\ c_1 &= m_1 m_2 [C_3 (b_2^2 + k_2^2) (k_1^2 + h_1^2) + C (a_2^2 + k_2^2) (k_1^2 + q_1^2)] \\ &\quad + m_1^2 C_3 k_1^2 l_2^2 + m_2^2 C k_2^2 (q_1^2 + h_1^2 + 2h_1 s_1) \\ c_2 &= \frac{1}{u} \left[ u^2 \left\{ m_1 C_3 l_2 \left( m_1 k_1^2 + m_2 \frac{b_2}{l_2} (k_1^2 + h_1^2) \right) - m_2 C (s_1 + h_1) \left( m_2 k_2^2 + m_1 \frac{s_1}{s_1 + h_1} (k_2^2 + a_2^2) \right) \right\} \right. \\ &\quad \left. + m_1 C C_3 l_2^2 (k_1^2 + q_1^2) + m_2 C \{ C_3 (q_1^2 + h_1^2 + 2h_1 s_1) (k_2^2 + b_2^2) + C (q_1^2 - s_1^2) (k_2^2 + a_2^2) \} \right] \\ c_3 &= \frac{C C_3 l_2}{u^2} \left[ u^2 \left\{ m_1 (q_1^2 + k_1^2 - s_1 l_2) + m_2 \frac{b_2}{l_2} (q_1^2 + h_1^2 + 2h_1 s_1) - m_2 \frac{1}{l_2} (s_1 + h_1) (b_2^2 + k_2^2) \right\} \right. \\ &\quad \left. + C l_2 (q_1^2 - s_1^2) \right] \\ c_4 &= \frac{C C_3 l_2}{u} \left[ -u^2 \left\{ m_2 \frac{b_2}{l_2} (s_1 + h_1) + m_1 s_1 \right\} + C (q_1^2 - s_1^2) \right] \end{aligned} \right\}.$$

To simplify these equations, new abbreviations,  $s_2$  and  $q_2$  are introduced in accordance with the abbreviations introduced for single vehicles in (3.7):

$$\left. \begin{aligned} C s_2 &= l_1^* C_1 + e_1 C_2 \\ s_2 &= h_1 + s_1 \\ C q_2^2 &= l_1^{*2} C_1 + e_1^2 C_2 \\ q_2^2 &= q_1^2 - s_1^2 + s_2^2 \\ &= q_1^2 + h_1^2 + 2h_1 s_1 \end{aligned} \right\}, \quad (3.16)$$

with  $l_1^*$  the distance between the front axle and hitch point. These abbreviations express parameters  $s_1$  and  $q_1$  defined in (3.7) with the hitch point instead of the centre of gravity as reference point.

The parameters are all positive in their physical ranges, except for the neutral steer parameters  $s_1$  and  $s_2$ ,  $e_1$  and  $b_2$ . Only forward driving is considered;  $u > 0$ . The Hurwitz criterion explained in equation (3.3) is used to analysed the stability boundaries. The following should hold:

$$\left. \begin{aligned} c_0 > 0 &: \text{always fulfilled} \\ c_1 > 0 &: \text{always fulfilled} \\ c_2 > 0 &: \left\{ \begin{aligned} D_{c_2} < 0 &: \text{always fulfilled} \\ D_{c_2} = 0 &: u < \infty \Rightarrow \text{always fulfilled} \\ D_{c_2} > 0 &: u < V_{crit,c_2} \end{aligned} \right. \\ c_3 > 0 &: \left\{ \begin{aligned} D_{c_3} < 0 &: \text{always fulfilled} \\ D_{c_3} = 0 &: u < \infty \Rightarrow \text{always fulfilled} \\ D_{c_3} > 0 &: u < V_{crit,c_3} \end{aligned} \right. \\ c_4 > 0 &: \left\{ \begin{aligned} D_{c_4} < 0 &: \text{always fulfilled} \\ D_{c_4} = 0 &: u < \infty \Rightarrow \text{always fulfilled} \\ D_{c_4} > 0 &: u < V_{crit,c_4} \end{aligned} \right. \\ H_1 > 0 &: \text{always fulfilled} \\ H_3 > 0 &: c_1 c_2 c_3 - c_0 c_3^2 - c_4 c_1^2 > 0 \end{aligned} \right\}, \quad (3.17)$$

with,

$$\left. \begin{aligned} V_{crit,c_2} &= \sqrt{\frac{m_1 C C_3 l_2^2 (k_1^2 + q_1^2) + m_2 C \{ C_3 q_2^2 (k_2^2 + b_2^2) + C (q_1^2 - s_1^2) (k_2^2 + a_2^2) \}}{-m_1 C_3 l_2 \left\{ m_1 k_1^2 + m_2 \frac{b_2}{l_2} (k_1^2 + h_1^2) \right\} + m_2 C s_2 \left\{ m_2 k_2^2 + m_1 \frac{s_1}{s_2} (k_2^2 + a_2^2) \right\}}} \\ V_{crit,c_3} &= \sqrt{\frac{C l_2 (q_1^2 - s_1^2)}{-m_1 (q_1^2 + k_1^2 - s_1 l_2) - m_2 \frac{b_2}{l_2} q_2^2 + m_2 \frac{s_2}{l_2} (b_2^2 + k_2^2)}} \\ V_{crit,c_4} &= \sqrt{\frac{C (q_1^2 - s_1^2)}{m_2 \frac{b_2}{l_2} s_2 + m_1 s_1}}, \end{aligned} \right\}, \quad (3.18)$$

and  $D_{c_2}$ ,  $D_{c_3}$ ,  $D_{c_4}$  the denominators of the critical speeds  $V_{crit,c_2}$ ,  $V_{crit,c_3}$  and  $V_{crit,c_4}$  respectively. The vehicle combination experiences a saddle-node bifurcation when all coefficients are initially positive and when the last coefficient,  $c_4$  passes zero due to a parameter variation. In this case, the fourth critical speed determines monotonic stability. It shows a strong similarity with the critical speed derived for a single vehicle in (3.10). This relation is investigated in section 3.2.2. The critical speeds of all coefficients are discussed in section 3.2.3 by assuming the normalised cornering stiffness. The third Hurwitz determinant which determines the Hopf bifurcation is analysed in section 3.2.3 as well.

### 3.2.2 Saddle-node bifurcation

The analogy between the last critical speed of a single vehicle and a vehicle with one articulation is discussed in this section. The normalised cornering stiffness is not applied.

Figure 3.9a shows the vertical forces acting on the towing vehicle, with:

$$\left. \begin{aligned} m_{cp} &= m_2 \frac{b_2}{l_2} \\ F_{z_1} &= m_1 g \frac{b_1}{l_1} - m_2 g \frac{b_2}{l_2} \frac{e_1}{l_1^*} \\ F_{z_2} &= m_1 g \frac{a_1}{l_1} + m_2 g \frac{b_2}{l_2} \frac{l_1^*}{l_1} \end{aligned} \right\}, \quad (3.19)$$

where  $m_{cp}$  is the mass of the trailer supported by the towing vehicle in the coupling point.

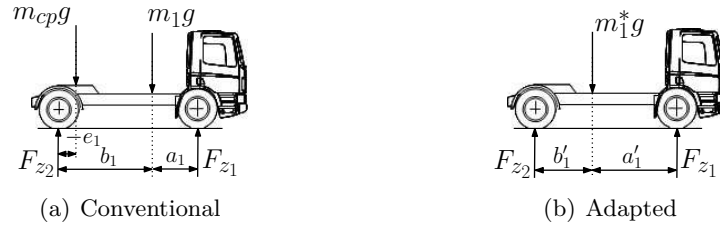


Figure 3.9: Vertical forces acting on the tractor

Figure 3.9b shows how the vertical forces of the towing vehicle mass and portion of the trailer mass carried by the towing vehicle, can be lumped. Obviously, the axle loads should remain the same, which yields:

$$\left. \begin{aligned} m_1^* &= m_1 + m_2 \frac{b_2}{l_2} \\ a_1' &= a_1 + \frac{m_2}{m_1^*} \frac{b_2}{l_2} h_1 \\ b_1' &= b_1 - \frac{m_2}{m_1^*} \frac{b_2}{l_2} h_1 \end{aligned} \right\}. \quad (3.20)$$

For the vehicle in figure 3.9b, the neutral steer parameter becomes:

$$\begin{aligned}
s'_1 &= a'_1 \frac{C_1}{C} - b'_1 \frac{C_2}{C} \\
&= a_1 \frac{C_1}{C} - b_1 \frac{C_2}{C} + \frac{m_2 \frac{b_2}{l_2}}{m_1^*} h_1 \\
&= s_1 + \frac{m_2 \frac{b_2}{l_2}}{m_1^*} h_1.
\end{aligned} \tag{3.21}$$

To adapt the critical speed of a single vehicle to the critical speed of the articulated vehicle, the total mass of the towing vehicle  $m_1^*$  and new neutral steer parameter  $s'_1$  have to be substituted for  $m_1$  and  $s_1$ :

$$\begin{aligned}
V_{crit, \text{single vehicle}} &= \sqrt{\frac{C(q_1^2 - s_1^2)}{m_1 s_1}} \Rightarrow V_{crit_{c_4}, \text{one articulation}} = \sqrt{\frac{C(q_1^2 - s_1'^2)}{m_1^* s_1'}} \\
V_{crit_{c_4}, \text{one articulation}} &= \sqrt{\frac{C(q_1^2 - s_1'^2)}{s_1 m_1 + m_2 \frac{b_2}{l_2} s_2}},
\end{aligned} \tag{3.22}$$

which is equal to the critical speed  $V_{crit, c_4}$  derived in (3.18). The combination is stable at any speed in the sense of the saddle-node bifurcation when the denominator of the root is negative. This means that this vehicle combination is understeered and stable for all speeds if  $s'_1 < 0$ , oversteered if  $s'_1 > 0$ , and unstable if oversteered and the speed exceeds the critical speed.

The trailer has a strong influence on the stability of the combination. Table 3.1 shows how the trailer can stabilise an unstable towing vehicle (bottom left) or destabilise a stable towing vehicle (top right). Furthermore, the trailer can increase understeer (top left) or oversteer (bottom right). However, it should be noted that the hitch point is located in front of the center of gravity of the towing vehicle in case  $h_1 < 0$ , which does not occur in practise.

	$h_1 < 0$ ; hitch point in front of cog	$h_1 > 0$ ; hitch point behind cog
$s_1 < 0$ understeered towing vehicle	$s'_1 < 0 \rightarrow \text{stable } \forall u$ $s_2 = s_1 + h_1 < 0$	if $s'_1 < 0$ stable $\forall u$ if $s'_1 > 0$ stable if $u < V_{crit}$
$s_1 > 0$ oversteered towing vehicle	if $s'_1 < 0$ stable $\forall u$ if $s'_1 > 0$ stable if $u < V_{crit}$	$s'_1 > 0 \rightarrow \text{stable if } u < V_{crit}$ $s_2 = s_1 + h_1 > 0$

Table 3.1: Stability as function of  $s_1$  and  $h_1$

The trailer has no effect on the stability of the towing vehicle when the trailer mass is carried entirely by the trailer axle ( $a_2 = l_2$ ,  $b_2 = 0$ ). In this case  $s'_1 = s_1$ . This is for instance for a truck-centre axle trailer, where the centre of gravity of the trailer is located near the trailer wheels. In this case equations (3.22) for a single vehicle and vehicle with one articulation are equal and stability is determined by the towing vehicle; the centre axle trailer has no effect on monotonic stability of a truck-centre axle trailer combination. There is only little load transfer between these units; the mass coupling is little.

The effect of the trailer on stability increases as  $b_2$  gets larger. This is for instance for a tractor-semitrailer, where the centre of gravity of the trailer is between the hitch point and trailer axle.

For stability, this means that  $m_2 \frac{b_2}{l_2} s_2$  gets larger in (3.22). Assuming an initially understeered towing vehicle ( $s_1 < 0$ ), the vehicle combination becomes oversteered when  $m_2 \frac{b_2}{l_2} s_2 > -s_1 m_1$ . The combination then becomes unstable when the speed exceeds the critical speed. This means that mass of the trailer supported by the towing vehicle in the coupling point effects stability; there is a strong mass coupling. Therefore, it can be concluded that a tractor-semitrailer with an initially stable towing vehicle becomes unstable (in the sense of the saddle-node bifurcation) when the mass of the trailer supported by the towing vehicle in the coupling point becomes too large. This bifurcation was also found by Pacejka as reported in the literature review (section 2.2, page 7).

### Numerical case study

This case study illustrates a numerical example of the saddle-node bifurcation for a tractor-semitrailer. The following parameters are used, see also appendix B:

Variable	Unit	Value
$m_1$	kg	7449
$m_2$	kg	32551
$a_1$	m	1.1062
$a_2$	m	4.98
$l_1$	m	3.6
$l_2$	m	8.13
$e_1$	m	-0.68

Table 3.2: Parameters of a tractor-semitrailer

The cornering stiffnesses are calculated as function of vertical load for the reference vehicle. Once the cornering stiffnesses are obtained, they do not scale with the vertical axle loads. Normalised cornering stiffnesses are thus not applied. For the calculation of the cornering stiffnesses  $f = f_1 = f_2 = f_3 = 5.73$  [1/rad].

Two parameters are varied separately in figure 3.10. Figure 3.10a illustrates a variation of the trailer mass,  $m_2$ . Figure 3.10b shows the effect of changing the location of the centre of gravity,  $\frac{a_2}{l_2}$ . From figure 3.10a it turns out that the critical speed is infinite when  $m_2 \approx 32$  tonnes. The reference vehicle has an infinity critical speed since it is neutrally steered ( $f_1 = f_2$ ). A trailer mass of 47 tonnes is required for a critical speed of 30 m/s. Figure 3.10b shows that  $\frac{a_2}{l_2} = 0.61$  [-] results in an infinite critical speed when the reference trailer mass listed in table 3.2 is used. The total mass should be located closer to the hitch point,  $\frac{a_2}{l_2} = 0.44$ , for the critical speed to be 30 m/s.

These numerical examples show the required trailer mass for the vehicle combination to become monotonically unstable at 30 m/s is not physical. Moreover, the examples used in this case study are not very likely to occur in reality, as the cornering stiffness scales with vertical load in reality. This effect is investigated in the next section.

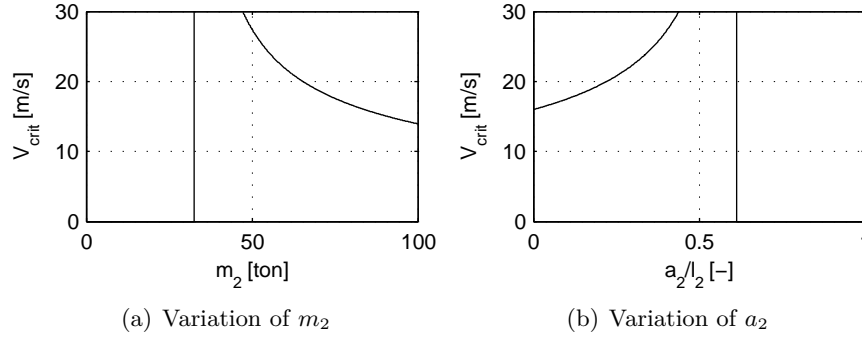


Figure 3.10: Numerical saddle-node bifurcation example for a tractor-semitrailer

Finally, it is very important to notice that the analysis presented in this section only account for the fourth critical speed and thus for the saddle-node bifurcation, assuming that all other coefficients of the characteristic equation are larger than zero. For the vehicle combination to be stable, all inequalities in (3.17) should be considered. They are studied in the next section.

### 3.2.3 Stability using the normalised cornering stiffness

It is interesting to study stability under normal driving conditions when normalised cornering stiffnesses can be assumed, as performed for single vehicles in section 3.1.2 (page 16) also. To simplify this stability problem, the tyres on all axles are assumed to have the same normalised cornering stiffness  $f = f_1 = f_2 = f_3$ . This assumption seems to be quite fair as explained by Houben, see figure 3.6 (section 3.1.2, page 18).

The cornering stiffness is a linear combination of the vertical load on the tyre according to (3.11):

$$\left. \begin{aligned} C_1 = fF_{z_1} &\Rightarrow F_{z_1} = m_1 g \frac{b_1}{l_1} - m_2 g \frac{b_2}{l_2} \frac{e_1}{l_1^*} \\ C_2 = fF_{z_2} &\Rightarrow F_{z_2} = m_1 g \frac{a_1}{l_1} + m_2 g \frac{b_2}{l_2} \frac{l_1^*}{l_1} \\ C_3 = fF_{z_3} &\Rightarrow F_{z_3} = m_2 g \frac{a_2}{l_2} \end{aligned} \right\}. \quad (3.23)$$

The cornering stiffnesses of an axle becomes zero when their is no road contact. Mathematically, this means that the cornering stiffnesses cannot become negative. For  $C_3$  this means that  $a_2 > 0$ . Table 3.3 lists the limits on the masses and dimensions for  $C_1$  and  $C_2$  for a tractor-semitrailer and truck-centre axle trailer.

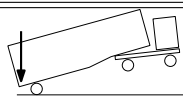
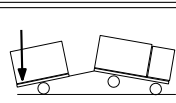
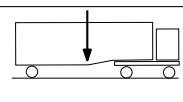
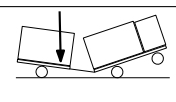
	$e_1 < 0$	Tractor-semitrailer	$e_1 > 0$	Truck centre-axle trailer
$b_2 < 0$		$C_1 : m_1 \frac{b_1}{e_1} < m_2 \frac{b_2}{l_2}$ $C_2 : -m_1 \frac{a_1}{l_1^*} < m_2 \frac{b_2}{l_2}$		$C_1 : \text{ok}$ $C_2 : -m_1 \frac{a_1}{l_1^*} < m_2 \frac{b_2}{l_2}$
$b_2 > 0$		$C_1 : \text{ok}$ $C_2 : \text{ok}$		$C_1 : m_1 \frac{b_1}{e_1} > m_2 \frac{b_2}{l_2}$ $C_2 : \text{ok}$

Table 3.3: Limits on masses and dimensions to avoid zero vertical axle forces

All critical speeds derived in (3.18) are investigated next. Distinction is made between the tractor-semitrailer and truck-centre axle trailer combinations. Some critical speeds determine the saddle-node and some determine the Hopf bifurcation. The effect of the individual critical speeds on the bifurcations is investigated after they are discussed individually.

In the next enumeration, the boundary for stability at any speed and stability when the speed is smaller than the critical speed is investigated for each coefficient of the characteristic equation individually. This boundary is reached when the denominator of the corresponding critical speed is zero. A negative denominator of the critical speed yields stability at any speed, a positive denominator of the critical speed yields stability when the speed is smaller than the critical speed.

#### Denominators for a tractor-semitrailer combination

Applying the denominators for a tractor-semitrailer yields:

$D_{c_2}$  : The denominator of  $V_{crit_2}$  can be rewritten to:

$$D_{c_2} = -m_1 C_3 l_2 I_1^* + m_2 C s_2 I_2^*, \quad (3.24)$$

with,

$$\left. \begin{aligned} I_1^* &= m_1 k_1^2 + m_2 \frac{b_2}{l_2} (k_1^2 + h_1^2) \\ I_2^* &= m_2 k_2^2 + m_1 \frac{s_1}{s_2} (k_2^2 + a_2^2) \\ &= m_2 k_2^2 - m_2 \frac{b_2}{l_2} (k_2^2 + a_2^2) \\ &= m_2 \frac{a_2^2}{l_2} (k_2^2 - a_2 b_2) \end{aligned} \right\}. \quad (3.25)$$

These terms do not equal the exact moments of inertias of the units independently due to the mass coupling between the units. Substituting  $f = f_1 = f_2 = f_3$  and (3.23) into (3.24) yields for stability at any speed:

$$\frac{I_1^*}{h_1} > \frac{I_2^*}{a_2}. \quad (3.26)$$

This criterion shows, that the moments of inertia of the units should be in relation to the distance between the centre of gravities of the units and the coupling point; a relatively light towing vehicle ( $I_1 = m_1 k_1^2$  is small) with heavy trailer ( $I_2 = m_2 k_2^2$  is large) may suffer from stability problems sooner than a vehicle combination of the same size with a heavy towing vehicle and light trailer. Decreasing the distance between the towing vehicles centre of gravity and the hitch point (reducing  $h_1$ ) reduces the risk of instability, as well as increasing the distance between the coupling point and the centre of gravity of the trailer (increasing  $a_2$ ).

Inequality (3.26) is fulfilled in any case if  $I_2^* < 0$ , or  $k_2^2 < a_2 b_2$ , since  $I_1^* > 0$ ,  $h_1 > 0$  and  $a_2 > 0$  in practise. For a tractor-semitrailer, the centre of gravity of the trailer is always between the hitch point and trailer axle,  $0 < a_2 < l_2$ . A homogenous mass distribution between these points ( $a_2 = b_2 = \frac{1}{2} l_2$ ) results in:

$$k_2^2 = \frac{1}{12} l_2^2 < \frac{1}{2} l_2 \frac{1}{2} l_2, \quad (3.27)$$

so  $I_2^* < 0$  and the combination is stable at any speed in the sense of this coefficient of the characteristic equation. Figure 3.11a shows some other mass distributions for which  $k_2^2 < a_2 b_2$  is fulfilled. The trailer mass is divided in two masses in the last two figures. The right mass  $m_{21}$  is a distance  $x_1$  from the centre of gravity, the left mass  $m_{22}$  is at distance  $x_2$ .

Figure 3.11b shows some examples of load distributions that may lead to  $k_2^2 > a_2b_2$ , such that  $I_2^* > 0$ . An example is one mass positioned on top of the hitch point and the other on top of the trailer axle, with both masses having large individual moments of inertia. Another option is that a great part of the total load is located at the rear or the front of the trailer, so in front of the hitch point or behind the trailer axle.

However, if  $k_2^2 > a_2b_2$ , inequality (3.26) can still be fulfilled. Moreover, the sketched mass distributions require very extreme parameters for a tractor-semitrailer combination. These mass distributions show more similarity with the lay-out of a truck-centre axle trailer combination. In practise, a tractor-semitrailer is expected not to experience this instability, which is illustrated with a numerical case study at the end of this section. Moving the masses towards each other enhances stability as  $k_2$  decreases. Furthermore, increasing  $a_2b_2$  enhances stability, which means moving the centre of gravity of the trailer halfway between the hitch point and the semitrailer axle.

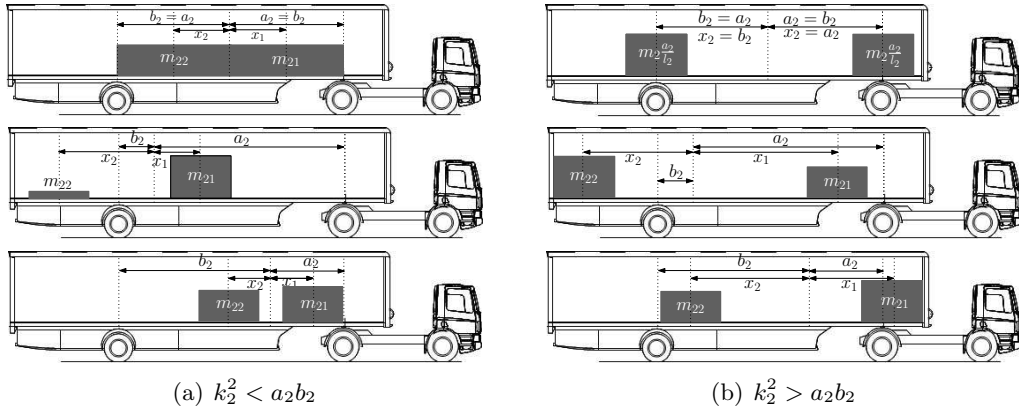


Figure 3.11: Cases where  $k_2^2 < a_2b_2$  is and is not fulfilled for a tractor-semitrailer

$D_{c3}$  : The denominator of the third critical speed is given by:

$$D_{c3} = -m_1(q_1^2 + k_1^2 - s_1l_2) - m_2\frac{b_2}{l_2}q_2^2 + m_2\frac{s_2}{l_2}(b_2^2 + k_2^2). \quad (3.28)$$

To simplify this problem for a tractor-semitrailer combination, it is assumed that the coupling plate is located on top of the rear axle of the towing vehicle,  $e_1 = 0$  (in reality it is located 0.68 m in front of the rear axle, which is fairly small in relation to the wheelbase of 3.6 m). This results in the following criterion for stability at any speed:

$$I_1^* + m_1a_1b_1 > -m_2\frac{b_2}{l_2}b_1l_1 - b_1m_2\frac{1}{l_2}(a_2b_2 - k_2^2). \quad (3.29)$$

This criterion is fulfilled in any case if  $k_2^2 < a_2b_2$ , which has already been discussed before for  $D_{c2}$ .

$D_{c4}$  : The denominator of the fourth critical speed is given by:

$$D_{c4} = m_2\frac{b_2}{l_2}s_2 + m_1s_1. \quad (3.30)$$

The combination is stable at any speed in the sense of this coefficient of the characteristic equation, when the denominator is smaller than zero. Assuming an initially understeered towing vehicle ( $f_1 - f_2 < 0$ , as concluded for stability of the towing vehicle in equation (3.13), section 3.1.2, page 18) yields for the stability of a tractor-semitrailer combination with the hitch point in front of the rear axle ( $e_1 < 0$ ):

$$\left. \begin{aligned} m_2 \frac{b_2}{l_2} &> m_1 \frac{b_1}{e_1} \\ m_2 \frac{b_2}{l_2} &> -m_1 \frac{a}{l_1^*} \end{aligned} \right\}, \quad (3.31)$$

which means that the wheels may not be lifted of the ground, as illustrated in table 3.3. These extreme cases do not occur in reality due to physical boundaries and legal axle loads. Therefore,  $D_{c_4}$  is negative for any speed when the cornering stiffness scales linearly with vertical load, even for  $f_1 \neq f_2 \neq f_3$ ,  $b_2 \neq 0$  and  $e_1 \neq 0$ .

### Denominators for a truck-centre axle trailer combination

Applying the denominators for a truck-centre axle trailer yields:

$D_{c_2}$  : In contrast to a tractor-semitrailer combination, the second denominator can become zero for a truck-centre axle trailer. The centre of gravity of the centre axle trailer is located near the trailer axle. As a result, there is no load transfer between the units when assuming  $b_2 \approx 0$  and thus  $a_2 \approx l_2$ . In this case, the inertias  $I_1^*$  and  $I_2^*$  reduce to  $I_1$  and  $I_2$ , which means that the inertia term of the trailer,  $I_2$ , cannot become negative anymore which is in contrast to the tractor-semitrailer evaluation. Criterion (3.26) reduces for a truck-centre axle trailer to:

$$\left. \begin{aligned} \frac{I_1}{h_1} &> \frac{I_2}{l_2} \\ \frac{m_1 k_1^2}{h_1} &> \frac{m_2 k_2^2}{l_2} \end{aligned} \right\}. \quad (3.32)$$

Assuming the same mass distribution in the loading space of the towing vehicle and trailer,  $k_1 \approx k_2$ , and assuming  $h_1 \approx l_2$  shows that the mass of the towing vehicle should be larger than the mass of the trailer. A fully laden trailer with empty truck will become unstable if the speed exceeds the critical speed. This will be illustrated with a numerical case study at the end of this section. Moreover, this criterion shows that placing the coupling point more towards the centre of gravity of the towing vehicle (decreasing  $h_1$ ) and making the drawbar longer (increasing  $l_2$ ) enhances stability of a truck-centre axle trailer.

$D_{c_3}$  : The denominator of the third critical speed is given by:

$$D_{c_3} = -m_1(q_1^2 + k_1^2 - s_1 l_2) - m_2 \frac{b_2}{l_2} q_2^2 + m_2 \frac{s_2}{l_2} (b_2^2 + k_2^2). \quad (3.33)$$

The problem is simplified for a truck-centre axle trailer by assuming  $b_2 \approx 0$ ,  $a_2 \approx l_2$ ,  $e_1 \neq 0$  in accordance with the simplification performed for  $D_{c_2}$ . This results in the following criterion of stability at any speed:

$$\frac{m_1(k_1^2 + a_1 b_1)}{h_1} > \frac{m_2 k_2^2}{l_2}, \quad (3.34)$$

which is less strict than (3.32) as  $a_1 > 0$  and  $b_1 > 0$ .



$D_{c_4}$  : The denominator of the fourth critical speed is given by:

$$D_{c_4} = m_2 \frac{b_2}{l_2} s_2 + m_1 s_1. \quad (3.35)$$

Assuming an initially understeered towing vehicle ( $f_1 - f_2 < 0$ ), the following yields for the stability of a truck-centre axle trailer with an positive coupling rear overhang ( $e_1 > 0$ ):

$$-m_1 \frac{a_1}{l_1^*} < m_2 \frac{b_2}{l_2} < m_1 \frac{b_1}{e_1}, \quad (3.36)$$

which means that the wheels may not be lifted of the ground, as illustrated in table 3.3. Therefore,  $D_{c_4}$  is negative for any speed when the cornering stiffness scales linearly with vertical load, even for  $f_1 \neq f_2 \neq f_3$ ,  $b_2 \neq 0$  and  $e_1 \neq 0$ .

### Numerical case study

This case study shows the effect of parameter changes of a tractor-semitrailer and truck-centre axle trailer on the denominator of the second critical speed  $D_{c_2}$ . The following parameters are used, see also appendix B:

Variable	Unit	Tractor-semitrailer	Truck-centre axle trailer
$m_1$	kg	7449	15000
$m_2$	kg	32551	25000
$k_1$	m	1.8881	1.433
$k_2$	m	4.053	2.4104
$a_1$	m	1.1062	2.5
$a_2$	m	4.98	7
$l_1$	m	3.6	5
$l_2$	m	8.13	7
$e_1$	m	-0.68	0.5

Table 3.4: Parameters of a tractor-semitrailer and a truck-centre axle trailer

The cornering stiffnesses are calculated as function of vertical load, with  $f = f_1 = f_2 = f_3 = 5.73$  [1/rad].

Figure 3.12a shows the effect of changing the location of the centre of gravity on (3.26) for a tractor-semitrailer. All other parameters are kept the same. The solid line represents the variation of  $\frac{I_1^*}{h_1}$  as function of  $a_2$ , the dashed line represents the variation of  $\frac{I_2^*}{a_2}$  as function of  $a_2$ . Equation 3.26 is not fulfilled when  $\frac{I_1^*}{h_1} < \frac{I_2^*}{a_2}$ , this is when  $\frac{a_2}{l_2} > 0.85$  [-]. This extreme parameter setting does not occur for a tractor-semitrailer with the parameters listed in table 3.4 as the legal axle loads must be obeyed.

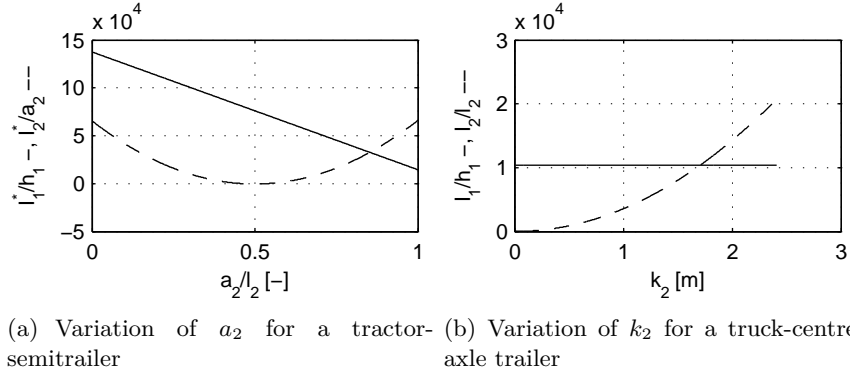


Figure 3.12: Numerical examples of inequalities (3.26) and (3.32)

Figure 3.12b shows the effect of changing the moment of inertia of the trailer,  $k_2$ , on inequality (3.32) for a truck-centre axle trailer. The solid line indicates that  $\frac{l_1}{h_1}$  does not vary as function of  $k_2$ , the dashed line shows the variation of  $\frac{l_2}{l_2}$  as function of  $k_2$ . Equation (3.32) is not fulfilled when  $\frac{l_1}{h_1} < \frac{l_2}{l_2}$ , this is for  $k_2 > 1.5$  m. Table 3.4 shows that the reference fully homogeneously laden trailer results in  $k_2 = 2.4$  m. This means that a truck-centre axle trailer may become unstable in the sense of the second critical speed when the speed exceeds the critical speed.

### Effect of the denominators on the saddle-node and Hopf bifurcations

The denominators of the critical speeds determine stability at any speed for the saddle-node and Hopf bifurcations. A saddle-node bifurcation occurs due to a parameter variation, when the last coefficient of the characteristic equation ( $c_4$ ) passes zero, assuming all other coefficients positive. It can be concluded that a vehicle with one articulation does not become divergently unstable when the towing vehicle alone is initially understeered ( $f_1 - f_2 < 0$ ); the denominator of the fourth critical speed is always smaller than zero for physical boundaries and when the cornering stiffness scales linearly with vertical load. Adding mass, relocating mass or changing other dimensions does not affect this monotonic stability. This conclusion holds for both the tractor-semitrailer and truck-centre axle trailer combination.

The evaluation of the Hopf bifurcation is more difficult, as the coefficients of the characteristic equation have to be multiplied:  $H_3 = c_1 c_2 c_3 - c_0 c_3^2 - c_4 c_1^2$ . From (3.17), (3.36) and (3.31) it follows that  $c_0 > 0$ ,  $c_1 > 0$  and  $c_4 > 0$ . Therefore, a Hopf bifurcation does not occur when all coefficients are initially positive and when due to a parameter variation the following inequality still holds:

$$c_2 c_3 > \frac{c_0 c_3^2 + c_4 c_1^2}{c_1}. \quad (3.37)$$

This inequality is not fulfilled when:

1.  $c_2 < 0$  and  $c_3 > 0$
2.  $c_2 > 0$  and  $c_3 < 0$
3.  $c_2 > 0$  and  $c_3 > 0$  but  $c_2 c_3 < \frac{c_0 c_3^2 + c_4 c_1^2}{c_1}$

$$4. \ c_2 < 0 \text{ and } c_3 < 0 \text{ but } c_2 c_3 < \frac{c_0 c_3^2 + c_4 c_1^2}{c_1}$$

In the first two cases either  $c_2$  or  $c_3$  is smaller than zero, while the right hand side of (3.37) is always larger than zero. Therefore, the denominators of the critical speeds of these two coefficients of the characteristic equation,  $D_{c_2}$  and  $D_{c_3}$ , determine stability at any speed partly for the Hopf bifurcation. From the evaluation of the denominators and the numerical case study, it turns out that a tractor-semitrailer has a relatively small inertia coupling; the inertia of the trailer can make the vehicle combination unstable in only very extreme cases. This in contrast to a truck-centre axle trailer combination.

It can be concluded that the vehicle combination becomes unstable in an oscillatory manner if the yaw moments of inertia are relatively large in relation to the dimensions of the combinations; a small towing vehicle with heavy trailer will suffer stability problems sooner than a large towing vehicle with small trailer. It was concluded in the previous overview, that this occurs sooner for a truck-centre axle trailer combination than for a tractor-semitrailer. The critical speeds derived for  $c_2$  and  $c_3$  in (3.18) apply.

However, (3.37) can also change sign when both  $c_2$  and  $c_3$  are positive or negative. This bifurcation is studied for a truck-centre axle trailer combination. The following simplifications are applied for the truck-centre axle trailer model:

- The centre of gravity of the trailer is on the trailer axle:  $a_2 = l_2$  and  $b_2 = 0$ .
- The hitch point is located at the rear axle:  $e_1 = 0$ .
- The normalised cornering stiffnesses of all tyres are the same:  $f = f_1 = f_2 = f_3$ .

With these simplifications, the coefficients of the characteristic equation reduce to:

$$\left. \begin{aligned} c_0 &= u [m_1 k_1^2 (k_2^2 + l_2^2) + m_2 k_2^2 (k_1^2 + b_1^2)] \\ c_1 &= f [m_1 \{(k_1^2 + a_1 b_1)(k_2^2 + l_2^2) + l_2^2 k_1^2\} + m_2 k_2^2 (b_1^2 + k_1^2 + b_1 l_1)] \\ c_2 &= \frac{f}{u} [u^2 \{-m_2 k_2^2 b_1 + l_2 m_1 k_1^2\} + f \{m_2 k_2^2 b_1 l_1 + m_1 (a_1 b_1 (k_2^2 + l_2^2) + l_2^2 (a_1 b_1 + k_1^2))\}] \\ c_3 &= \frac{f^2}{u^2} [u^2 \{-m_2 k_2^2 b_1 + l_2 m_1 (k_1^2 + a_1 b_1)\} + f a_1 b_1 m_1 l_2^2] \\ c_4 &= \frac{1}{u} l_2 m_1 f^3 a_1 b_1 \end{aligned} \right\}. \quad (3.38)$$

The stability of a vehicle combination can change due to parameter variations. Figure 3.13 shows the critical Hopf bifurcation speed as function of a parameter variation. The parameter to be varied is indicated with  $x$ , but it can be any parameter such as vehicle mass, length or any other dimension. Three areas are distinguished; (1) stability at any speed, (2) stability when the speed is smaller than the critical speed, and (3) instability when the speed is larger than the critical speed. The dotted line divides the graph in two parts; stability at any speed and stability as function of the vehicle speed. It is assumed, that the critical speed is infinite at the intersection of these areas;  $V_{crit, H_3} = \infty \Rightarrow H_3 = 0$ . This was also concluded for the coefficients of the characteristic equation in (3.17) and for a single vehicle saddle-node bifurcation in (3.10). The intersection of these two regions is investigated, such that stability at any speed can be analysed. This means that the parameter value of  $x$  at the dotted line is calculated.

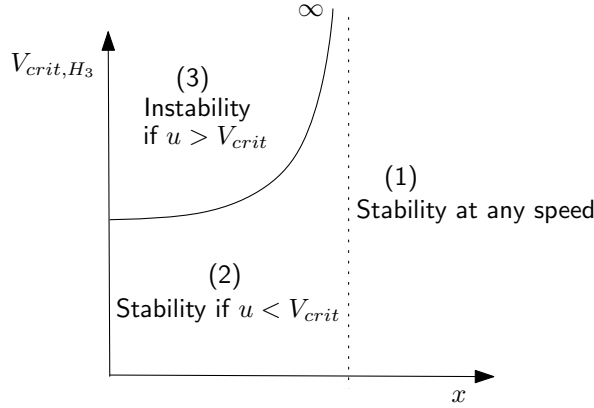


Figure 3.13: Stability and instability areas

When the speed is infinite, the coefficients approach to:

$$\left. \begin{aligned} c_0 &\rightarrow uc_{0_r} \\ c_1 &\rightarrow fc_{1_r} \\ c_2 &\rightarrow fuc_{2_r} \\ c_3 &\rightarrow f^2c_{3_r} \\ c_4 &\rightarrow 0 \end{aligned} \right\}, \quad (3.39)$$

with  $c_{i_r}$  reduced coefficients:

$$\left. \begin{aligned} c_{0_r} &= m_1k_1^2(k_2^2 + l_2^2) + m_2k_2^2(k_1^2 + b_1^2) \\ c_{1_r} &= m_1\{(k_1^2 + a_1b_1)(k_2^2 + l_2^2) + l_2^2k_1^2\} + m_2k_2^2(b_1^2 + k_1^2 + b_1l_1) \\ c_{2_r} &= -m_2k_2^2b_1 + l_2m_1k_1^2 \\ c_{3_r} &= -m_2k_2^2b_1 + l_2m_1(k_1^2 + a_1b_1) \end{aligned} \right\}. \quad (3.40)$$

As explained, it is assumed that the Hurwitz determinant is zero at the limit when speed goes to infinity. Filling in (3.39) for Hurwitz determinant ( $H_3 = c_1c_2c_3 - c_0c_3^2 - c_4c_1^2$ ) yields:

$$\begin{aligned} \lim_{u \rightarrow \infty} H_3 &= fc_{1_r}fuc_{2_r}f^2c_{3_r} - uc_{0_r}f^4c_{3_r}^2 - c_4f^2c_{1_r}^2 \\ &= f^4u(c_{1_r}c_{2_r}c_{3_r} - c_{0_r}c_{3_r}^2) \\ &= f^4uc_{3_r}(c_{1_r}c_{2_r} - c_{0_r}c_{3_r}) \\ &= 0 \end{aligned} \quad (3.41)$$

From (3.41) it follows that the intersection of the two areas in figure 3.13 can be reached in three ways; (1)  $f = 0$ , (2)  $c_{3_r} = 0$  and (3)  $c_{1_r}c_{2_r} - c_{0_r}c_{3_r} = 0$ . The first option means that the cornering stiffnesses on all axes are zero, which does not occur in practise. The second option was discussed for the denominator of  $c_3$  also. In this case the inertias should be in proportion the size of the units:  $\frac{m_2k_2^2}{l_2} = \frac{m_1(k_1^2 + a_1b_1)}{b_1}$ .

For the third option  $c_{1_r}c_{2_r} = c_{0_r}c_{3_r}$  should hold. Rewriting yields:

$$\begin{aligned} m_1a_1b_1I_2\{l_2(b_1^2 + k_1^2) + b_1(k_2^2 + l_2^2)\} &= (I_1l_2^2 + I_2b_1l_1)(I_1l_2 - I_2b_1) \\ I_1l_2 - I_2b_1 &= \frac{m_1a_1b_1I_2\{l_2(b_1^2 + k_1^2) + b_1(k_2^2 + l_2^2)\}}{(I_1l_2^2 + I_2b_1l_1)}. \end{aligned} \quad (3.42)$$

This evaluation reveals that the vehicle combination reaches the point where the Hopf bifurcation occurs sooner, than the point where the second denominator passes zero ( $I_1 l_2 = I_2 b_1$ ) and  $V_{crit, c_2}$  becomes relevant. However, if  $D_{c_2} < 0$  the combination is always unstable with an oscillatory behaviour.

Finally, it can be concluded that a Hopf bifurcation does not occur at any speed when:

$$\left. \begin{aligned} \frac{m_1(k_1^2 + a_1 b_1)}{b_1} &> \frac{m_2 k_2^2}{l_2} \\ I_1 l_2 - I_2 b_1 &> \frac{m_1 a_1 b_1 I_2 \{l_2(b_1^2 + k_1^2) + b_1(k_2^2 + l_2^2)\}}{(I_1 l_2^2 + I_2 b_1 l_1)} \end{aligned} \right\}. \quad (3.43)$$

In theory, there is also a small area for stability at any speed when both  $c_2$  and  $c_3$  are negative. However, this area corresponds to non physical parameter ranges.

### Numerical case study

This case study shows the effect of changing the moment of inertia of the trailer,  $k_2$ , on the Hopf bifurcation of a truck-centre axle trailer. The reference truck-centre axle trailer has the following parameters (see appendix B):

Variable	Unit	Value tractor-semitrailer
$m_1$	kg	15000
$m_2$	kg	25000
$k_1$	m	1.433
$k_2$	m	2.4104
$a_1$	m	2.5
$a_2$	m	7
$l_1$	m	5
$l_2$	m	7
$e_1$	m	0.5

Table 3.5: Parameters of a truck-centre axle trailer

The cornering stiffnesses are calculated as function of vertical load, with  $f = f_1 = f_2 = f_3 = 5.73$  [1/rad].

Figure 3.14 shows the critical Hopf bifurcation speed as function of  $k_2$ . The towing vehicle is loaded as listed in table 3.5 in figure 3.14a. The towing vehicle is empty ( $m_1 = 7000$  kg) in figure 3.14b. These figures show that the truck-centre axle trailer can experience a Hopf bifurcation when the moment of inertia of the trailer and the vehicle speed are large. Furthermore, the critical speed decreases when the mass of the towing vehicle decreases.

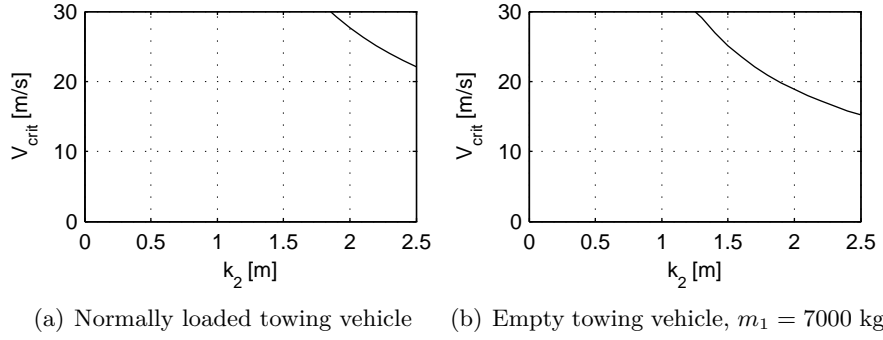


Figure 3.14: Effect of the moment of inertia of the trailer on the critical speed which determines the Hopf bifurcation for truck-centre axle trailer

From the analysis presented in this chapter, it turns out that in practise many vehicles with one articulation are stable. The analysis in this section helps in understanding the stability boundaries. However, a clear distinction between the combinations cannot be made, as they are practically all stable. A similar conclusion was drawn for single vehicles. It is investigated in the next section whether this conclusion also holds for conventional vehicles with two articulations.

### 3.3 Stability of vehicles with two articulations

A truck-full trailer is the only conventional truck combination with two articulations, see figure 3.15. The steering dolly has an articulation angle with respect to the towing vehicle, and the trailer chassis makes an additional articulation angle with respect to the steering dolly.

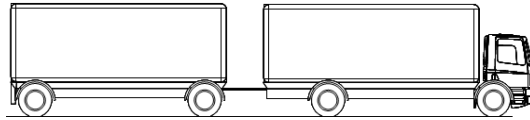


Figure 3.15: Truck-full trailer; conventional vehicle with two articulations

The stability boundaries are analysed by evaluating the characteristic equation derived from the equations of motion. Figure 3.16 shows the free body diagram. The equations of motion of this vehicle system are derived in appendix A. The following abbreviations are used, in accordance with (3.7) and (3.16):

$$\left. \begin{aligned} C_t &= C_3 + C_4 \\ C_t s_3 &= C_3 a_3 - C_4 b_3 \\ C_t q_3^2 &= C_3 a_3^2 + C_4 b_3^2 \\ l_2^* &= l_2 + e_2 \end{aligned} \right\} \quad (3.44)$$

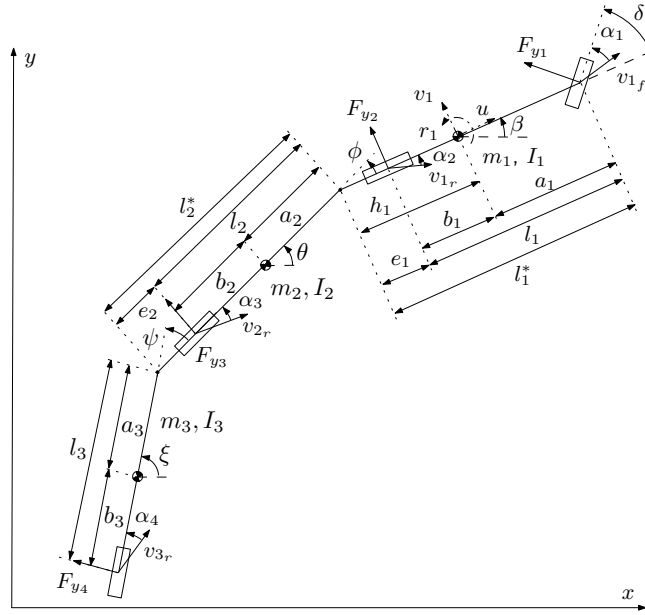


Figure 3.16: Free body diagram vehicle with two articulations

The equations of motion read:

$$\left. \begin{aligned}
 & \{m_1 + m_2 + m_3\} (\dot{v}_1 + ur_1) - \{m_2(h_1 + a_2) + m_3(h_1 + l_2^* + a_3)\} \dot{r}_1 \\
 & - \{m_2 a_2 + m_3(l_2^* + a_3)\} \ddot{\phi} - m_3 a_3 \ddot{\psi} = \\
 & -\frac{1}{u} [\{C + C_t\} v_1 + \{C s_1 - C_3(h_1 + l_2) - C_4(h_1 + l_2^* + l_3)\} r_1 \\
 & - \{C_3 l_2 + C_4(l_2^* + l_3)\} \dot{\phi} - C_4 l_3 \dot{\psi} - C_t u \phi - C_4 u \psi] + C_1 \delta_1 \\
 & - h \{m_2 + m_3\} (\dot{v}_1 + ur_1) + \{I_1 + m_2 h_1(h_1 + a_2) + m_3 h_1(h_1 + l_2^* + a_3)\} \dot{r}_1 \\
 & + \{m_2 h_1 a_2 + m_3 h_1(l_2^* + a_3)\} \ddot{\phi} + m_3 h_1 a_3 \ddot{\psi} = \\
 & -\frac{1}{u} [\{C s_1 - C_t h_1\} v_1 + \{C q_1^2 + C_3 h_1(h_1 + l_2) + C_4 h_1(h_1 + l_2^* + l_3)\} r_1 \\
 & + \{C_3 h_1 l_2 + C_4 h_1(l_2^* + l_3)\} \dot{\phi} + C_4 h_1 l_3 \dot{\psi} + C_t h_1 u \phi + C_4 h_1 u \psi] + C_1 a_1 \delta_1 \\
 & - \{m_2 a_2 + m_3 l_2^*\} (\dot{v}_1 + ur_1) + \{I_2 + m_2 a_2(h_1 + a_2) + m_3 l_2^*(h_1 + l_2^* + a_3)\} \dot{r}_1 \\
 & + \{I_2 + m_2 a_2^2 + m_3 l_2^*(l_2^* + a_3)\} \ddot{\phi} + m_3 a_3 l_2^* \ddot{\psi} = \\
 & -\frac{1}{u} [-\{C_3 l_2 + C_4 l_2^*\} v_1 + \{C_3 l_2(h_1 + l_2) + C_4 l_2^*(h_1 + l_2^* + l_3)\} r_1 \\
 & + \{C_3 l_2^2 + C_4 l_2^*(l_2^* + l_3)\} \dot{\phi} + C_4 l_3 l_2^* \dot{\psi} + \{C_3 l_2 + C_4 l_2^*\} u \phi + C_4 l_2^* u \psi] \\
 & - m_3 a_3 (\dot{v}_1 + ur_1) + \{I_3 + m_3 a_3(h_1 + l_2^* + a_3)\} \dot{r}_1 + \{I_3 + m_3 a_3(l_2^* + a_3)\} \ddot{\phi} \\
 & + \{I_3 + m_3 a_3^2\} \ddot{\psi} = -\frac{1}{u} [-C_4 l_3 v_1 + C_4 l_3 \{h_1 + l_2^* + l_3\} r_1 \\
 & + C_4 l_3 \{l_2^* + l_3\} \dot{\phi} + C_4 l_3^2 \dot{\psi} + C_4 l_3 u \phi + C_4 l_3 u \psi]
 \end{aligned} \right\}. \quad (3.45)$$

These equations apply for all vehicles with two articulations. Simplifications can be made for a truck-full trailer combination, by assuming the dolly mass and inertia to be small in relation to the trailer mass ( $m_2 \approx 0$ ,  $I_2 \approx 0$ ,  $a_2 \approx l_2$ ,  $b_2 \approx 0$ ) and by assuming no mechanical trail at the

front axle of the trailer ( $e_2 \approx 0$ ,  $l_2^* \approx l_2$ ). The equations reduce to:

$$\left. \begin{aligned} m_1 a_{y_1} &= F_{y_1} + F_{y_2} \\ I_1 \ddot{\beta} &= a_1 F_{y_1} - b_1 F_{y_2} \\ m_3 a_{y_3} &= F_{y_3} + F_{y_4} \\ I_3 \ddot{\xi} &= a_3 F_{y_3} - b_3 F_{y_4} \end{aligned} \right\}, \quad (3.46)$$

with  $a_{y_1}$  and  $a_{y_3}$  the lateral accelerations at the centre of gravities of the towing vehicle and full trailer respectively, which are expressed as:

$$\left. \begin{aligned} a_{y_1} &= \dot{v}_1 + ur_1 \\ a_{y_3} &= \dot{v}_3 + ur_3 \end{aligned} \right\}. \quad (3.47)$$

The lateral velocity at the centre of gravity of the full trailer,  $v_3$ , and yaw velocity of the full trailer,  $r_3 = \dot{\xi}$ , can be expressed as a function of the lateral velocity at the centre of gravity of the towing vehicle,  $v_1$ , the towing vehicle yaw velocity,  $r_1 = \dot{\beta}$ , and the articulation angles with  $\rho = \phi + \psi$  the total articulation angle:

$$\left. \begin{aligned} v_3 &= v_1 - h_1 r_1 - l_2 \dot{\theta} - a_3 \dot{\xi} - u\rho \\ r_3 &= \dot{\xi} \\ &= \dot{\beta} + \dot{\phi} + \dot{\psi} \\ &= r_1 + \dot{\rho} \end{aligned} \right\}. \quad (3.48)$$

This yields for the lateral acceleration of the trailer:

$$\begin{aligned} a_{y_3} &= \dot{v}_3 + ur_3 \\ &= \dot{v}_1 - h_1 \dot{r}_1 - l_2 \ddot{\theta} - a_3 \ddot{\xi} - u\dot{\rho} + ur_3 \\ &= \dot{v}_1 - h_1 \dot{r}_1 - l_2 \ddot{\theta} - a_3 \ddot{\xi} - ur_1. \end{aligned} \quad (3.49)$$

Equation (3.46) show that in this case the combination behaves like a linked pair of two single vehicles. This was also found in literature by Ellis [10] and Fancher et al. [13] (see section 2.3, page 8).

The lateral acceleration and tyre forces of the trailer are expressed in the coordinates of the towing vehicle. The state-space description reads:

$$\begin{bmatrix} m_1 & 0 & 0 & 0 & 0 & 0 \\ 0 & I_1 & 0 & 0 & 0 & 0 \\ m_3 & -m_3(h_1 + l_2 + a_3) & -m_3(l_2 + a_3) & -m_3 a_3 & 0 & 0 \\ 0 & I_3 & I_3 & I_3 & 0 & 0 \\ 0 & 0 & 0 & 0 & 1 & 0 \\ 0 & 0 & 0 & 0 & 0 & 1 \end{bmatrix} \begin{bmatrix} \dot{v}_1 \\ \dot{r}_1 \\ \ddot{\phi} \\ \ddot{\psi} \\ \dot{\phi} \\ \dot{\psi} \end{bmatrix} = \begin{bmatrix} C_1 \\ a_1 C_1 \\ 0 \\ 0 \\ 0 \\ 0 \end{bmatrix} \delta_1 - \frac{1}{u} \begin{bmatrix} C \\ C s_1 + m_1 u^2 \\ C q_1^2 \\ -C_t(h_1 + l_2) - C_4 l_3 + m_3 u^2 \\ -C_t s_3(h_1 + l_2) + C_4 l_3 b_3 \\ 0 \\ 0 \end{bmatrix} \begin{bmatrix} v_1 \\ r_1 \\ \dot{\phi} \\ \dot{\psi} \\ \phi \\ \psi \end{bmatrix}, \quad (3.50)$$



with state vector  $(v_1, r_1, \dot{\phi}, \dot{\psi}, \phi, \psi)$ , with  $v_1$  the lateral velocity at the centre of gravity of the towing vehicle,  $r_1$  the yaw velocity of the towing vehicle,  $\phi$  the relative articulation angle between the first articulation and the towing vehicle, and  $\psi$  the relative articulation angle between the second and first articulation.

The first two rows in the state-space description account for the towing vehicle, and match the equations derived in (3.6). This is in contrast to vehicles with one articulation. In the previous section, it was concluded that a truck-centre axle trailer has a strong inertia coupling, but a relative small mass coupling. For a tractor-semitrailer the opposite is true. Due to the massless steering dolly in a truck-full trailer combination, the coupling is no longer dynamic, but only kinematic in nature; the trailer does not affect the dynamics of the towing vehicle, but the steering wheel angle of the steering dolly is a function of the location and orientation of the trailer with respect to the towing vehicle and the states of the trailer are expressed in the states of the towing vehicle. There is no load transfer between the units due to the kinematic coupling, which means that the truck-full trailer can be modelled as two kinematically coupled single vehicles.

From the equations of motion it follows that an unstable towing vehicle in a truck-full trailer combination cannot be stabilised by the trailer, which means that the combination is at least unstable if  $s_1 > 0$  and  $u > V_{crit}$ . Furthermore, it is expected that this truck combination cannot experience a Hopf bifurcation. This is, since it was concluded in section 3.1 (page 14) that the towing vehicle alone does not become unstable with an oscillatory motion, which cannot be affected by the trailer. In a similar way, the full trailer alone cannot experience a Hopf bifurcation, as it can be considered as a second single vehicle. Nevertheless, to make the stability analysis in this chapter complete, these hypotheses are checked by applying the Hurwitz criterion.

The characteristic equation reads:

$$c_0\lambda^6 + c_1\lambda^5 + c_2\lambda^4 + c_3\lambda^3 + c_4\lambda^2 + c_5\lambda + c_6 = 0, \quad (3.51)$$

with,

$$\left. \begin{aligned} c_0 &= m_3^2 k_3^2 l_2 u^2 m_1^2 k_1^2 \\ c_1 &= u m_3 l_2 m_1 \{ k_1^2 k_3^2 (C m_3 + C_t m_1) + m_1 k_1^2 C_t q_3^2 + m_3 k_3^2 C q_1^2 \} \\ c_2 &= u^2 \{ m_1 k_1^2 (C_3 (a_3^2 + k_3^2) + C_4 b_3 l_2) - m_3 k_3^2 C s_1 l_2 \} + \\ &\quad l_2 \left\{ C C_t (k_1^2 + q_1^2) (k_3^2 + q_3^2) + \frac{1}{m_1} C^2 (q_1^2 - s_1^2) m_3 k_3^2 + \frac{1}{m_3} C_t^2 (q_3^2 - s_3^2) m_1 k_1^2 \right\} \\ c_3 &= m_1 u^2 \{ m_3 C C_3 (q_1^2 + k_1^2) (a_3^2 + k_3^2) - m_3 l_2 s_1 C C_t (q_3^2 + k_3^2) + m_1 k_1^2 C_4 C_3 a_3 (l_2 + l_3) \\ &\quad + C_4 b_3 C l_2 m_3 (k_1^2 + q_1^2) \} + C C_t l_2 \{ m_3 C (q_1^2 - s_1^2) (q_3^2 + k_3^2) \\ &\quad + m_1 C_t (q_3^2 - s_3^2) (q_1^2 + k_1^2) \} \\ c_4 &= A_{c_4} u^4 + B_{c_4} u^2 + C_{c_4} \\ c_5 &= -C_4 C_3 C l_3 \{ -u^2 m_1 (k_1^2 + q_1^2 - s_1 (l_2 + l_3)) + C (s_1^2 - q_1^2) (l_2 + l_3) \} \\ c_6 &= -C_4 C_3 C l_3 \{ C (s_1^2 - q_1^2) + s_1 u^2 m_1 \} \end{aligned} \right\},$$

with,

$$\left. \begin{aligned} A_{c_4} &= m_1 \{ -C s_1 m_3 [C_3 (k_3^2 + a_3^2) + C_4 b_3 l_2] + m_1 k_1^2 C_3 C_4 l_3 \} \\ B_{c_4} &= C^2 m_3 (q_1^2 - s_1^2) [C_3 (k_3^2 + a_3^2) + C_4 b_3 l_2] + C_t^2 m_1 C (q_3^2 - s_3^2) \left[ (q_1^2 + k_1^2) (1 + \frac{l_2}{l_3} - s_1 l_2) \right] \\ C_{c_4} &= C^2 C_t^2 l_2 (q_1^2 - s_1^2) (q_3^2 - s_3^2) \end{aligned} \right\}. \quad (3.52)$$

All vehicle parameters are considered to be positive for this combination, except the neutral steer

parameters  $s_1$  and  $s_3$ . Only forward driving is considered;  $u > 0$ . This yields for stability:

$$\left. \begin{aligned} c_0 > 0 & : \text{always fulfilled} \\ c_1 > 0 & : \text{always fulfilled} \\ c_i > 0 & : \begin{cases} s_1 < 0 & : \text{always fulfilled} \\ s_1 \geq 0 & : u < V_{crit, c_i} \end{cases} \\ & \text{(for } i = 2 \dots 6) \\ H_1 > 0 & : \text{always fulfilled} \\ H_3 > 0 & : c_1 c_2 c_3 - c_0 c_3^2 - c_4 c_1^2 > 0 \\ H_5 > 0 & : \begin{vmatrix} c_1 & c_0 & 0 & 0 & 0 \\ c_3 & c_2 & c_1 & c_0 & 0 \\ c_5 & c_4 & c_3 & c_2 & c_1 \\ 0 & c_6 & c_5 & c_4 & c_3 \\ 0 & 0 & 0 & c_6 & c_5 \end{vmatrix} > 0 \end{aligned} \right\}, \quad (3.53)$$

with,

$$\left. \begin{aligned} V_{crit, c_2} &= \sqrt{\frac{l_2 \left\{ CC_t(k_1^2 + q_1^2)(k_3^2 + q_3^2) + \frac{1}{m_1} C^2(q_1^2 - s_1^2)m_3 k_3^2 + \frac{1}{m_3} C_t^2(q_3^2 - s_3^2)m_1 k_1^2 \right\}}{-m_1 k_1^2 (C_3(a_3^2 + k_3^2) + C_4 b_3 l_2) + m_3 k_3^2 C s_1 l_2}} \\ V_{crit, c_3} &= \sqrt{\frac{CC_t l_2 \left\{ m_3 C(q_1^2 - s_1^2)(q_3^2 + k_3^2) + m_1 C_t(q_3^2 - s_3^2)(q_1^2 + k_1^2) \right\}}{-m_1 \left\{ m_3 C C_3(q_1^2 + k_1^2)(a_3^2 + k_3^2) - m_3 l_2 s_1 C C_t(q_3^2 + k_3^2) + m_1 k_1^2 C_4 C_3 a_3(l_2 + l_3) + C_4 b_3 C l_2 m_3(k_1^2 + q_1^2) \right\}}} \\ V_{crit, c_4} &= \sqrt{\frac{-B_{c_4} \pm \sqrt{B_{c_4}^2 - 4A_{c_4}C_{c_4}}}{2A_{c_4}}} \\ V_{crit, c_5} &= \sqrt{\frac{C(q_1^2 - s_1^2)(l_2 + l_3)}{-m_1(k_1^2 + q_1^2 - s_1(l_2 + l_3))}} \\ V_{crit, c_6} &= \sqrt{\frac{C(q_1^2 - s_1^2)}{s_1 m_1}} \end{aligned} \right\}. \quad (3.54)$$

As expected when evaluating the state-space description, the critical speed of the saddle-node bifurcation derived for a single vehicle in (3.10) also applies to a truck-full trailer. Therefore, it can be concluded that a truck-full trailer is stable in the sense of the saddle-node bifurcation when  $s_1 < 0$ . The conclusions when the normalised cornering stiffness is assumed as discussed in section 3.1.2 (page 16) thus apply for the truck-full trailer also. This means that the normalised cornering stiffness of the towing vehicles rear axle should be larger than the normalised cornering stiffness of the towing vehicles front axle ( $f_2 > f_1$ ) for stability at any speed; the towing vehicle should be understeered. When this is not the case, only the wheelbase of the towing vehicle and the nominal cornering stiffnesses can affect the critical speed. Relocating the centre of gravity of the towing vehicle, or changing any trailer parameter does not affect monotonic stability.

The fifth Hurwitz determinant should be calculated to evaluate the Hopf bifurcation. From (3.53) follows:

$$H_5 = -c_6 \begin{vmatrix} c_1 & c_0 & 0 & 0 \\ c_3 & c_2 & c_1 & 0 \\ c_5 & c_4 & c_3 & c_1 \\ 0 & c_6 & c_5 & c_3 \end{vmatrix} + c_5 \begin{vmatrix} c_1 & c_0 & 0 & 0 \\ c_3 & c_2 & c_1 & c_0 \\ c_5 & c_4 & c_3 & c_2 \\ 0 & c_6 & c_5 & c_4 \end{vmatrix}. \quad (3.55)$$

Like in the previous section on vehicles with one articulation, two regions are considered; (1) stability at any speed, and (2) stability if the speed is smaller than the critical speed. It is again assumed that the critical speed is infinite at the intersection of these two regions;  $V_{crit, H_5} = \infty \Rightarrow H_5 = 0$ . Normalised cornering stiffnesses are assumed, with  $f = f_1 = f_2 = f_3 = f_4$  (which

means that  $s_1 = s_3 = 0$ ), and all coefficient of the characteristic equation in (3.51) are divided by  $u^2$ . When the speeds approaches infinity,

$$\left. \begin{array}{l} c_5 \rightarrow 0 \\ c_6 \rightarrow 0 \end{array} \right\}. \quad (3.56)$$

Therefore, from (3.55) it then follows that:

$$\lim_{u \rightarrow \infty} H_5 = 0. \quad (3.57)$$

This confirms that a truck-full trailer combination does not experience a Hopf bifurcation when normalised cornering stiffnesses on all axles are the same and when the initial vehicle is stable, as the expression in (3.57) is no function of any vehicle parameter, and since the bifurcation occurs at an infinity vehicle speed.

Further analysis is not performed as it can be concluded that under normal driving conditions when the normalised cornering stiffness can be assumed, a truck-full trailer combination with an initially stable towing vehicle remains stable when changing the masses and dimensions of either the truck or trailer. In accordance with the conclusions of the other vehicles discussed, stability may not be the right criterion to study dynamic vehicle behaviour of a truck-full trailer combination either. The case  $m_2 \neq 0$  and  $I_2 \neq 0$  (which should be applied for some Ecocombi combinations) has not been studied.

### 3.4 Concluding remarks

In this chapter, the stability of single vehicles and conventional vehicles with one and two articulations is studied. The following conclusions can be drawn in general:

- Most vehicle combinations hardly become unstable in yaw for physical parameter settings when the cornering stiffness scales linearly with vertical load.
- All vehicle combinations are unstable when the towing vehicle in the combination (so including the load of the trailer carried by the towing vehicle) is oversteered and when the speed exceeds the critical speed.
- The normalised cornering stiffness can be assumed up to relatively high axle loads, which means that the axle cornering stiffness scales linearly with vertical load.

Furthermore, the following conclusions can be drawn for the individual vehicle combinations:

**Single vehicle:** A single vehicle does not become unstable in an oscillatory way. A saddle-node bifurcation only occurs when the vehicle is oversteered and when the speed exceeds the critical speed.

**Tractor-semitrailer:** A tractor-semitrailer experiences a saddle-node bifurcation when the tractor in the combination is oversteered and the speed exceeds the critical speed. Oversteer occurs when the tractor individually is oversteered initially and the normalised cornering stiffness can be assumed, or when the tractor individually is understeered initially but the

cornering stiffnesses do not scale linearly with vertical load. In the latter case, the portion of the mass of the trailer supported by the towing vehicle in the coupling point becomes too large; the tractor-semitrailer has a strong mass coupling. However, this vehicle combination is stable for all speeds when the towing vehicle without trailer is understeered initially and the cornering stiffness scales linearly with vertical load. A Hopf bifurcation does not occur for a tractor-semitrailer combination when the normalised cornering stiffness is assumed and when applying physical parameter settings.

**Truck-centre axle trailer:** The truck-centre axle trailer has a strong inertia coupling. In contrast to the tractor-semitrailer, the mass coupling is almost zero as the centre of gravity of a centre axle trailer is often nearly located on top of the trailer axle. Therefore, a saddle-node bifurcation does not occur for a truck-centre axle trailer when the towing vehicle is stable, also when the normalised cornering stiffness cannot be assumed. The inertia coupling may lead to a Hopf bifurcation, when the inertia of the trailer is relatively large in relation to the inertia of the towing vehicle and when the speed exceeds the critical speed.

**Truck-full trailer:** In contrast to the conventional vehicles with one articulation, a truck-full trailer is not dynamically coupled when the steering dolly mass and inertia are neglected as they are much smaller than the trailer mass and inertia. In this case a kinematic coupling determines the relative location and orientation of the full trailer with respect to the towing vehicle. As a result, the truck and full trailer can be modelled as two kinematically coupled single vehicles. Monotonic stability is determined by the towing vehicle. A Hopf bifurcation does not occur.

The stability analysis presented in this chapter did not show explicit differences between the vehicle combinations, as most combinations were concluded to be stable. Nevertheless, it was concluded in the literature review that there are large differences in the dynamic performance of the combinations. Rearward amplification is often used in literature to analyse the dynamic behaviour of articulated vehicles. It is studied in the next chapter.

---

## Rearward Amplification

---

It was concluded in the previous chapter, that conventional truck combinations are stable for many parameter settings. Nevertheless, it was concluded in the literature review (section 2.5, page 9) that the amount of yaw damping may vary considerably between different vehicle configurations. Yaw damping is a measure for the out swing of the trailing units in a truck combination during a dynamic vehicle manoeuvre. Little yaw damping results in a large amplification of the motion of a trailing unit with respect to its towing unit.

Rearward amplification ( $RA$ ) is a performance measure that quantifies the amount of lateral acceleration magnification in a system and it is often used to investigate the lateral dynamics of articulated vehicles. An introduction was given in the literature review. It was concluded that the values of  $RA$  depend on driving conditions, such as the vehicle speed and the manoeuvre. These conditions differ for the studies analysed. As a result, different rearward amplification values for similar vehicles are observed.

Furthermore, it has been concluded in many studies in the literature review, that rearward amplification is a function of the input frequency and vehicle speed. In general, the amount of damping decreases as the vehicle speed increases, which result in higher rearward amplification values.

The reason for the differences in resulting rearward amplification between the studies is analysed in section 4.1 and a more generic way is proposed to investigate the effect of parameter changes on the dynamic performance of truck combinations. Rearward amplification is studied for the conventional vehicles in section 4.2 and 4.3. Section 4.4 presents a comparison between all conventional and Ecocombi combinations. The conclusions are presented in section 4.5.

### 4.1 Definitions for rearward amplification

Rearward amplification is defined in two ways. The first definition uses a time domain approach. A dynamic vehicle manoeuvre is carried out, and the lateral acceleration of the centre of gravity of the towing vehicle,  $a_{y1}$ , and the largest lateral acceleration at the centre of gravities of the first and second trailing units,  $a_{yn}$ , are used:

$$RA_t = \frac{\max(\text{abs}(a_{yn}))}{\max(\text{abs}(a_{y1}))}. \quad (4.1)$$

Note that the lateral acceleration of the centre of gravity of the trailing unit which results in the highest rearward amplification value is used. This is not necessarily the last trailing unit. These lateral accelerations are responses of the vehicle to a dynamic vehicle manoeuvre, mostly a single or double lane change. Figure 4.1 gives an illustration of a single lane change. Both the steering wheel angle and the resulting lateral accelerations are shown.

Figure 4.1a also reveals that the original steering wheel angle can be approximated with a single sine-wave function. In general, two types of lane changes are distinguished; (1) a path-following lane change where a driver follows a desired path, resulting in a sine shaped lateral acceleration response (the original signal), and (2) a single sine-wave steering wheel input (the approximated signal). The first method is closed-loop, as the driver steers the combination through the lane change while reacting to the motion of the vehicle. The second method is open-loop. In this thesis, both methods are used. However, the path-following lane change input as shown in figure 4.1a is used as an open-loop input as well, as the behaviour of the vehicle combination is studied and not the closed-loop system consisting of the driver and the vehicle. The same signal is used for all vehicle combinations and all vehicle speeds.

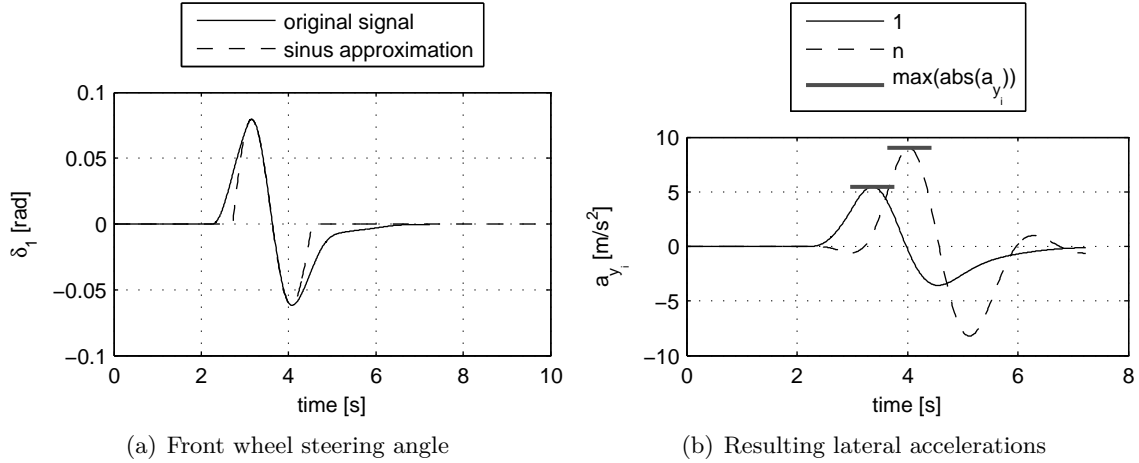


Figure 4.1: Rearward amplification using the time domain definition, responses of the reference truck-full trailer model (see appendix B) ( $n=3$ ) with  $u = 25$  [m/s],  $RA_t = \frac{9.0}{5.5} = 1.6$

In the second definition for rearward amplification the lateral acceleration to steering wheel angle gain of the trailer,  $H_{a_{y_n}, \delta_1}(\omega) = \left| \frac{a_{y_n}(\omega)}{\delta_1(\omega)} \right|$ , and the lateral acceleration to steering wheel angle gain of the towing vehicle,  $H_{a_{y_1}, \delta_1}(\omega) = \left| \frac{a_{y_1}(\omega)}{\delta_1(\omega)} \right|$ , are used:

$$RA_f = \max \left| \frac{H_{a_{y_n}, \delta_1}(\omega)}{H_{a_{y_1}, \delta_1}(\omega)} \right| = \max |H_{a_{y_n}, a_{y_1}}(\omega)|. \quad (4.2)$$

The state-space matrices derived in appendix A are used to calculate frequency response functions, FRF's. Figure 4.2 gives an illustration of FRF's of the reference truck-full trailer model. The maximum value for rearward amplification over the frequency range is indicated.

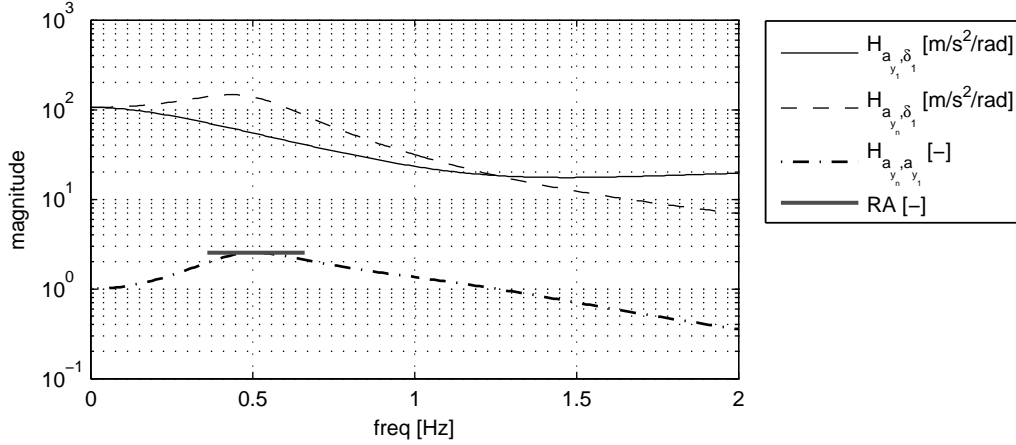


Figure 4.2: Rearward amplification in the frequency domain, data from the reference truck-full trailer combination (see appendix B) ( $n=3$ ) with  $u=25$  [m/s],  $RA_f = 2.5$  at  $f_r = 0.7$  Hz

#### 4.1.1 Differences between frequency domain approach and time domain approach

The time domain definition is often used during full scale testing, whereas the frequency approach is typically used for numerical analysis. The resulting values for rearward amplification are different. This section explains why and gives an overview of the advantages and disadvantages of the two approaches.

**Calculation order:** In the time definition the absolute maxima are divided, whereas in the frequency approach the magnitudes of the gains are divided first and then the maximum is calculated. This means that the phase information is lost in the time definition, as the absolute values are taken regardless of the moments in time where these maxima occur. On the contrary, a frequency response function used to calculate the amplification gain contains both phase and magnitude information.

Due to the different calculating order, the time signals cannot be calculated from the  $H_{a_{y_n}, a_{y_1}}$  FRF. No mathematical relation has been found for the relation between the definitions, though it is observed that the relation is a function of the amount of damping in the system. Furthermore, it is hard to obtain an algebraic equation to analytically calculate rearward amplification in the time domain definition from the equations of motion. This is in contrast to the frequency domain definition, where the FRF's can be calculated directly from the state-space matrices.

**Transient behaviour of the initial conditions:** The second difference is the result of transient behaviour of the initial conditions and is illustrated in figure 4.3. This figure shows the responses of the lateral accelerations on a steering wheel input of a 10 period sine. The lateral accelerations used in the time domain definition are indicated at the beginning of the manoeuvre. An FRF gives the response of a system to a sinusoidal input, after the transient responses as a result of initial conditions have died out. The maximum values used in

the frequency domain approach are indicated in the steady-state part in figure 4.3. The indicated maximum levels of lateral acceleration cause a deviation in rearward amplification value for the two definitions.

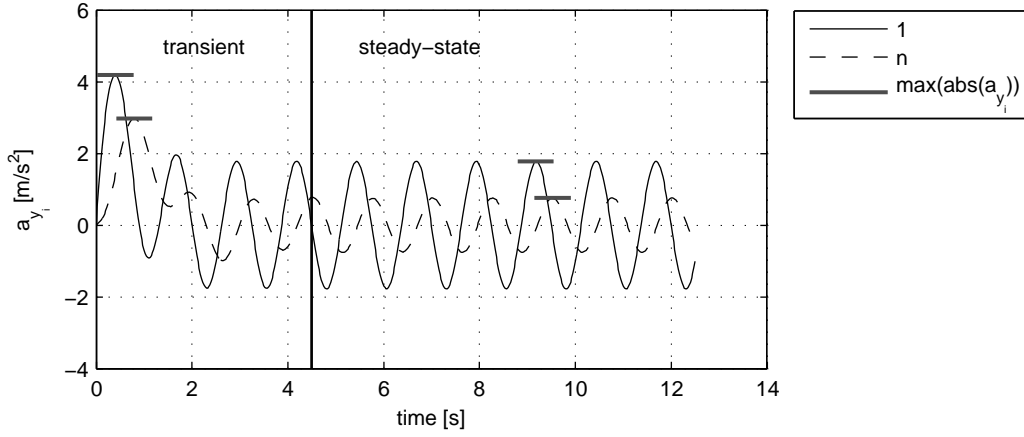


Figure 4.3: Difference between the definitions with a 10 period sine as input, data from the reference tractor-semitrailer combination (see appendix B) ( $n=2$ ),  $RA_t = \frac{4.2}{3.0} = 1.4$ ,  $RA_f = \frac{1.8}{0.8} = 2.3$

**Input signal:** It was concluded in the literature review, and it can be concluded from figure 4.2, that rearward amplification is a function of the input frequency. A lane change is performed at one steering wheel frequency, whereas a FRF gives information over the entire frequency range. With the frequency domain approach, the worst frequency can be selected from the FRF. Moreover, the rearward amplification of only one dynamic vehicle manoeuvre is calculated in the time domain. One can think of many other manoeuvres to perform, which all give different values for rearward amplification. The frequency domain definition uses a well defined input.

Considering these differences the frequency domain approach is selected in this study to calculate rearward amplification. An important reason is the possibility to derive algebraic equations of motion which can be used to calculate the FRF's. Furthermore, the results from the frequency approach are driver independent and independent from the steering wheel input. The most critical frequency can be selected, as this approach gives information over the entire frequency range. Finally, it gives more consistent results.

Nevertheless, the time domain approach is used in many other studies. This is mainly because it is relatively easy to obtain the performance measure during full scale vehicle testing. However, the results are relatively hard to reproduce, as a lane change is a closed-loop vehicle manoeuvre; the outcome of the rearward amplification value is driver dependent. Also, different lane changes were used in the studies analysed in the literature review, which makes comparison even more difficult.

The translation from the time approach to the frequency approach and visa versa is not straightforward, due to the different order of calculating the absolute values and maxima of the signals and due to the transient behaviour as a result of the initial conditions. The relation between the



two definitions is investigated in the next section, as to be able to compare the results of other studies with the calculations presented in this study.

#### 4.1.2 Relation between frequency domain approach and time domain approach

In this section, the relation between the rearward amplification values obtained with a FRF, path following lane change input and single sine-wave input as shown in figure 4.1a is studied for different vehicle configurations.

Figure 4.4 shows the FRF's of rearward amplification of a tractor-semitrailer, truck-centre axle trailer and truck-full trailer combination for several vehicle speeds. In these figures, three graphs are shown; (1) the magnitude of the FRF, (2) the value obtained when applying the time domain approach using the single lane change path following manoeuvre shown in figure 4.1a as input. For comparison the time based rearward amplification values are calculated at several steering input frequencies. And (3) the value obtained when applying the time domain approach using a single sine-wave function as input.

It can be observed that around the maximum amplification, the FRF gives values of the same order of magnitude as the time definitions for the tractor-semitrailer and truck-centre axle trailer. For the truck-full trailer, a large resonance peak can be seen in the FRF compared to the time domain. In general, the lane change and sine approach give quite similar results.

The following conclusions can be drawn:

- It is important to perform the vehicle manoeuvres at the frequencies where the rearward amplification is largest. This frequency differs for individual combinations and is a function of vehicle speed.
- Increasing vehicle speed results in less damping in the system which results in a larger rearward amplification value. Therefore, the vehicle speed should be as large as possible. In this study the numerical simulations are performed with a vehicle speed of 25 m/s.
- The frequency approach can be used to calculate the frequency where rearward amplification is largest. This gives an indication for the frequency at which a lane change or single sine-wave manoeuvre should be carried out during full scale testing or when using complex multibody simulation models.

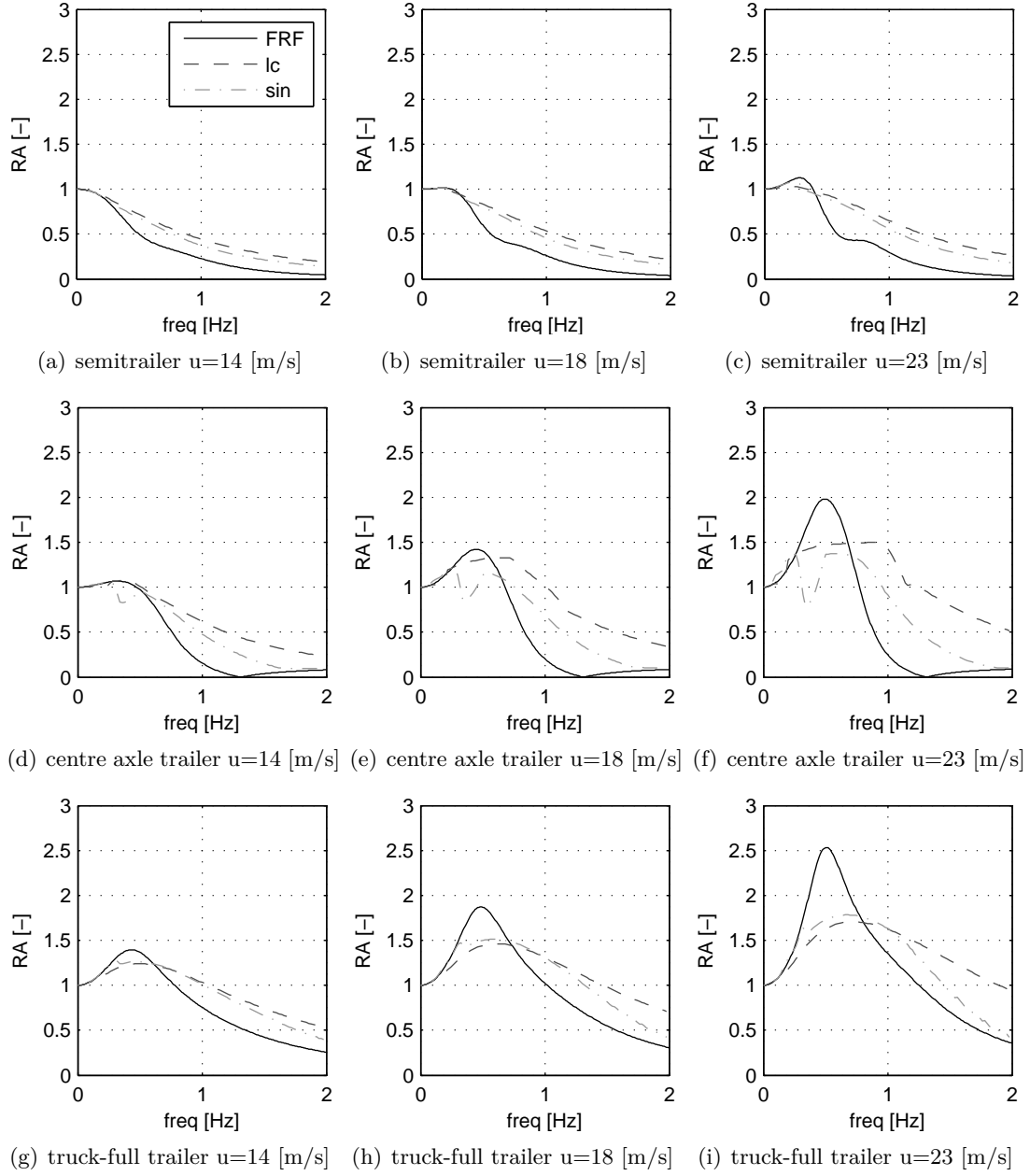


Figure 4.4: Comparison of the approaches as function of excitation frequency and vehicle speed, 'FRF' = frequency response function, 'lc' = result with a path following lane change as input, 'sin' = result with a single sine-wave function as input, for vehicle parameters see appendix B

## 4.2 Rearward amplification of a conventional vehicle with two articulations

The literature review shows that the truck-full trailer combination has the highest rearward amplification value. Therefore, this combination is investigated first. Equations for the rearward amplification of a truck-full trailer are derived and the effect of parameter changes is investigated in this section.

### 4.2.1 Equations for the rearward amplification of a truck-full trailer

As concluded in the previous chapter, the truck-full trailer combination can be modelled as two kinematically coupled single vehicles, assuming that the steering dolly mass and inertia are zero ( $m_2 = 0$ ,  $I_2 = 0$ ), and assuming no mechanical trail of the steering dolly ( $e_2 = 0$ ). Rearward amplification can then be calculated as the lateral acceleration gain of each unit to its front axle steering input, multiplied by the ratio of the inputs (which is given by the kinematic coupling between the units):

$$\begin{aligned} RA_{tf} &= \max \left| H_{a_{y_3}, a_{y_1}}(\omega) \right| \\ &= \max \left| \frac{H_{a_{y_3}, \delta_1}(\omega)}{H_{a_{y_1}, \delta_1}(\omega)} \right| \\ &= \max \left| \frac{H_{a_{y_3}, \delta_3}(\omega) H_{\delta_3, \delta_1}(\omega)}{H_{a_{y_1}, \delta_1}(\omega)} \right|, \end{aligned} \quad (4.3)$$

with  $H_{a_{y_i}, \delta_i}$  the lateral acceleration to front steering wheel angle gains of each unit, with  $i = 1$  for the towing vehicle and  $i = 3$  for the trailer, and  $H_{\delta_3, \delta_1}$  the kinematic coupling between the units.

The advantage of this modelling approach, is that the total FRF for rearward amplification can be split up and analysed in three steps; (1) the lateral acceleration to front steering wheel angle response of the towing vehicle  $H_{a_{y_1}, \delta_1}$ , (2) the lateral acceleration response of the trailer to its steering dolly input  $H_{a_{y_3}, \delta_3}$ , and (3) the kinematic coupling  $H_{\delta_3, \delta_1}$ . Equations can be derived for these three FRF's separately.

The lateral acceleration to steering wheel angle gains for the two single vehicles,  $H_{a_{y_1}, \delta_1}$  and  $H_{a_{y_3}, \delta_3}$ , have been investigated by for instance Pacejka [28] and Mitschke [26] and can be applied for both the towing vehicle and full trailer separately. This leaves only the kinematic coupling between the units,  $H_{\delta_3, \delta_1}$ , to be modelled.

An FRF for rearward amplification can also be derived directly from  $H_{a_{y_3}, a_{y_1}}$ . However, the resulting equation is very lengthy and hard to interpret. Furthermore, not the total FRF, but only the kinematic coupling gain FRF has to be derived for the approach in (4.3), as the lateral acceleration to steering wheel angle gains of single vehicles are known from literature. Finally, when the parameters of the towing vehicle and full trailer are the same  $H_{a_{y_1}, \delta_1} = H_{a_{y_3}, \delta_3}$  the equation for rearward amplification reduces to  $RA_{tf} = \max |H_{\delta_3, \delta_1}(\omega)|$ .

The modelling of the kinematic coupling is discussed in the next section. The equations for  $H_{a_{y_1}, \delta_1}$ ,  $H_{a_{y_3}, \delta_3}$ ,  $H_{\delta_3, \delta_1}$  and finally for  $RA_{tf}$  are given after that.

### Modelling of the kinematic coupling between truck and full trailer

Figure 4.5a shows the free body diagrams of two single vehicles. Their equations of motion expressed in the lateral velocities and yaw rates of the individual units ( $v_1, \dot{\beta} = r_1, v_3$  and  $\dot{\xi} = r_3$ ), with inputs  $\delta_1$  and  $\delta_3$  are (assuming  $u = u_1 = u_2$ ):

$$M_1 \dot{x}_1 = D_1 x_1 + F_1 U_1, \quad (4.4)$$

with,

$$x_1 = \begin{bmatrix} v_1 \\ r \\ v_3 \\ \dot{\xi} \end{bmatrix}, \quad U_1 = \begin{bmatrix} \delta_1 \\ \delta_3 \end{bmatrix}, \quad M_1 = \begin{bmatrix} m_1 & 0 & 0 & 0 \\ 0 & I_1 & 0 & 0 \\ 0 & 0 & m_3 & 0 \\ 0 & 0 & 0 & I_3 \end{bmatrix}$$

$$D_1 = -\frac{1}{u} \begin{bmatrix} C & C s_1 + m_1 u^2 & 0 & 0 \\ C s_1 & C q_1^2 & 0 & 0 \\ 0 & 0 & C_t & C_t s_3 + m_3 u^2 \\ 0 & 0 & C_t s_3 & C_t q_3^2 \end{bmatrix}, \quad F_1 = \begin{bmatrix} C_1 & 0 \\ a_1 C_1 & 0 \\ 0 & C_3 \\ 0 & a_3 C_3 \end{bmatrix}.$$

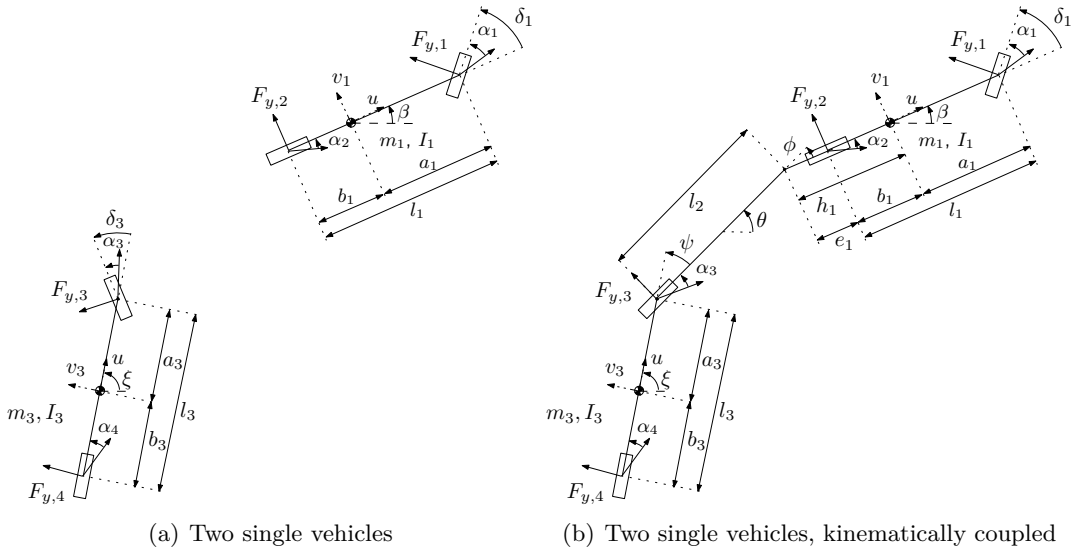


Figure 4.5: Free body diagrams

In the truck-full trailer combination, the second input,  $\delta_3$ , is a function of the relative location and orientation of the full trailer with regard to the towing vehicle, see figure 4.5b. Therefore,  $\delta_3$  is a function of the state variables of both single vehicles;  $\delta_3 = D_3 x_1$ , where  $D_3$  is yet unknown. This yields the equations of motion:

$$M_1 \dot{x}_1 = D_1 x_1 + F_{1,1} \delta_1 + F_{1,2} \delta_3$$

$$= (D_1 + F_{1,2} D_3) x_1 + F_{1,1} \delta_1, \quad (4.5)$$

with  $F_{1,1}$  the first column of  $F_1$  and  $F_{1,2}$  the second column of  $F_1$ . Solving this equation for  $D_3$  gives an expression for the kinematic coupling.

In order to find this expression, a coordinate transformation is applied on the state-space description of a truck-full trailer, which was given in the previous chapter and derived in appendix A. The new state vector,  $x_2$ , contains  $v_3$ , the lateral velocity of the trailer, and  $\dot{\xi}$ , the yaw velocity gain of the trailer, such that both towing vehicle and trailer are expressed in their own coordinates. The new state-space description reads:

$$M_2 \dot{x}_2 = D_2 x_2 + F_2 U_2, \quad (4.6)$$

with,

$$x_2 = \begin{bmatrix} v_1 \\ r \\ v_3 \\ \dot{\xi} \\ \rho \\ \theta \\ \beta \end{bmatrix}, \quad U_2 = \delta_1, \quad M_2 = \begin{bmatrix} m_1 & 0 & 0 & 0 & 0 & 0 & 0 \\ 0 & I_1 & 0 & 0 & 0 & 0 & 0 \\ 0 & 0 & m_3 & 0 & 0 & 0 & 0 \\ 0 & 0 & 0 & I_3 & 0 & 0 & 0 \\ 0 & 0 & 0 & 0 & 1 & 0 & 0 \\ 0 & 0 & 0 & 0 & 0 & 1 & 0 \\ 0 & 0 & 0 & 0 & 0 & 0 & 1 \end{bmatrix}, \quad F_2 = \begin{bmatrix} C_1 \\ a_1 C_1 \\ 0 \\ 0 \\ 0 \\ 0 \\ 0 \end{bmatrix}$$

$$D_2 = -\frac{1}{u} \begin{bmatrix} C & C s_1 + m_1 u^2 & 0 & 0 & 0 & 0 & 0 \\ C s_1 & C q_1^2 & 0 & 0 & 0 & 0 & 0 \\ 0 & 0 & C_t & C_t s_3 + m_3 u^2 & C_3 u & -C_3 u & C_3 u \\ 0 & 0 & C_t s_3 & C_t q_3^2 & C_3 a_3 u & -C_3 a_3 u & C_3 a_3 u \\ 0 & u & 0 & -u & 0 & 0 & 0 \\ -u/l_2 & u h_1/l_2 & u/l_2 & a_3 u/l_2 & u^2/l_2 & 0 & 0 \\ 0 & -u & 0 & 0 & 0 & 0 & 0 \end{bmatrix},$$

with  $\rho = \phi + \psi$  the total articulation angle and by using

$$v_3 = v_1 - h_1 r - l_2 \dot{\theta} - a_3 \dot{\xi} - u \rho. \quad (4.7)$$

The last three equations and states of (4.6) can be added to (4.5), such that  $x_1 = x_2$ ,  $M_1 = M_2$  and  $F_{1,1} = F_2$ . Therefore,  $D_1 + F_{1,2} D_3 = D_2$ , which yields for  $D_3$ :

$$D_3 = \begin{bmatrix} 0 & 0 & 0 & 0 & -1 & 1 & -1 \end{bmatrix}. \quad (4.8)$$

The steering wheel angle for the trailer can now be expressed as:

$$\begin{aligned} \delta_3 &= D_3 x_2 \\ &= -\rho + \theta - \beta \\ &= -\psi. \end{aligned} \quad (4.9)$$

The free body diagram shown in figure 4.5b illustrates this steering wheel angle. It is defined as the angle between the drawbar of the trailer and its longitudinal axis, which is  $\psi$ . The kinematic coupling shows a negative gain; the steering wheel angle and dolly angle have an opposite sign. This explains why a trailer initially steers in the opposite direction when steering into a corner. As illustration, figure 4.6 shows the steering wheel angle  $\delta_1$ , and the dolly angle  $\delta_3$ , during a lane change manoeuvre.

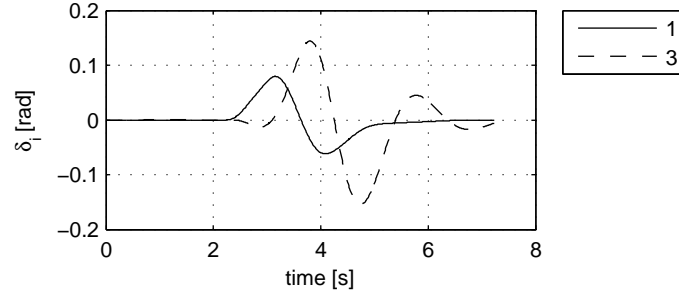


Figure 4.6: Input  $\delta_1$  and response  $\delta_3$  during a lane change

The kinematic coupling FRF,  $H_{\delta_3, \delta_1}$ , can now be calculated:

$$H_{\delta_3, \delta_1}(\omega) = C_s(j\omega I - A_s)^{-1}B_s + D_s, \quad (4.10)$$

with  $j$  the complex variable ( $j^2 = -1$ ),  $I$  a unity matrix, and  $A_s = M_2^{-1}D_2$ ,  $B_s = M_2^{-1}F_2$ ,  $C_s = D_3$  and  $D_s = 0$  the state-space matrices.

Finally, figure 4.7 shows a new way to express the dynamics of a truck-full trailer. The scheme contains two single vehicle blocks for the towing vehicle and full trailer, and a kinematic coupling as a feedback signal. The complex truck-full trailer dynamics is now split up in four less complex blocks. Block  $C$  contains the three last equations of (4.6):

$$\left. \begin{aligned} \xi &= \int \dot{\xi} dt \\ \beta &= \int r dt \\ \rho &= \xi - \beta \\ \dot{\theta} &= -\frac{v_3}{l_2} + \frac{v_1}{l_2} - \frac{h_1 r_1}{l_2} - \frac{a_3 \dot{\xi}}{l_2} - \frac{u \rho}{l_2} \\ \theta &= \int \dot{\theta} dt \end{aligned} \right\}. \quad (4.11)$$

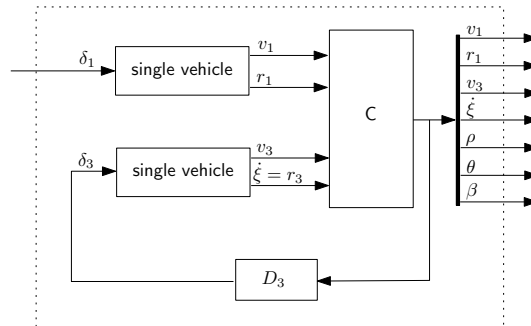


Figure 4.7: A new way to model a truck-full trailer as two single vehicles with kinematic coupling

### Expressions for the frequency response functions

The lateral acceleration to steering wheel angle gains for a single vehicle can now be calculated

in analogy with (4.10), with  $A_s = M_2^{-1}D_2$ ,  $B_s = M_2^{-1}F_2$ . The state-space output matrix  $C_s$  and feed through matrix  $D_s$  for the towing vehicles lateral acceleration are given by:

$$\begin{aligned} a_{y1} &= \dot{v}_1 + ur_1 \\ C_{s_{ay1}, \delta_1} &= A_s(1, :) + \begin{bmatrix} 0 & u & 0 & 0 & 0 & 0 & 0 \end{bmatrix} \\ D_{s_{ay1}, \delta_1} &= B_s(1). \end{aligned} \quad (4.12)$$

For the full trailer, the state-space output and feed through matrices become:

$$\begin{aligned} a_{y3} &= \dot{v}_3 + u\dot{\xi} \\ C_{s_{ay3}, \delta_3} &= A_s(3, :) + \begin{bmatrix} 0 & 0 & 0 & u & 0 & 0 & 0 \end{bmatrix} \\ D_{s_{ay3}, \delta_3} &= B_s(3). \end{aligned} \quad (4.13)$$

Solving these equations yields:

$$H_{a_{y_i}, \delta_i}(\omega) = \left( H_{a_{y_i}, \delta_i} \right)_{ss} \cdot \frac{\text{num}_{a_{y_i}, \delta_i}}{\text{den}_{a_{y_i}, \delta_i}}, \quad (4.14)$$

with,

$$\left. \begin{aligned} \left( H_{a_{y_i}, \delta_i} \right)_{ss} &= \frac{u^2}{l_i} \left( \frac{1}{1 - \frac{u^2}{V_{crit,i}^2}} \right) \\ \text{num}_{a_{y_i}, \delta_i} &= (j\omega)^2 \frac{m_i k_i^2}{l_i C_{i+1}} + \frac{b_i}{u} j\omega + 1 \\ \text{den}_{a_{y_i}, \delta_i} &= (j\omega)^2 \left( \frac{m_i^2 u^2 k_i^2}{\left( 1 - \frac{u^2}{V_{crit,i}^2} \right) C^{*2} (q_i^2 - s_i^2)} + \frac{m_i u (k_i^2 + q_i^2)}{\left( 1 - \frac{u^2}{V_{crit,i}^2} \right) C^* (q_i^2 - s_i^2)} j\omega + 1 \right) \end{aligned} \right\}, \quad (4.15)$$

with  $C^* = C$  for  $i = 1$  and  $C^* = C_t$  for  $i = 3$ , and

$$V_{crit,i}^2 = \frac{C^* (q_i^2 - s_i^2)}{s_i m_i}. \quad (4.16)$$

Figure 4.8 shows the free body diagram with all parameters.

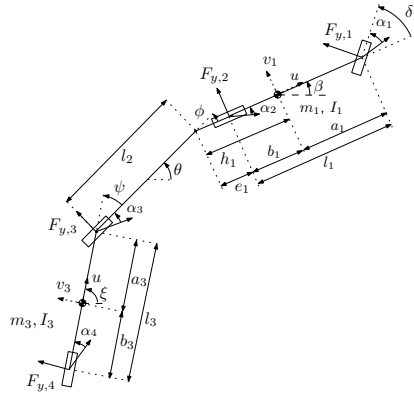


Figure 4.8: Free body diagram truck-full trailer

The kinematic coupling gain can be expressed from (4.10):

$$H_{\delta_3, \delta_1}(\omega) = (H_{\delta_3, \delta_1})_{ss} \cdot \frac{\text{num}_{\delta_3, \delta_1}}{\text{den}_{\delta_3, \delta_1}}. \quad (4.17)$$

The numerator and denominator of the  $H_{\delta_3, \delta_1}$  contain dynamics of both the towing vehicle and trailer, as the kinematic coupling determines the location and orientation of the full trailer with respect to the towing vehicle. Equation (4.17) can be expressed as:

$$\begin{aligned} H_{\delta_3, \delta_1}(\omega) &= (H_{\delta_3, \delta_1})_{ss} \cdot \frac{\text{num}_{\delta_3, \delta_1}}{\text{den}_{\delta_3, \delta_1}} \\ &= (H_{\delta_3, \delta_1})_{ss} \cdot \frac{\text{den}_{a_{y3}, \delta_3}}{\text{den}_{a_{y1}, \delta_1}} \cdot \frac{\text{num}_{\delta_3, \delta_1}^*}{\text{den}_{\delta_3, \delta_1}^*}, \end{aligned} \quad (4.18)$$

with,

$$\left. \begin{aligned} (H_{\delta_3, \delta_1})_{ss} &= \frac{1 - \frac{u^2}{V_{crit,3}^2}}{1 - \frac{u^2}{V_{crit,1}^2}} \frac{l_3}{l_1} \\ \text{num}_{\delta_3, \delta_1}^* &= (j\omega)^2 \frac{m_1(k_1^2 - a_1 h_1)}{l_1 C_2} - \frac{e_1}{u} j\omega + 1 \\ \text{den}_{\delta_3, \delta_1}^* &= \frac{l_2 l_3}{u^2} \left( 1 - \frac{u^2}{V_{crit,3}^2} \right) \cdot (j\omega)^2 \cdot \text{den}_{a_{y3}, \delta_3} + (j\omega)^2 \frac{m_3(k_3^2 + a_3^2 + a_3 l_2)}{l_3 C_4} + \frac{l_2 + l_3}{u} j\omega + 1 \end{aligned} \right\}. \quad (4.19)$$

The FRF of the kinematic coupling gain can thus be split up as follows; (1) a steady-state part  $(H_{\delta_3, \delta_1})_{ss}$ , (2) the characteristic equations of two single vehicles (the towing vehicle and full trailer),  $\text{den}_{a_{y1}, \delta_1}$  and  $\text{den}_{a_{y3}, \delta_3}$ , which are required to determine the relative location and orientation of the units, (3) the dynamics describing the connection of the two units;  $\text{num}_{\delta_3, \delta_1}^*$  and  $\text{den}_{\delta_3, \delta_1}^*$ .

Finally, the equation for rearward amplification as defined in (4.3) can be expressed as:

$$\begin{aligned} RA_{tf} &= \max \left| \frac{H_{a_{y3}, \delta_3}(\omega) H_{\delta_3, \delta_1}(\omega)}{H_{a_{y1}, \delta_1}(\omega)} \right| \\ &= \max \left( \frac{(H_{a_{y3}, \delta_3})_{ss} (H_{\delta_3, \delta_1})_{ss}}{(H_{a_{y1}, \delta_1})_{ss}} \cdot \left| \frac{\text{num}_{a_{y3}, \delta_3} \text{den}_{a_{y3}, \delta_3} \text{num}_{\delta_3, \delta_1}^*}{\text{den}_{a_{y3}, \delta_3} \text{den}_{a_{y1}, \delta_1} \text{den}_{\delta_3, \delta_1}^*} \right| \right) \\ &= \max \left| \frac{\text{num}_{a_{y3}, \delta_3}}{\text{num}_{a_{y1}, \delta_1}} \cdot \frac{\text{num}_{\delta_3, \delta_1}^*}{\text{den}_{\delta_3, \delta_1}^*} \right|. \end{aligned} \quad (4.20)$$

#### 4.2.2 Effect of parameter changes on rearward amplification of a truck-full trailer

The effect of parameter variations on rearward amplification of a truck-full trailer is illustrated with case studies in this section. It is assumed that normalised cornering stiffnesses can be



applied. The following parameters apply for the reference vehicle (see appendix B):

$$\left. \begin{aligned} l &= l_1 = l_3 = 5 \text{ m} \\ a &= a_1 = a_3 = 2.5 \text{ m} \\ k &= k_1 = k_3 = 1.44 \text{ m} \\ f &= f_1 = f_2 = f_3 = f_4 = 56.25 \text{ 1/rad} \end{aligned} \right\}. \quad (4.21)$$

Furthermore, in contrast to the data listed in appendix B also the masses of the full trailer and truck are chosen identical:

$$m = m_1 = m_3 = 15000 \text{ kg}. \quad (4.22)$$

With this simplification, the full trailer and truck are two identical single vehicles. It should be noted that the masses have no effect on rearward amplification, as the cornering stiffness scales linearly with vertical load. This will be discussed in case study 2.

Only the parameters of interest are varied. Furthermore, a uniform mass distribution is assumed, and the centre of gravity is assumed to be at half the wheelbase:

$$\left. \begin{aligned} k_1 &= \sqrt{\frac{1}{12} l_1^2} \\ k_3 &= \sqrt{\frac{1}{12} l_3^2} \\ \frac{a_1}{l_1} &= \frac{a_3}{l_3} = 0.5 \end{aligned} \right\}. \quad (4.23)$$

**Case study 1: Effect of the kinematic coupling:** The FRF's of the towing vehicle and trailer are the same as they are modelled as two identical single vehicles:  $H_{ay_1, \delta_1}(\omega) = H_{ay_3, \delta_3}(\omega)$ . The equation for rearward amplification reduces to:

$$RA_{tf} = \max \left| \frac{\text{num}_{\delta_3, \delta_1}^*}{\text{den}_{\delta_3, \delta_1}^*} \right|. \quad (4.24)$$

This means that rearward amplification is only determined by the FRF elements in (4.19) of the kinematic coupling.

The damping ratio of the zeros is investigated first. It can be derived from the nominator of the kinematic coupling gain in (4.19):

$$\begin{aligned} \text{num}_{\delta_3, \delta_1}^* &= (j\omega)^2 \frac{m_1(k_1^2 - a_1 h_1)}{l_1 C_2} - \frac{e_1}{u} j\omega + 1 \\ &= \frac{(j\omega)^2}{\omega_{\text{num}\delta_3\delta_1}^2} + 2 \frac{\zeta_{\text{num}\delta_3\delta_1}}{\omega_{\text{num}\delta_3\delta_1}} j\omega + 1, \end{aligned} \quad (4.25)$$

with  $\omega_{\text{num}}$  the natural frequency and  $\zeta_{\text{num}}$  the damping ratio. This yields for the damping ratio of the kinematic coupling:

$$\zeta_{\text{num}\delta_3\delta_1} = -\frac{1}{2} \frac{e_1}{u} \sqrt{\frac{l C_2}{m(k^2 - a h_1)}}. \quad (4.26)$$

The coupling point of a truck is behind the rear axle,  $e_1 > 0$ , which yields that the zeros are in the right hand complex plane; they are non-minimum phase. This means, that an input to the system in one direction,  $\delta_1$  is for instance positive, results in an initial negative

steering wheel angle of the trailer. This is also concluded in (4.9) and it is illustrated in figure 4.6.

A second observation from (4.24) is that the nominator of the FRF contains the distance between the rear axle of the towing vehicle and the coupling point  $e_1$ , whereas the drawbar length  $l_2$  is in the denominator. These two parameters determine, with the articulation angles, the location and orientation of the trailer with respect to the towing vehicle. Numerical simulations are performed to investigate the effect of these parameters.

Figure 4.9a shows the values for rearward amplification as function of the coupling rear overhang. From this figure, it turns out that increasing  $e_1$  results in an increase of rearward amplification and thus a decrease of the dynamic performance of the vehicle combination. This is because a large coupling rear overhang results in a larger input to the trailer; the rear of the truck swings out more when the coupling rear overhang is larger.

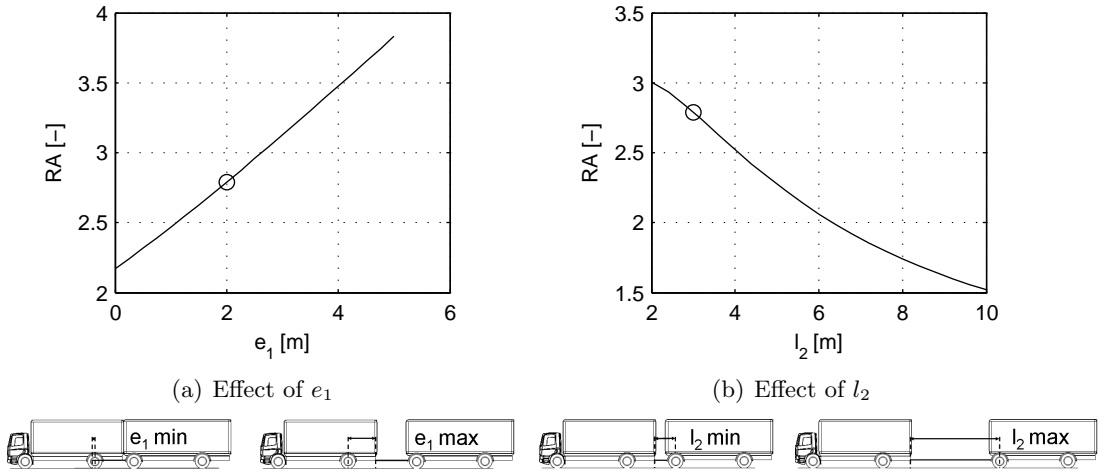


Figure 4.9: Effect of  $e_1$  and  $l_2$  on rearward amplification of the simplified truck-full trailer model, o is the reference combination

Figure 4.9b shows the effect of changing the drawbar length. When increasing  $l_2$ , the trailer starts cutting the corner and makes a smaller path than the shorter drawbar combination, which results in a smaller rearward amplification value. The trailer has to travel a longer distance before it makes the same motion as the towing vehicle; it filters the towing vehicle's motion.

**Case study 2: Effect of loading conditions:** In practise, the truck and full trailer are often homogeneously loaded. Therefore, very extreme loading cases are not considered. However, both the masses, moments of inertia and the longitudinal location of the centre of gravities can change.

As explained before, the lateral dynamics of the towing vehicle are not affected by the trailer; the truck and trailer are assumed to be kinematically coupled. Therefore, changing the load or load distribution of the trailer has no effect on the stability of the combination. Furthermore, normalised cornering stiffnesses are assumed, which means that increasing or

decreasing weight has no effect on rearward amplification, as long as the lateral cornering stiffness dependency with vertical load is in its linear range. Simulations confirm that changing only the load ratio,  $\frac{m_1}{m_3}$ , or the inertia of the trailer,  $k_3$ , does not affect rearward amplification in this case.

Changing the moments of inertia of the towing vehicle,  $k_1$ , results in a change of the performance measure, see figure 4.10. Increasing the moment of inertia of the towing vehicle results in a larger yaw motion, and thus in a larger lateral velocity of the coupling point. A larger lateral motion at the coupling point results in a larger input to the trailer. However, this effect is much smaller in comparison to the effect of the coupling rear overhang and drawbar length illustrated in figure 4.9.

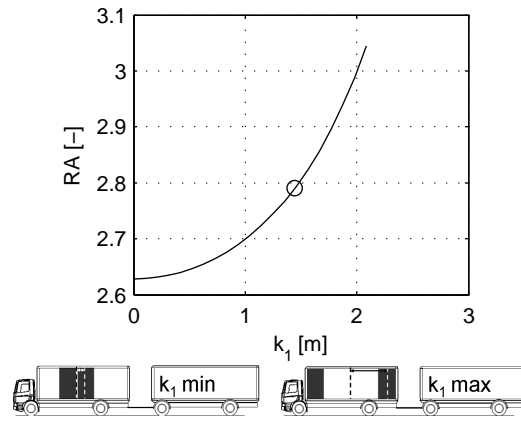


Figure 4.10: Effect of  $k_1$  on rearward amplification of the simplified truck-full trailer model, o is the reference combination

A second way to explain the effect of the moment of inertia on rearward amplification is by considering the FRF  $H_{a_{y_1}, \delta_1}$ . Rearward amplification is high at the anti-resonance frequency of  $H_{a_{y_1}, \delta_1}$ , as  $H_{a_{y_1}, \delta_1}$  is in the denominator of the rearward amplification equation in (4.3). Adding damping to the system at this frequency, results in a smaller value of the anti-resonance of  $H_{a_{y_1}, \delta_1}$ , and thus in a smaller value for rearward amplification.

The damping can be derived from the nominator of the lateral acceleration gain in (4.15):

$$\begin{aligned} \text{num}_{a_{y_1} \delta_1} &= (j\omega)^2 \frac{m_1 k_1^2}{l_1 C_2} + \frac{b_1}{u} j\omega + 1 \\ &= \frac{(j\omega)^2}{\omega_{\text{num}_{a_{y_1} \delta_1}}^2} + 2 \frac{\zeta_{\text{num}_{a_{y_1} \delta_1}}}{\omega_{\text{num}_{a_{y_1} \delta_1}}} j\omega + 1, \end{aligned} \quad (4.27)$$

This yields for the damping ratio:

$$\zeta_{\text{num}_{a_{y_1} \delta_1}} = \frac{1}{2} \frac{b_1}{u} \sqrt{\frac{l_1 C_2}{m_1 k_1^2}}, \quad (4.28)$$

which indicates that decreasing the moment of inertia ( $I_1 = m_1 k_1^2$ ) results in a larger value for  $\zeta_{\text{num}_{a_{y_1} \delta_1}}$  and thus in a smaller anti-resonance peak and a smaller value for rearward amplification.

The last parameter variation to be considered when changing the load distribution is the longitudinal location of the centre of gravities. Changing this location also changes the vertical load on each axle. When normalised cornering stiffnesses are assumed, this does not affect rearward amplification, as the lateral tyre cornering stiffness scales with vertical load. When the cornering stiffness does not scale linearly with vertical load, the location of the centre of gravity changes the neutral steer parameters. The effect of the neutral steer parameters on rearward amplification is investigated in the next case study.

**Case study 3: Effect of neutral steer parameters:** Both the towing vehicle and full trailer are often nearly neutrally steered. In practise, this is for instance when the centre of gravity is exactly centered between the front and rear axle,  $a_i = b_i$ , and when the cornering stiffness of the front and rear axle are the same,  $C_i = C_{i+1}$ . The normalised cornering stiffnesses should be the same for a neutrally steered vehicle,  $f_i = f_{i+1}$ , which was concluded in the previous chapter to be often true for trucks (see figure 3.6, section 3.1.2, page 18). Nevertheless, this case study handles the cases where  $s_1 \neq 0$  and  $s_3 \neq 0$ .

The neutral steer parameter  $s_1$  is determined by the location of the centre of gravity and the tyre stiffness of the towing vehicle:  $Cs_1 = a_1C_1 - b_1C_2$ . In the previous case study, it was concluded that the anti-resonance peak of  $|H_{a_{y1},\delta_1}|$  is important for rearward amplification. The damping ratio  $\zeta_{\text{num}a_{y1}\delta_1}$  given in (4.28) indicates, that increasing  $b_1$  and  $C_2$  results in more damping of the anti-resonance, and thus in a smaller value for rearward amplification. This means that the towing vehicle should become more understeered.

This effect can also be explained by the lever effect of the towing vehicle, as concluded in the previous case studies also. The motion at the coupling point decreases when the yaw motion of the towing vehicle decreases. The yaw motion decreases as the vehicle becomes more understeered.

The lateral acceleration to steering wheel angle gain of the full trailer is in the denominator of the rearward amplification equation in (4.3). The damping of its poles should be large, such that the resonance peak is small as well as the rearward amplification value. Pacejka [28] gives the following approximation for the damping ratio of a single vehicle:

$$\begin{aligned}\zeta &\approx \frac{1}{\sqrt{1 + \frac{\eta}{g}u^2}} \\ &= \frac{1}{\sqrt{1 - \frac{u^2}{V_{crit}^2}}},\end{aligned}\tag{4.29}$$

with  $\eta$  the understeer coefficient;  $\eta_i = \frac{-s_i m_i g (C_i + C_{i+1})}{l_i C_i C_{i+1}}$ . Figure 4.11 shows the approximation of the damping ratio by Pacejka as function of vehicle speed. The damping ratio is large for an oversteered vehicle and goes to infinity when the speed equals the critical speed. This approximation of the damping ratio is one for a neutrally steered vehicle and decreases for an understeered vehicle. This means that a tendency of the trailer towards oversteer enhances the dynamic performance of the vehicle combination as the resonance peak of the trailers FRF decreases, which decreases rearward amplification.

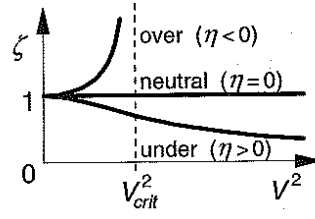


Figure 4.11: Damping ratio as function of vehicle speed [28]

The effect of the neutral steer parameters is investigated numerically by changing the normalised cornering stiffnesses. The neutral steer parameter of the towing vehicle,  $s_1$ , is investigated by changing  $f_2$ . The effect of the neutral steer parameter of the trailer,  $s_3$ , is investigated by changing  $f_4$ . Figure 4.12 gives the results. It confirms that the towing vehicle should be towards understeer;  $f_2$  should be large. The trailer should be towards oversteer;  $f_4$  should be small to enhance the dynamic performance of the vehicle combination. The effect of the trailer on the resulting value for rearward amplification is much smaller than the effect of the towing vehicle. Note that an oversteered vehicle has a critical speed; it becomes unstable if the speed exceeds the critical speed. Therefore, in practise the full trailer is often understeered, to prevent swing out of its rear end. Rearward amplification then decreases as the full trailer becomes less understeered, towards neutral steer.

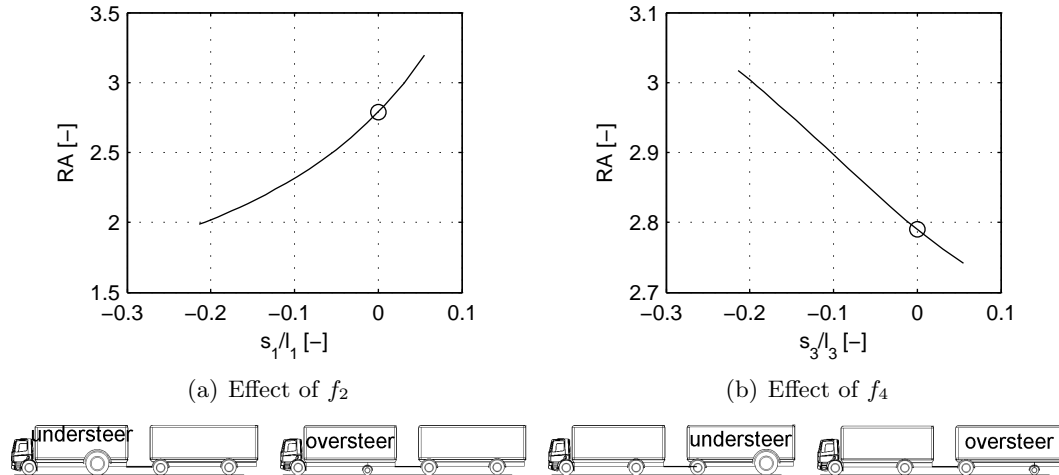


Figure 4.12: Effect of  $f_2$  and  $f_4$  on rearward amplification of the simplified truck-full trailer model, o is the reference combination

**Case study 4: Effect of lengths of the units:** Some Ecocombi configurations show similarities with a truck-full trailer. Ecocombi C has both a longer towing vehicle and a longer trailer, whereas the towing vehicle of Ecocombi D is similar to the towing vehicle of the conventional combination, but it has a very long full trailer. The effect of the individual wheelbases of the towing vehicle and full trailer is investigated in this case study. It is assumed that the location of the centre of gravities and the gyration arms scale with the

wheelbases:

$$\left. \begin{aligned} k_1 &= \sqrt{\frac{1}{12} l_1^2} \\ k_3 &= \sqrt{\frac{1}{12} l_3^2} \\ \frac{a_1}{l_1} &= \frac{a_3}{l_3} = 0.5 \end{aligned} \right\}. \quad (4.30)$$

The other parameters are the same for the towing vehicle and full trailer.

First, the effect of the wheelbases on the FRF  $H_{\delta_3, \delta_1}$  is investigated. The kinematic coupling gain is in the nominator of the rearward amplification in equation (4.3) and should therefore be small for a good dynamic performance of the vehicle combination. Its steady-state gain can be calculated as follows. The steady-state gain of a single vehicle unit can be calculated by considering the equations for steady-state driving as expressed in the literature review (equation (2.2), section 2.1, page 6):

$$\delta_i = \frac{l_i}{R} + \alpha_i - \alpha_{i+1}. \quad (4.31)$$

Pacejka [28] formulates this expression as:

$$\begin{aligned} \delta_i &= \frac{l_i}{R} + \eta_i \frac{a_{y_i}}{g} \\ &= \frac{l_i}{R} - a_{y_i} l_i \frac{1}{V_{crit_i}^2} \\ &= l_i \left( \frac{1}{R} - \frac{a_{y_i}}{V_{crit_i}^2} \right). \end{aligned} \quad (4.32)$$

Filling in  $i = 1$  for the towing vehicle and  $i = 3$  for the trailer and by applying  $a_{y_i} = \frac{u^2}{R}$  yields the expression of the steady-state gain in equation (4.15). As the steady-state gain is only determined by the individual single vehicles, it is not a function of the coupling parameters  $e_1$  (coupling rear overhang) and  $l_2$  (drawbar length).

In practise, both the towing and trailing units are nearly neutrally steered. The steady-state kinematic coupling gain reduces to  $\frac{l_3}{l_1}$  when assuming  $s_1 = 0$  and  $s_3 = 0$ . The following cases can then be distinguished:

- $l_3 > l_1$  The steady-state magnitude of the kinematic coupling is larger than one, which means that the steering wheel angle of the dolly is larger than the steering wheel angle of the towing vehicle.
- $l_3 = l_1$  The steady-state magnitude of the kinematic coupling is one, which means that both units steer with the same amount.
- $l_3 < l_1$  The steady-state magnitude of the kinematic coupling is smaller than one, which means that the steering wheel angle of the towing vehicle is larger than the steering wheel angle of the dolly.

Figure 4.13 shows the effect of changing the wheelbases of the single vehicles individually on rearward amplification over the entire frequency range. A smaller wheelbase of the towing vehicle results in a smaller distance between the centre of gravity and the coupling point, which results in a smaller lateral motion of the coupling point. This leveraging effect was also explained in the other case studies. A longer wheelbase of the trailer results in a

motion with a smaller deviation from the original straight line path; the trailer filters the path of the towing vehicle. The longer the wheelbase, the more time it takes before the trailer follows the path of the towing vehicle. This effect can be compared with the effect of making the drawbar longer.

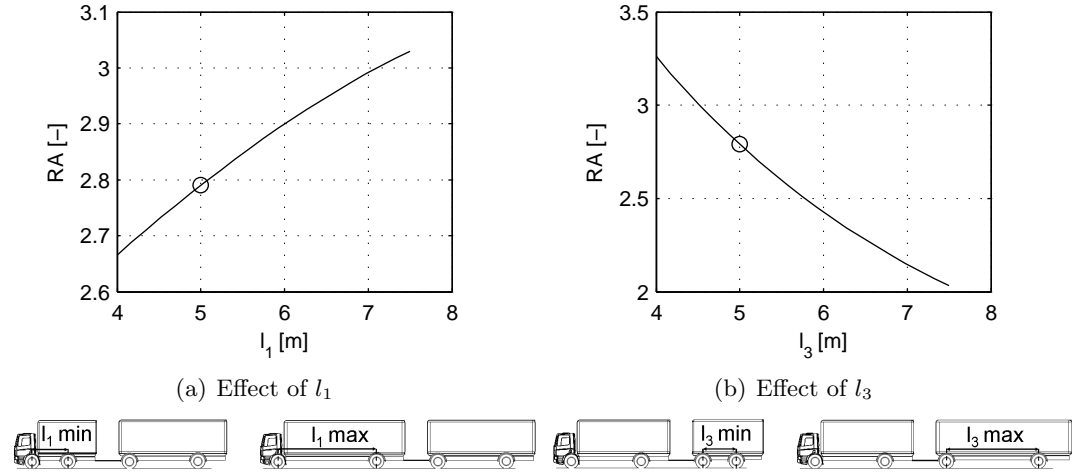


Figure 4.13: Effect of  $l_1$  and  $l_3$  on rearward amplification of the simplified truck-full trailer model, o is the reference combination

### Summary

The lateral dynamic performance of a truck-full trailer improves when rearward amplification decreases. The performance measure can be investigated by modelling the truck combination as two kinematically coupled identical single vehicles. Due to the nature of the kinematic coupling, the motion of the truck is not affected by the dynamics of the trailer. The rearward amplification can be reduced in two ways; (1) by minimizing the input to the trailer, and (2) by minimizing the response of the trailer separately.

The input of the trailer is a function of the relative location and orientation of the trailer with respect to the towing vehicle. It can be reduced by;

- reducing the coupling rear overhang,
- making the towing vehicle more understeered,
- reducing the moment of inertia of the towing vehicle,
- reducing the wheelbase of the towing vehicle.

The rearward amplification response of the trailer can for instance be reduced by;

- increasing the drawbar length,
- making the wheelbase of the trailer longer,
- reducing the amount of understeer of the trailer towards neutral steer.

For the assumptions used in this study, the inertia of the trailer and the load of the towing vehicle and trailer have no effect on rearward amplification.

### 4.3 Rearward amplification of conventional vehicles with one articulation

The effect of parameter changes on the rearward amplification of the other conventional vehicles, the tractor-semitrailer and truck-centre axle combination, is briefly illustrated in this section. The simulations are performed at 25 m/s as it was concluded in figure 4.4 (page 46) that rearward amplification increases with vehicle speed for all combinations. The reference vehicle parameters are listed in appendix B. In contrast to the parameters listed in the appendix, the centre axle trailer is loaded to  $m_2 = 10000$  kg. The combination becomes unstable with an oscillatory motion when the trailer mass becomes too large with the parameter variations used in this section. This was concluded in the stability analysis in section 3.2.3 (page 25).

Figures 4.14 and 4.15 illustrate the effect of changing the coupling rear overhang and trailer wheelbase for both combinations. The distance between the centre of gravity of the towing vehicle and the coupling point should be small and the trailers wheelbase should be large for a small rearward amplification value.

The tractor-semitrailer combination has a smaller value for rearward amplification, as the distance between the hitch point and the trailer axle is much larger than the same distance of the truck-centre axle trailer, and because the fifth wheel is located closer to the centre of gravity of the towing vehicle compared to the truck-centre axle trailers coupling point.

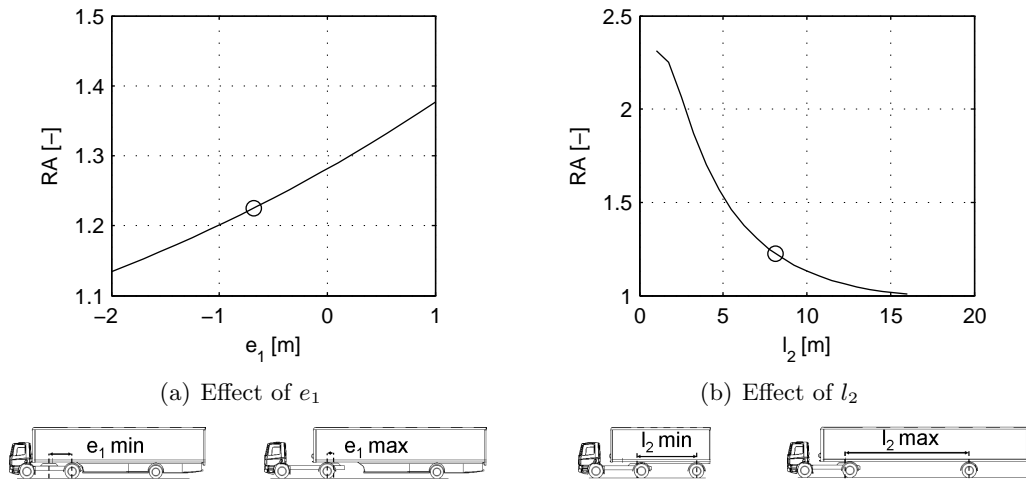


Figure 4.14: Effect of  $e_1$  and  $l_2$  on rearward amplification of a tractor - semitrailer, o is the reference combination



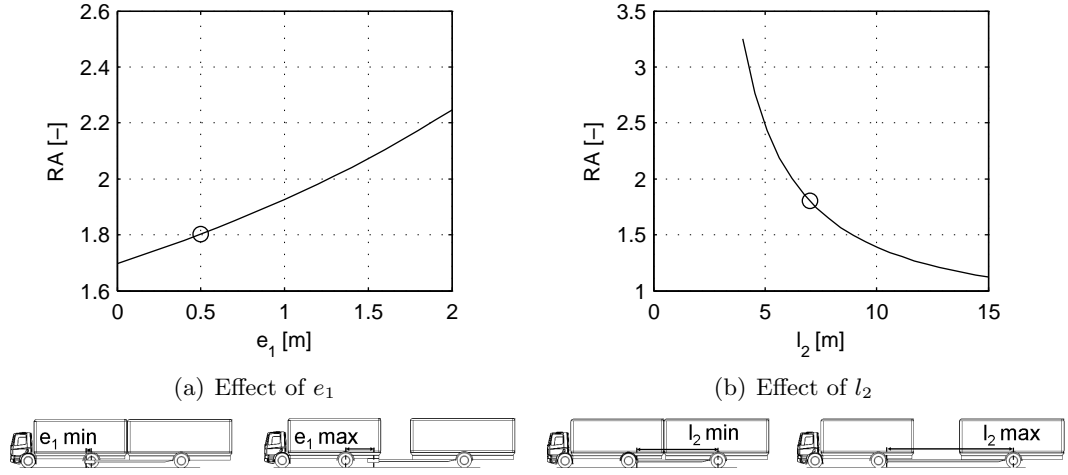


Figure 4.15: Effect of  $e_1$  and  $l_2$  on rearward amplification of a truck-centre axle trailer, o is the reference combination

The effect of the neutral steer parameter of the towing vehicle,  $s_1$ , on rearward amplification is investigated for the conventional vehicles with one articulation in figure 4.16 by changing  $f_2$ . Making the towing vehicle more understeered (increasing  $f_2$ ) results for both the tractor-semitrailer and truck-full trailer in a smaller rearward amplification value, as the input to the trailer decreases.

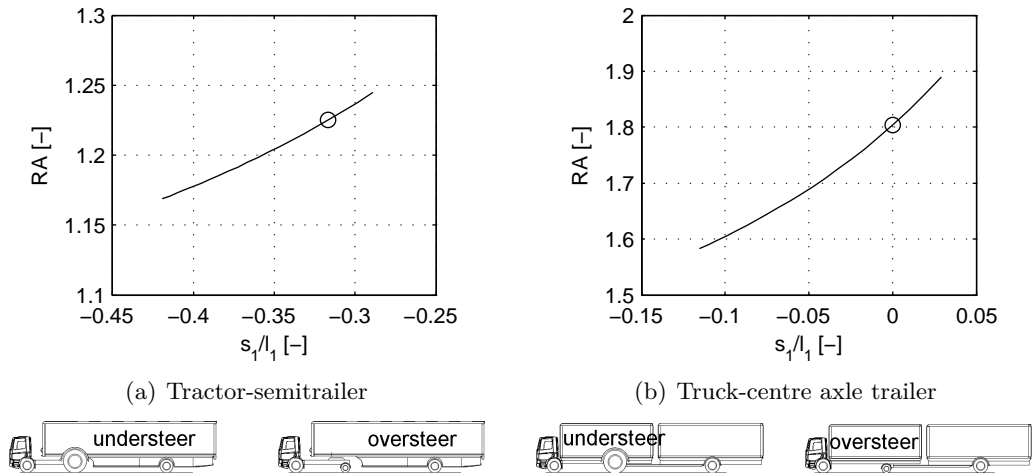


Figure 4.16: Effect of  $f_2$  on rearward amplification of a tractor-semitrailer and a truck-centre axle trailer, o is the reference combination

Finally, the loading ratio,  $\frac{m_1}{m_2}$ , is investigated for the truck-centre axle trailer as it has an inertia coupling. The trailer mass is changed in figure 4.17; increasing the trailer mass (and therefore also the inertia of the trailer  $I_2 = m_2 k_2^2$ ) increases rearward amplification. Changing the towing vehicles mass has a similar opposite effect.

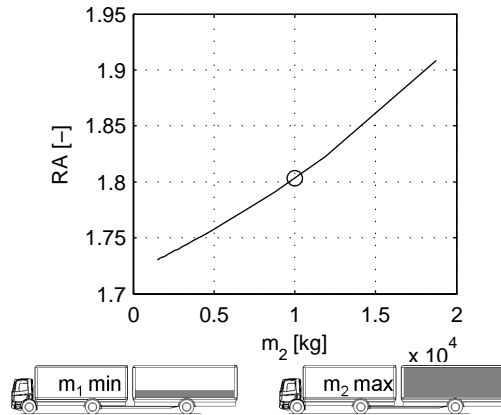


Figure 4.17: Effect of  $m_2$  on rearward amplification of a truck-centre axle trailer, o is the reference combination

### Summary

Summarising the observations of the three conventional vehicles (truck-full trailer, tractor-semitrailer and truck-centre axle trailer), the following conclusions can be drawn:

- A semitrailer results in a smaller rearward amplification value than a centre axle trailer, as the distance between the coupling point and the trailer wheels is larger and because the coupling point is located closer to the centre of gravity of the towing vehicle in comparison with a truck-centre axle trailer.
- For all combinations, decreasing the distance between the centre of gravity of the towing vehicle and the coupling point and increasing the trailer wheelbases reduces rearward amplification. This qualitative effect of the coupling rear overhang and trailer wheelbase is independent of the type of coupling between the units, as the same conclusion is drawn for a truck-full trailer which has a kinematic coupling, and for both the tractor-semitrailer and truck-centre axle trailers which have dynamic couplings.
- On the other hand, the truck-centre axle trailer also differs from the truck-full trailer. Due to the kinematic coupling, the loading ratio (trailer mass divided by towing vehicle mass) has no effect on rearward amplification of the truck-full trailer. For the truck-centre axle trailer, the loading ratio changes rearward amplification.

## 4.4 Comparison of rearward amplification values for all conventional and Ecocombi configurations

This section gives an overview of the resulting rearward amplification values of all conventional vehicles and Ecocombi's. The Ecocombi's are loaded to a gross vehicle weight of 60 tonnes. The load in each unit is assumed to be homogeneous and in proportion to the length of the loading length of the unit. All vehicles are modelled with single axles, such that the equations of motion

derived in the previous chapter can be used. The parameters of the vehicles are taken from [31] and are listed in appendix B. The simulations are performed with a speed of 25 m/s.

Furthermore, the gain at the centre of gravity of the articulation which results in the highest rearward amplification is used. Vehicles with one articulation have only two centers of gravity, which means that the FRF of the first articulation,  $H_{a_{y2},a_{y1}}$ , is used. Truck-full trailer combinations have also two centers of gravity, though they have two articulations, when the steering dolly is assumed massless ( $m_2 = 0$ ). Therefore, rearward amplification for truck-full trailers is calculated with the  $H_{a_{y3},a_{y1}}$  FRF. For the other Ecocombi's (A, B and E), the following equation is used:

$$RA = \max \left[ \max |H_{a_{y2},a_{y1}}|, \max |H_{a_{y3},a_{y1}}| \right]. \quad (4.33)$$

Figure 4.18 shows both  $|H_{a_{y2},a_{y1}}|$  and  $|H_{a_{y3},a_{y1}}|$  for Ecocombi's A, B and E. It turns out that for Ecocombi's A and B  $\max |H_{a_{y3},a_{y1}}|$  results in the largest rearward amplification value, though  $|H_{a_{y2},a_{y1}}|$  might be larger at specific frequencies. Finally, the amplification increases at the same frequency when going from the first to the second articulation for Ecocombi E as the trailer units have comparable weights and dimensions.

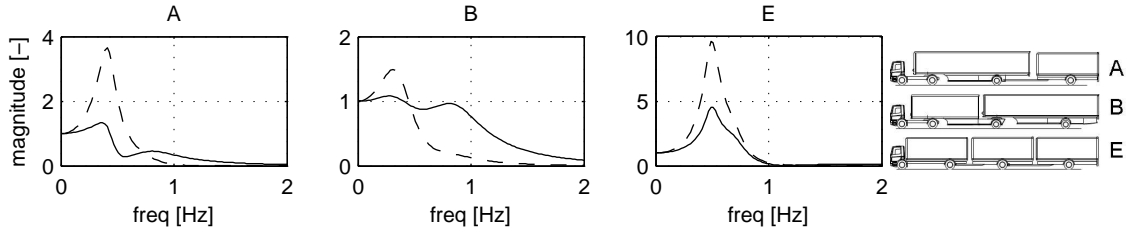


Figure 4.18:  $|H_{a_{y2},a_{y1}}|$  — and  $|H_{a_{y3},a_{y1}}|$  — for the conventional vehicles and Ecocombi's with two articulations

The resulting values for rearward amplification and the frequency where the maximum occurs are compared by configuration type in the next figures. A distinction between truck-full trailers, truck-centre axle trailers and tractor-semitrailers is made.

**Truck-full trailers:** The truck-full trailer combinations are compared first; the conventional combination, Ecocombi's C and D, see figure 4.19. Ecocombi C has about the same layout as the conventional truck-full trailer; the wheelbase of the towing vehicle and trailer increased both. However, Ecocombi D has a relative short towing vehicle, followed by a dolly carrying the front end of a semitrailer which together form a full trailer.

The longer wheelbase of the trailer results in a relative small rearward amplification value of Ecocombi D compared with the other full trailer combinations. Ecocombi C has a relative high rearward amplification value; the mass and inertia of both the towing vehicle and trailer increases compared to the conventional vehicle, as the length of the loading space increases. The inertia of the trailer should to be counteracted by trailer axles. However, both the conventional vehicle and the Ecocombi have single axles, though the mass and the inertia increased considerably. Normalised cornering stiffnesses are applied, which means that the total stiffness scales with the vertical load. However, the amount of damping in the system does not increase with the same amount, as the wheelbases do not change in

relation to the increased mass. Therefore, the Ecocombi has too little yaw damping in relation to its inertia and mass. In reality, more than one axle is applied on the trailer when such high loads are applied, which increases yaw damping. This will be studied in the next chapter.

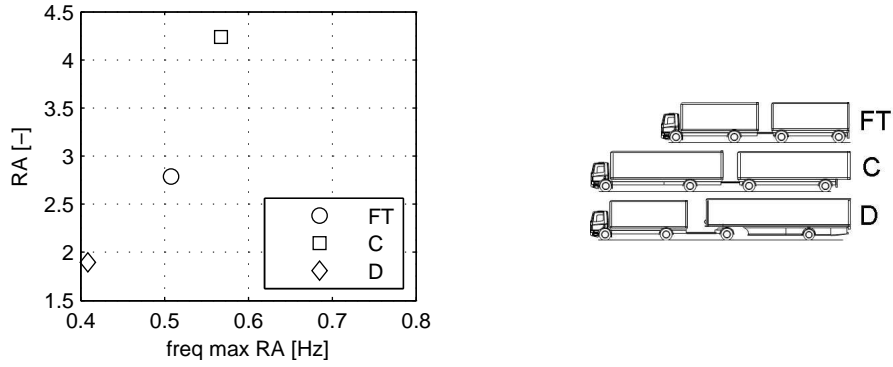


Figure 4.19: Rearward amplification value and frequency where the maximum occurs for all truck-full trailer combinations

**Tractor-semitrailers:** The second group to be evaluated are the tractor-semitrailers. Ecocombi B is a double semitrailer combination. Ecocombi F can be compared with a conventional tractor-semitrailer, with a larger and heavier towing vehicle. Their resulting values for rearward amplification and the frequency where this maximum occurs are shown in figure 4.20.

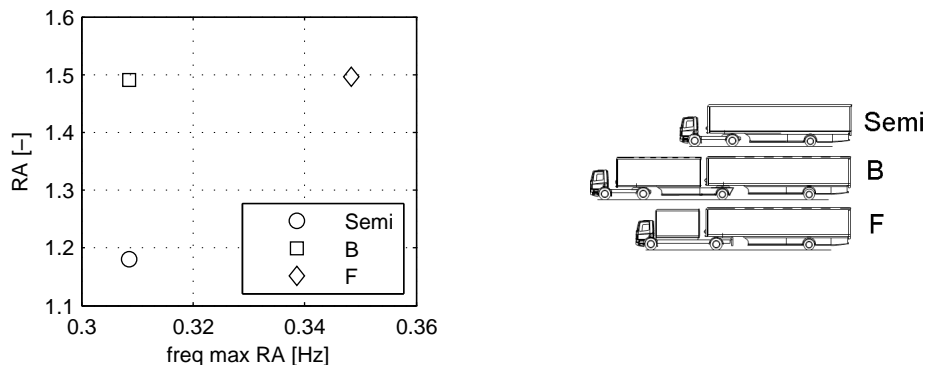


Figure 4.20: Rearward amplification value and frequency where the maximum occurs for all tractor-semitrailer combinations

As concluded in the previous section, the semitrailers are favourable for rearward amplification as their trailers wheelbase is large and because the coupling points are located relatively close to the centre of gravity of their leading unit. The resulting rearward amplification values of these three combinations are quite comparable and are the smallest of all combinations.

**Truck-centre axle trailers:** The third group of vehicles are the truck-centre axle trailers, see figure 4.21. Ecocombi G has the same lay-out as the conventional combination, but dimensions are larger. Its rearward amplification value is much higher than the conventional vehicle. This is unexpected, as it was concluded that increasing the distance between the coupling point and the trailer wheels reduces rearward amplification. The same effect was explained for Ecocombi C and a truck-full trailer also; in the Ecocombi combination, mass and inertia of both the towing vehicle and trailer increased compared to the conventional vehicle. The inertia of the trailer should to be counteracted by the truck in the coupling point and by the trailer wheels. However, both the conventional vehicle and the Ecocombi have similar couplings and the same amount of trailer axles. Therefore, the Ecocombi has too little yaw damping in relation to its inertia. In reality, more than one axle is applied on the trailer which increases yaw damping. This is discussed in the next chapter.

Furthermore, Ecocombi E consist of two smaller centre axle trailers. Although this combination is stable at this vehicle speed, the resulting rearward amplification value is very large. Two inertia couplings exist in this combination; from the truck to the first centre axle trailer and from the first centre axle trailer to the second.

Finally, Ecocombi A is a special combination. The semitrailer is favourable for rearward amplification, but the centre axle trailer is not.

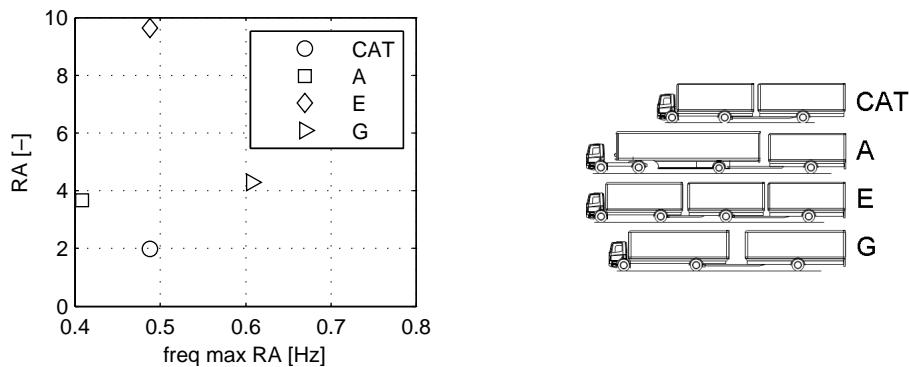


Figure 4.21: Rearward amplification value and frequency where the maximum occurs for all truck-centre axle trailers

The resulting values of rearward amplification are compared in figure 4.22 with the results of Pinxteren [31] as presented in the literature review (figure 2.6, section 2.5, page 11). The results of Pinxteren are used because he investigated all combinations analysed in this study also. Both the results of the frequency approach discussed in this section, and of a single lane change are shown. The input signal of the lane change is the same for all combinations, and illustrated in figure 4.1a (page 42). The input frequency of the lane change equals the frequency where rearward amplification is largest in the FRF.

It appears that the frequency domain rearward amplification results in larger differences between the combinations. This approach gives much higher values compared to Pinxteren and the single lane change. This is especially the case for the combinations containing full trailers and centre axle trailers. As explained before, this might be caused by the modelling of too little yaw damping, as in reality more axles are applied on these vehicles.

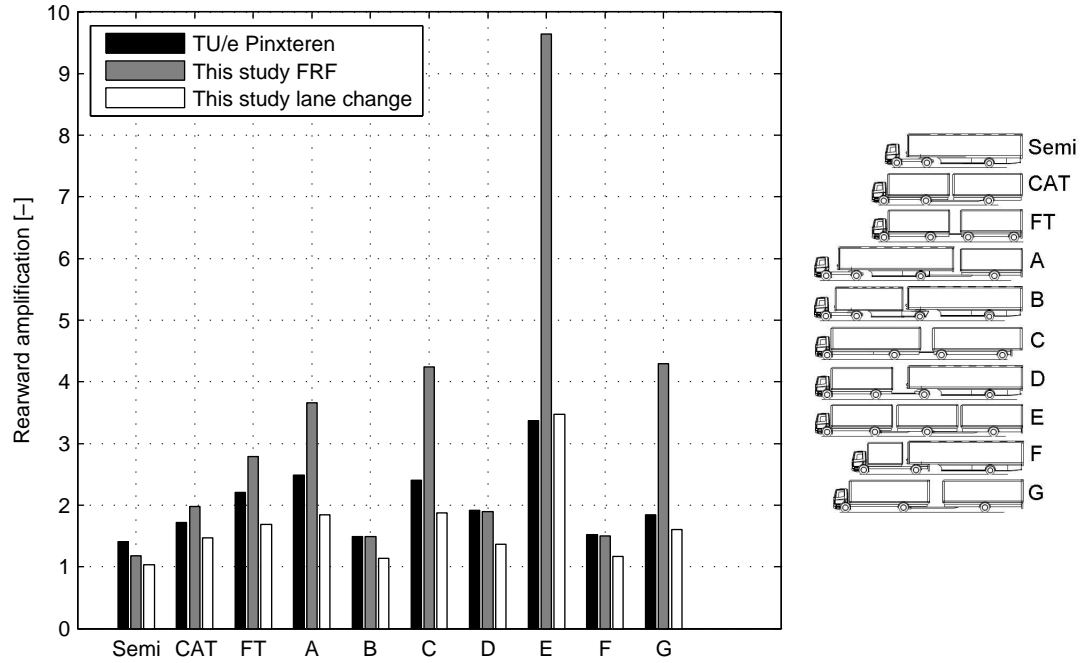


Figure 4.22: Ranking of the vehicle combinations in terms of rearward amplification, TU/e Pinxteren [31]

## 4.5 Concluding remarks

The performance measure rearward amplification is studied in this chapter. It turns out to be a better measure for the dynamic performance of truck combinations than stability, because a clear distinction between the various combinations can be made and the effect of parameter changes can be observed clearly.

The results of a time domain definition, which is used in many studies, appear not to be generic and reproducible; they largely depend on the steering wheel input frequency, the driver (as it is a closed-loop vehicle manoeuvre) and the vehicle speed. Therefore, a frequency domain approach is used in this thesis. In contrast to the time definition, equations can be derived for rearward amplification, which enhances the insight into the important phenomena causing amplification. Furthermore, the frequency domain approach can be used to calculate the frequency where rearward amplification is largest. This gives an indication for the frequency with which a lane change or single sine-wave manoeuvre should be carried out during full scale vehicle testing or when using complex multibody simulation models. Also, the results of the frequency domain approach for the different vehicles show a larger spread than the time domain approach.

The conventional and Ecocombi combinations are divided in three groups; (1) tractor-semitrailer combinations, (2) truck-centre axle trailer combinations, and (3) truck-full trailer combinations. The following conclusions can be drawn:

**Tractor-semitrailers:** The conventional vehicle combination, Ecocombi B and F are tractor-

semitrailer combinations. Table 4.1 shows the effect of the parameters having the most significant effect on rearward amplification of these vehicle combinations. The indicated requirements correspond to a small rearward amplification and a good dynamic performance of the vehicle combination.

Description	symbol	requirement
Distance between rear axle towing vehicle and coupling point	$e_1$	small
Distance between coupling point and trailer axle	$l_2$	large
Tendency to neutral steer or understeer	$s_1$	understeer

Table 4.1: Tractor-semitrailer requirements for a small rearward amplification value

The tractor-semitrailer combinations perform best compared to all other combinations. This is since the coupling point is located relatively far towards the centre of gravity of the towing vehicle and since the distance between the coupling point and the trailer axle is relatively large compared to the other vehicle combinations.

**Truck-centre axle trailers:** The conventional vehicle, Ecocombi A, E and G are of the group centre axle trailers. Table 4.2 shows the parameters which have most significant effect on the rearward amplification of the truck-centre axle trailers. The indicated requirements corresponds to a small rearward amplification value.

Description	symbol	requirement
Distance between rear axle towing vehicle and coupling point	$e_1$	small
Distance between coupling point and trailer axle	$l_2$	large
Tendency to neutral steer or understeer	$s_1$	understeer
Trailer inertia	$I_2 = m_2 k_2^2$	small

Table 4.2: Truck-centre axle trailer requirements for a small rearward amplification value

In contrast to the other combinations, the mass and inertia of the trailer are very important for the dynamic performance of combinations containing centre axle trailers.

**Truck-full trailers:** The conventional vehicle, Ecocombi C and D are truck-full trailers. Table 4.3 shows the parameters which have the most significant effect on rearward amplification of truck-full trailers. Again, the indicated requirements correspond to a better dynamic performance.

The mass of the trailer has no effect on rearward amplification of combinations containing full trailers, when the cornering stiffness scales linearly with vertical load and when a kinematic coupling between the units is assumed. This is in contrast to centre axle trailers. This distinction is caused by the different coupling between the towing unit and the trailer.

Description	symbol	requirement
Distance between rear axle towing vehicle and coupling point	$e_1$	small
Distance between coupling point and trailer axle	$l_2$	large
Inertia of the towing vehicle	$k_1$	small
Tendency to neutral steer or understeer towing vehicle	$s_1$	understeer
Tendency to neutral steer or understeer full trailer	$s_3$	neutral steer
Wheelbase towing vehicle	$l_1$	small
Wheelbase full trailer	$l_3$	large

Table 4.3: Truck-centre axle trailer requirements for a small rearward amplification value

Up till now, all vehicle combinations were modelled with single axles. However in reality, multiple axle per unit such as tandem or triple axles are applied in order to meet the maximum legal axle loads. They are used to reduce tyre and road wear while increasing the load capacity. The yaw damping can be increased by mounting more axles on the individual units. Therefore, the effect of mounting more axles on rearward amplification is explained in the next chapter.



---

## Effect of Multiple Axles on the Dynamic Performance of Articulated Vehicles

---

Segel et al. [33] conclude that multiple axles introduce yaw moments which resist the yaw motion of the vehicle. An equivalent wheelbase can be formulated, which is longer than the original geometric wheelbase. Therefore, as concluded by Houben [20] too, vehicles with multiple axles remain stable at higher vehicle speeds compared to the same vehicles with single axles. As a consequence, the evaluation of stability and rearward amplification with single axles corresponds to the worst case scenario.

It was concluded in the previous chapter, that the resulting rearward amplification values of some combinations is unrealistically high compared to the results of other studies. Equations are derived in this chapter to show the effect of multiple axles on rearward amplification. This chapter starts with a section which handles the modelling of multiple axles.

### 5.1 Modelling of multiple axles

The modelling of multiple axles is discussed in this section, by deriving the equation of motions for one application; a single vehicle with multiple axles on the rear. Furthermore, the equations of motion are generalised for a single vehicle with  $n$  axles per axle group. The equations for the other combinations are derived in appendix A. Furthermore, the effect of multiple axles and the distance between these axles is investigated numerically.

Figure 5.1 shows a free body diagram of a single vehicle with tandem axles at the rear. The following equations of motion can be derived, assuming the same lateral tyre stiffness on the tandem axles  $C_2$ , and a distance  $2j$  between the tandem axles:

$$\left. \begin{aligned} m_1(\dot{v}_1 + ur_1) &= -\frac{1}{u} \{ (C_1 + 2C_2)v_1 + (a_1C_1 - 2b_1C_2)r_1 \} + C_1\delta_1 \\ I_1\dot{r}_1 &= -\frac{1}{u} \{ (a_1C_1 - 2b_1C_2)v_1 + (a_1^2C_1 + 2b_1^2C_2 + 2j^2C_2)r_1 \} + a_1C_1\delta_1 \end{aligned} \right\}. \quad (5.1)$$

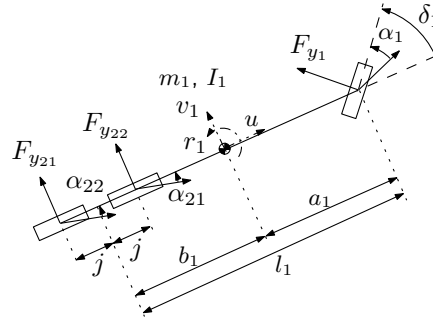


Figure 5.1: Free body diagram of a single vehicle with tandem rear axle

Abbreviations can be formulated in analogy with the abbreviations introduced for a single vehicle with single axles in (3.7) (section 3.1 page 15):

$$\left. \begin{aligned} C &= C_1 + 2C_2 \\ Cs_1 &= a_1C_1 - 2b_1C_2 \\ Cq_1^2 &= a_1^2C_1 + 2b_1^2C_2 + 2j^2C_2 \end{aligned} \right\}. \quad (5.2)$$

Comparing these expressions with the expressions for a vehicle with single axles in (3.7) shows that when the same parameters are used for single and multiple axles, the total cornering stiffness  $C$  increases compared to single axles, the vehicle becomes more understeered (as  $s_1$  becomes smaller) when mounting tandem axles at the rear, and the yaw damping increases (as  $q_1$  increases) compared to a vehicle with single axles.

It is assumed that the load on an axle group is evenly divided over the axles. This yields for the cornering stiffnesses, when assuming a linear relation between the cornering stiffness and vertical load as discussed in section 3.1.2 (page 16):

$$\left. \begin{aligned} C_1 &= f_1 m_1 \frac{b_1}{l_1} \\ C_2 &= \frac{1}{2} f_2 m_1 \frac{a_1}{l_1} \end{aligned} \right\}. \quad (5.3)$$

The abbreviations of (5.2) can be rewritten when normalised cornering stiffnesses are assumed to:

$$\left. \begin{aligned} C &= m_1 \frac{1}{l_1} (b_1 f_1 + a_1 f_2) \\ Cs_1 &= m_1 \frac{a_1 b_1}{l_1} (f_1 - f_2) \\ Cq_1^2 &= m_1 \frac{a_1}{l_1} (a_1 b_1 f_1 + (b_1^2 + j^2) f_2) \end{aligned} \right\}. \quad (5.4)$$

This yields that when the tyre stiffnesses scale with vertical load, the total cornering stiffness  $C$  and neutral steer parameter  $s_1$  are not affected, but the amount of yaw damping increases. This means for example that this vehicle remains stable for a higher vehicle speed in case it is oversteered compared to a two axle vehicle with the same parameters and single axles.

In general,  $i$  axle groups are assumed on a vehicle combination;  $i = 1$  for the front axle,  $i = 2$  for the rear axle,  $i = 3$  for the trailer axle of the first articulation, and  $i = 4$  for the trailer axle of the second articulation. Each axle group can have  $n_i$  axles, and the distance from the centre of gravity on an articulation to the symmetry axis of the axle group is  $x_i$ . Figure 5.2 illustrates these parameters. It is assumed that the cornering stiffness of all axles on one group is the same;  $C_i$ , and that all multiple axle groups are not steered.

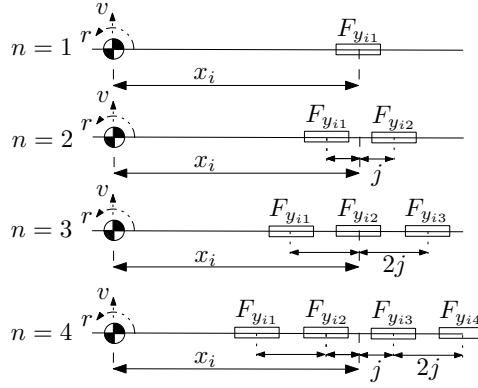


Figure 5.2: Modelling of multiple axles

Furthermore, the lateral forces can be expressed by two terms;  $F_{y_{in}}$  and  $F_{y_{ij}}$ . The first,  $F_{y_{in}}$ , equals the lateral tyre force when single axles are applied. The second,  $F_{y_{ij}}$ , has to be added for multiple axles. For the single vehicle discussed so far, these terms are expressed by:

$$\begin{aligned} F_{y_{in}} &= -\frac{1}{u}C_i(v_1 + x_i r_1) \\ F_{y_{ij}} &= -\frac{1}{u}C_i j r_1. \end{aligned} \quad (5.5)$$

This means that the lateral forces can be expressed as, see figure 5.2:

$$\begin{aligned} F_{y_1} &= C_1 \alpha_1 \\ &= -\frac{1}{u}C_1(v_1 + x_1 r_1) + C_1 \delta_1 \\ &= F_{y_{1n}} + C_1 \delta_1 \\ F_{y_{21}} &= C_2 \alpha_{21} \\ &= -\frac{1}{u}C_2(v_1 + x_2 r_1 - j r_1) \\ &= F_{y_{2n}} - F_{y_{2j}} \\ F_{y_{22}} &= C_2 \alpha_{22} \\ &= -\frac{1}{u}C_2(v_1 + x_2 r_1 + j r_1) \\ &= F_{y_{2n}} + F_{y_{2j}}, \end{aligned} \quad (5.6)$$

with  $x_1 = a_1$  and  $x_2 = -b_1$ .

The equations of motion can now be expressed as:

$$\left. \begin{aligned} m_1(\dot{v}_1 + u r_1) &= F_{y_1} + F_{y_{21}} + F_{y_{22}} \\ &= F_{y_{1n}} + F_{y_{2n}} + F_{y_{2j}} + C_1 \delta_1 \\ &= n_1 F_{y_{1n}} + n_2 F_{y_{2n}} + C_1 \delta_1 \\ I_1 \dot{r}_1 &= x_1 F_{y_1} + (x_2 - j) F_{y_{21}} + (x_2 + j) F_{y_{22}} \\ &= x_1 F_{y_{1n}} + (x_2 - j)(F_{y_{2n}} - F_{y_{2j}}) + (x_2 + j)(F_{y_{2n}} + F_{y_{2j}}) + a_1 C_1 \delta_1 \\ &= n_1 x_1 F_{y_{1n}} + n_2 x_2 F_{y_{2n}} + 2j F_{y_{2j}} + a_1 C_1 \delta_1 \end{aligned} \right\}, \quad (5.7)$$

with  $n_1 = 1$ ,  $n_2 = 2$ . The equations of motion of the other vehicle combinations discussed in this study are derived in appendix A.

Figure 5.3 illustrates the effect of adding axles and placing the axles further apart on the rearward amplification value of Ecocombi E (truck-centre axle trailer-centre axle trailer combination, for the parameters see appendix B). The reference combination has a single towing vehicle front axle, a tandem towing vehicle rear axle group, and tandem axles on both centre axle trailers. The number of axles on both trailers is changed in figure 5.3a. The distance between all axles on all axle groups is changed in figure 5.3b, so this is on both the towing vehicles rear axle group, and the first and second trailer axle groups. Note that the truck has a tandem rear axle in this case, in contrast to the simulations performed in the previous chapter. From figure 4.21 (section 4.4, page 65) it follows that rearward amplification is about 9.5 when single axles are applied on all axle groups. Figure 5.3a reveals that mounting tandem axles at the rear of the towing vehicle and single axles on all other axle groups, already results in a decrease of rearward amplification to 6.7.

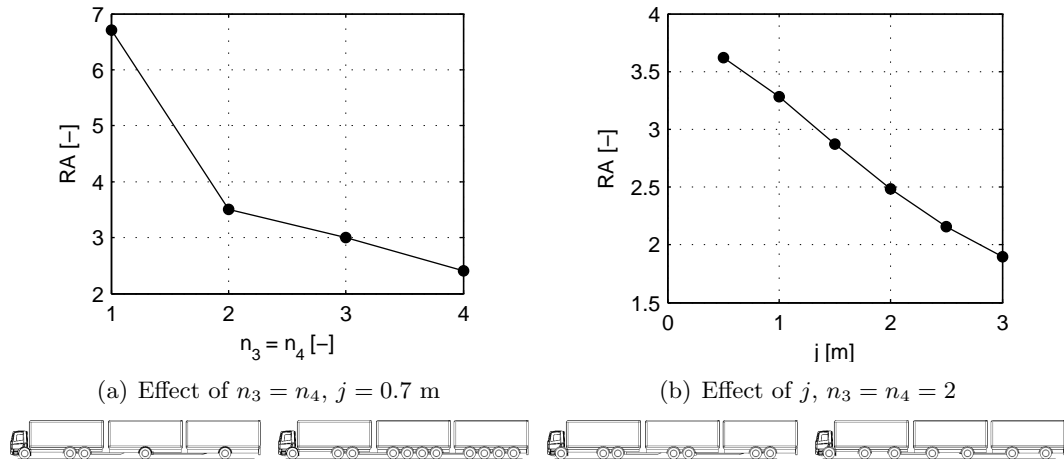


Figure 5.3: Effect of multiple axles on rearward amplification of an Ecocombi E combination, for parameters see appendix B

Finally, it can be concluded that rearward amplification decreases as the yaw damping increases when more axles are applied (increasing  $n$ ) and when the axles are placed further apart (increasing  $j$ ).

## 5.2 Effect of multiple axles on rearward amplification of all combinations

The effect of multiple axles on rearward amplification of all conventional vehicles and Ecocombi combinations is investigated in this section. The parameters used in the simulations are listed in appendix B. As concluded in the previous section, the yaw damping increases when applying more axles. Therefore, the value for rearward amplification decreases when multiple axles are applied.

Figure 5.4 shows the resulting value for rearward amplification and the frequency where the maximum occurs for both the vehicles with single axles and multiple axles. It appears that the values for rearward amplification decrease. The frequency where the maximum occurs generally decreases for the tractor-semitrailer combinations and increases for all other combinations.

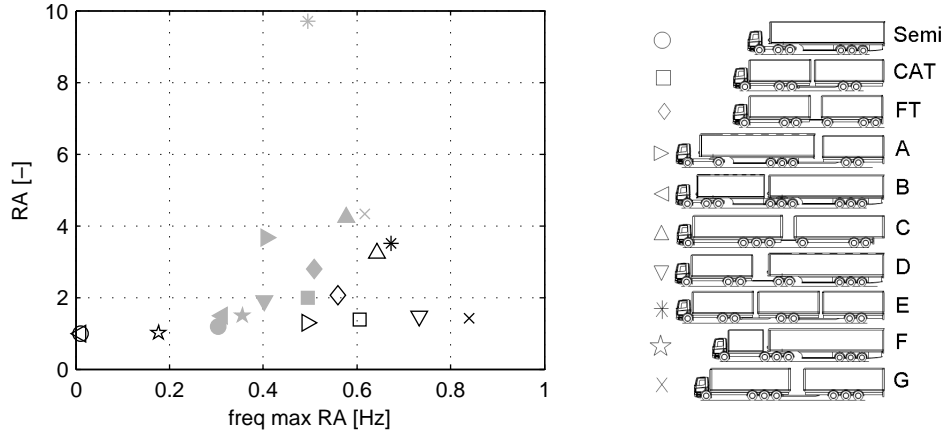


Figure 5.4: Rearward amplification value and frequency where the maximum occurs for all conventional vehicles and Ecocombi's, gray = single axles, black = multiple axles

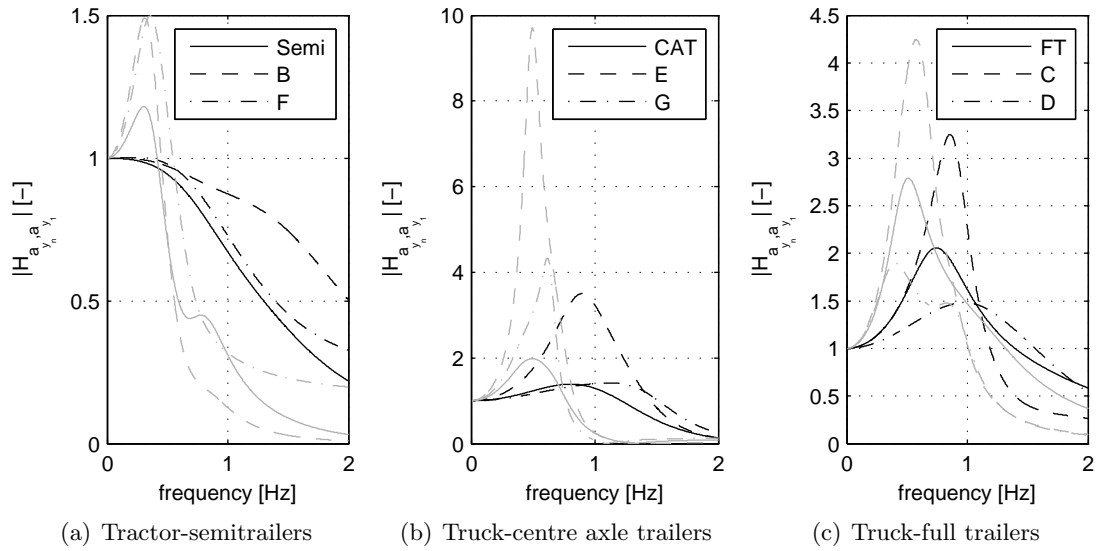


Figure 5.5: Comparison of  $|H_{a_{y_n}, a_{y_1}}|$  for single axles (gray) and multiple axles (black)

Figure 5.5 shows some magnitude plots of the lateral acceleration gains. The tractor-semitrailer combinations (the conventional vehicle, Ecocombi B and F) were already well damped with single axles due to the long wheelbase of the semitrailer. Adding axles increased yaw damping even further. As a result, figure 5.5a shows that the amplification is smaller than one for dynamic manoeuvres and obviously equal to one for steady-state driving. Therefore, the frequency where the

maximum occurs is close to or equal to zero. However, for some input frequencies the magnitude increased compared with the single axle simulation. Therefore, it is very important to compare the combination at the right input frequency.

For the other two groups, the truck-centre axle trailers and the truck-full trailers, adding yaw damping results in a larger damped eigen frequency compared to single axles. This is because the vehicle combination requires more steering input to excite the eigen frequency due to the increased damping.

Figure 5.6 shows a comparison of the resulting values for rearward amplification with single and multiple axles, calculated in the same way as illustrated in figure 4.22 (section 4.4, page 66). Four bar graphs are shown; (1) results of the FRF's with single axles, (2) results of the FRF's with multiple axles, (3) results of a single lane change with single axles (the steering wheel input frequency equals the frequency where the amplification is largest in the FRF of the single axles FRF), and (4) results of a single lane change with multiple axles (the input frequency equals the frequency where the amplification is largest in the multiple axles FRF).

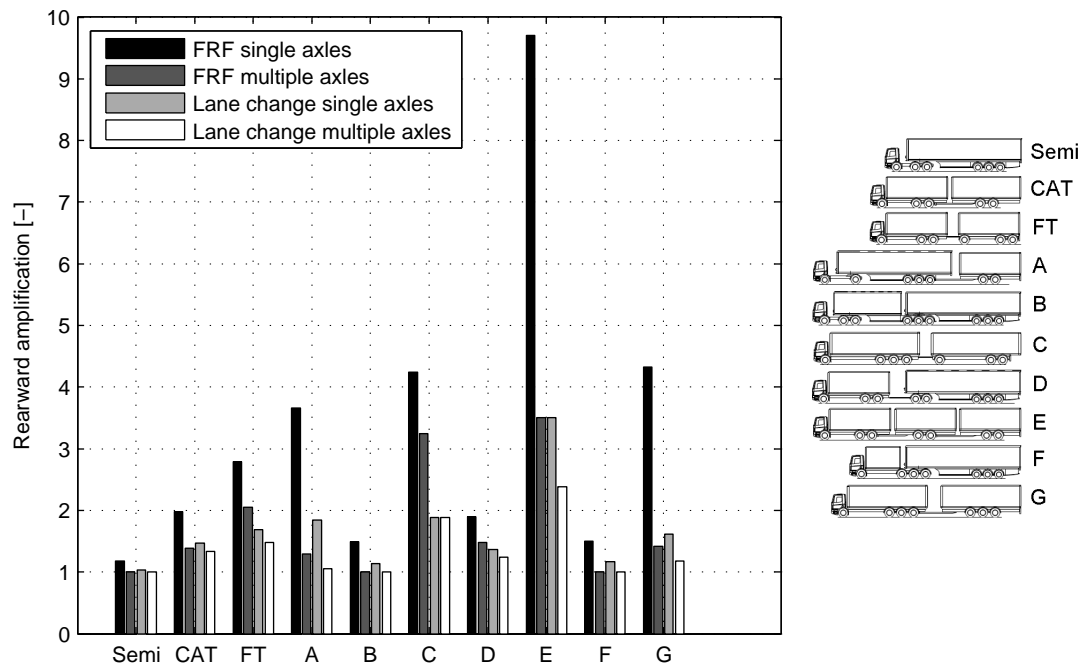


Figure 5.6: Comparison of the resulting rearward amplification with multiple and single axles

From this figure, it can be observed that all rearward amplification values decreased. However, the results of the FRF simulations with single axles and multiple axles deviate more than the results of the lane changes. Therefore, the FRF approach seems more sensitive to adding axles than the time domain approach.

In the next overview the results of the vehicle combinations are compared with the results of other studies. The combinations are divided in the following vehicle groups; tractor-semitrailers, truck-centre axle trailers and truck-full trailers.

**Tractor-semitrailers:** Figure 5.7 shows the resulting rearward amplification values in the frequency approach of the conventional tractor-semitrailer, Ecocombi B and F and the results of two studies presented in the literature review (figure 2.6, section 2.5, page 11).

The resulting rearward amplification differs per study, as concluded also in the literature review. The main reasons for these discrepancies are; (1) the vehicle parameters are not the same, (2) some studies use linear vehicle and tyre models, others use non-linear models, (3) some studies use one track vehicle models, others are based on a multibody simulation model or are obtained during full scale vehicle testing, (4) the input differs per study, and (5) the vehicle speed differs per study.

Nevertheless, the figure shows that the results of both the combinations with single and multiple axles are of the right order of magnitude. Note that the results of this study with multiple axles correspond to steady-state driving as the rearward amplification is one. Furthermore, the rearward amplification of Ecocombi B of the ARRB is smaller than one. It can be concluded from figure 5.5a that this is not the maximum over the frequency range, as rearward amplification is always one at steady-state driving.

Finally, it can be concluded that adding axles does not improve the results of the tractor-semitrailer combinations significantly. This is since most yaw damping is obtained by the long wheelbase of the semitrailer.

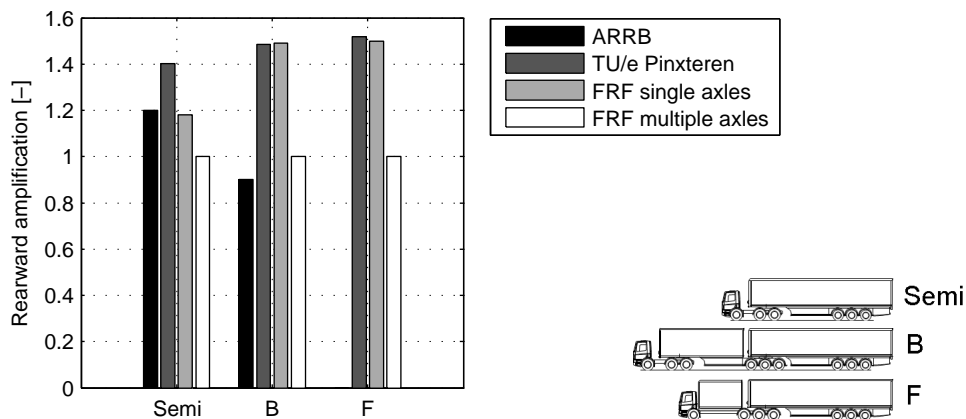


Figure 5.7: Comparison of the resulting rearward amplification of the tractor-semitrailer combinations with other studies, ARRB [16] and TU/e Pinxteren [31]

**Truck-centre axle trailers:** Figure 5.8 shows the results of the conventional tractor-centre axle trailer, Ecocombi A, E and G. In contrast to the tractor-semitrailer combinations rearward amplification decreases significantly when applying multiple axles, especially for the Ecocombi's. It appears that the axles have to account for most the damping of the centre axle trailer. The trailer axles are important as the centre of gravity of a centre axle trailer is directly above the trailer wheels. The increased yaw damping due to the application of multiple axles is now much better in proportion to the weight and dimensions of the Ecocombi's.

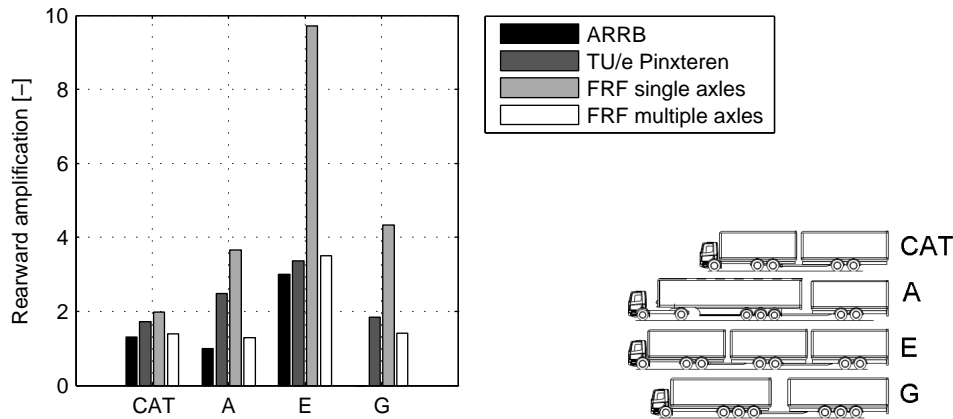


Figure 5.8: Comparison of the resulting rearward amplification of the truck-centre axle trailer combinations with other studies, ARRB [16] and TU/e Pinxteren [31]

**Truck-full trailers:** Figure 5.9 shows the results of rearward amplification of the conventional truck-full trailer, Ecocombi C and D. The rearward amplification decreases especially for Ecocombi C. This is since this vehicle combination has both an increase truck and trailer wheelbase in comparison with the conventional combination. In contrast, the trailer wheelbase of Ecocombi D is very large. Like for the tractor-semitrailers, even with single axles significant yaw damping is obtained in Ecocombi D with the large trailer wheelbase. For Ecocombi C the increased weight due to the larger loading space has to be counteracted by the multiple axle groups.

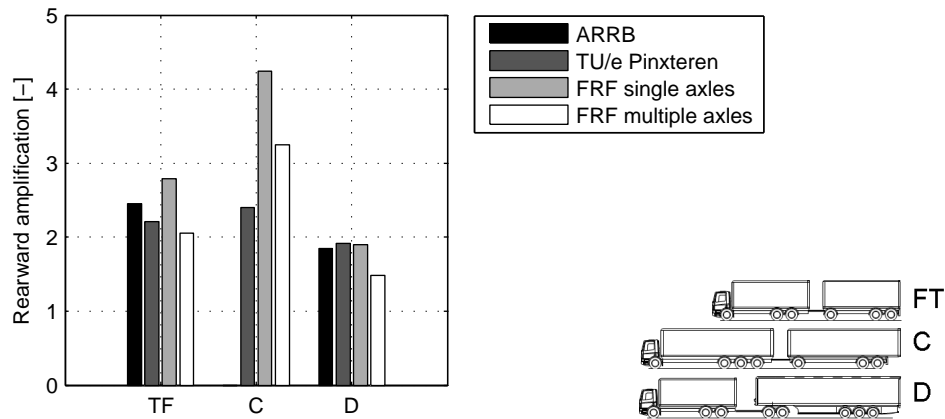


Figure 5.9: Comparison of the resulting rearward amplification of the truck-full trailer combinations with other studies, ARRB [16] and TU/e Pinxteren [31]

Finally, figure 5.10 illustrates the comparison of all vehicle combinations. The resulting rearward amplification differs per study, as concluded also in the literature review. However, in general the trend and ranking between the vehicle combinations is the same when comparing the combinations relative to each other. Note that the result of Pinxteren of Ecocombi A is an exception.



It can be concluded that the frequency domain approach can be used as a more generic and reproducible way to analyse rearward amplification.

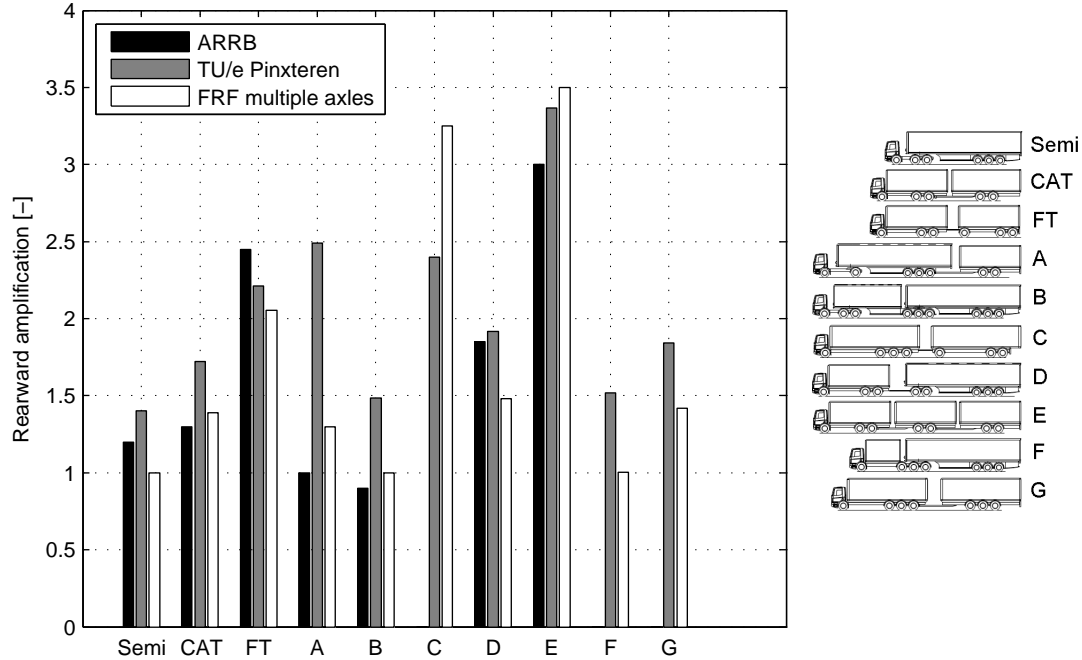


Figure 5.10: Ranking of the vehicle combinations in terms of rearward amplification, ARRB [16] and TU/e Pinxteren [31]

### 5.3 Concluding remarks

In this chapter the effect of applying multiple axles per axle group on rearward amplification is analysed. The values using the frequency domain approach dramatically decreases when multiple axles are applied. These results are now better comparable with other studies. Moreover, the frequency domain approach shows a larger difference in resulting rearward amplification values than the time domain approach, and is therefore more sensitive for these variations.

The following conclusions can be drawn for the three vehicle groups:

- For the tractor-semitrailers, the yaw damping is mostly obtained by the large distance between the coupling point and the trailer axle. This effect is more significant than adding trailer axles.
- In the truck-centre axle trailers, the trailer load is located close to, or directly above the trailer axles. Therefore, especially the trailer axle group has to account for the yaw damping of a centre axle trailer. Adding axles improves rearward amplification, as well as placing the axles further apart.
- For the full trailers adding trailer axles improves rearward amplification, as well as placing them further apart and increasing the wheelbase of the trailer.



---

## Conclusions and Recommendations

---

This research focusses on gaining fundamental understanding on the effects of various lay-outs and parameters on the lateral dynamic behaviour of articulated vehicles. A generic method is proposed which can be used to gain this understanding. The entire range of vehicles used on the European roads is addressed, which includes the conventional tractor-semitrailer, truck-centre axle trailer and truck-full trailer and seven Ecocombi combinations. The effect of multiple axles is investigated, steered axles other than the towing vehicles front axle are out the scope of this thesis. This chapter gives the main conclusions and recommendations.

### 6.1 Conclusions

The stability boundaries of the conventional vehicle combinations are investigated first. The normalised cornering stiffness can be assumed during nominal loading conditions; the tyre cornering stiffness scales linearly with the vertical force applied on the tyre. The following conclusions can be drawn:

- A single vehicle is stable and remains stable at any speed due to any parameter variation when the normalised cornering stiffness of the rear axle is larger than the normalised cornering stiffness of the front axle ( $f_2 > f_1$ ).
- The load of a semitrailer is partly carried by the towing vehicle. The tractor-semitrailer combination can experience a saddle-node bifurcation when the portion of the weight of the trailer carried by the towing vehicle becomes too large, such that normalised cornering stiffnesses at the rear axle of the towing vehicle cannot be assumed anymore. When the normalised cornering stiffness can be assumed, a tractor-semitrailer remains stable after a parameter variation for all speeds in terms of both the saddle-node and Hopf bifurcation when it is understeered initially.
- The centre of gravity of a centre axle trailer is located close to the trailer axle. Therefore, there is only little load transfer between the towing vehicle and the trailer. As a result, a saddle-node bifurcation does not occur for a truck-centre axle trailer combination. However, the combination can become unstable with an oscillatory motion when the inertia of the trailer is relatively large in relation to the inertia of the towing vehicle. The dimensions play

an important role in this balance as well; the distance between the coupling point and the trailer wheels should be relatively small, the distance between the centre of gravity of the towing vehicle and the coupling point should be relatively large to experience instability. Furthermore, instability occurs when the speed exceeds the critical speed.

- Finally, a truck-full trailer has no dynamic but only a kinematic coupling between its units when assuming a massless steering dolly with no inertia and no mechanical trail at the front axle of the full trailer. There is no load transfer between the units and the dynamics of the towing vehicle are not affected by the trailer at all. As a result, the stability problem reduces to the stability problem of a single vehicle.

The stability analysis gives insight into the stability boundaries of articulated vehicles. It appears that most vehicle combinations are stable during normal driving conditions where normalised cornering stiffnesses can be assumed. Only very extreme parameter combinations may lead to instability. It can be concluded that stability cannot distinguish between various lay-outs and parameter settings.

Therefore, the performance measure rearward amplification is used, which quantifies the lateral acceleration magnification in a vehicle system. It is often used to investigate the lateral damping in vehicle combinations, since although the combinations were concluded to be stable, their amount of damping is expected to differ. The following conclusions can be drawn from the analysis on rearward amplification:

- This performance measure is capable of distinguishing between the articulated vehicles.
- A frequency domain approach should be used, which gives information over the entire frequency range. A time domain approach is often used in literature where a dynamic vehicle manoeuvre such as a lane change is used as input. In contrast to the time domain approach, the frequency domain approach is better reproducible, more robust, driver independent and mathematic equations can be derived to investigate the effect of vehicle parameters on the dynamic performance of the combinations. Furthermore, a larger deviation of the resulting rearward amplification values can be observed for the frequency approach compared to the time domain approach, which makes the differences between the combinations more clearly.
- A semitrailer in a combination results in a relatively small rearward amplification. This is for the conventional tractor-semitrailer and for the Ecocombi's containing semitrailers. The two main reasons are; (1) the distance between the centre of gravity of the towing vehicle and the coupling point is relatively small, which results in a small input to the trailer as the motion at the coupling point is hardly amplified, and (2) the distance between the coupling point and the trailer wheels is relatively large, which results in much yaw damping. Reducing the distance between the centre of gravity of the towing vehicle and the coupling point and increasing the trailer wheelbase and drawbar length also reduces rearward amplification for the other combinations.
- The loading ratio, the mass of the trailer divided by the mass of the towing vehicle, is unimportant for the rearward amplification of the conventional and Ecocombi truck-full trailer combinations when assuming a linear relationship between the cornering stiffness and the vertical load applied on the axle. This is since the units are assumed to be kinematically

coupled; the dynamics of the towing vehicle is not affected by the dynamics of the trailer. However, due to the dynamic coupling of centre axle trailers, the loading ratio is very important for the rearward amplification when this unit is part of the combination.

Finally, the effect of multiple axles on the dynamic performance of articulated vehicles is investigated. This is because multiple axles per axle group are applied in order to meet the maximum legal axle loads and to reduce tyre and road wear. This is especially for the Ecocombi combinations. The following conclusions can be drawn:

- The resulting rearward amplification value of the frequency domain approach reduces significantly for the truck-centre axle trailer and truck-full trailer combinations when multiple axles are applied.
- Rearward amplification of semitrailer combinations does not change significantly when multiple axles are applied, as the yaw damping is obtained mostly by the large trailer wheelbase.
- The difference between the rearward amplification results in the time domain approach and the frequency domain approach reduces when multiple axles are applied due to the increased yaw damping.
- The effect of multiple axles can be observed more clearly with the frequency domain approach than with the time domain approach.
- For combinations containing either centre axle trailers or the full trailers it is important to model the amount of axles on the unit in proportion to the length, weight and inertia of the combination.

Note that these conclusions hold when performing simulations on smooth road surfaces under optimal simulation conditions. This is because in these simulations effects like side wind gusts, rutting, and excitation of for instance the steering dolly due to uneven road surfaces are not taken into account. Furthermore, single track vehicle models are used, which means that load transfer, uneven steering and uneven braking at the left and right wheels are not taken into account.

## **6.2 Recommendations for electronic stability control function tests at DAF**

At DAF these results can be used to examine new yaw stability control functions using a complex multibody simulation model. It is recommended to simulate with the most critical configurations such that the resulting rearward amplification is large and the stability control function is challenged most. Again note that these recommendations hold for the assumptions made in this study. The following recommendations are formulated:

- Analyse dynamic vehicle yaw behaviour with a performance measure like rearward amplification, which is capable of distinguishing between the vehicle combinations and parameters based on their yaw damping. Stability boundaries should not be studied.

- Use the linear one track models discussed in this study in a frequency domain approach to approximate the input frequency where rearward amplification is largest.
- Perform simulations with as little axles as possible on the combination as permitted by law, in order to simulate with a vehicle combination with little yaw damping which results in high amplifications.
- From all applications, select the vehicles with small trailer wheelbases, large coupling rear overhangs and short drawbars. At DAF this is for instance an FA with a small wheelbase, large coupling rear overhang and a full trailer with a sort wheelbase.
- For a tractor-semitrailer; place the load of the trailer as far as possible to the front of the trailer.
- For a truck-centre axle trailer; simulate with an unladen towing vehicle and laden trailer and with a high inertia.
- For a truck-full trailer combination; do not spend time on investigating the effect of the load or load distribution in the trailer.

### 6.3 Recommendations for further research

Finally, the following recommendations are formulated for further research:

- Investigate the effect of excitations of the vehicle other than the towing vehicle's front wheel steering wheel input on the dynamic yaw behaviour and the conclusions formulated in this study. For example the effect of side wind gusts, rutting, and steering inputs from other axles in the vehicle combination.
- Investigate the effect of mechanical and pneumatic trail, different excitation on the left and right wheels (two track model), load transfer between left and right wheels, the effect of roll, camber, flexibilities etc on the results presented in this study.
- Investigate which open-loop dynamic vehicle manoeuvre is better reproducible and generic than the closed-loop lane change. This open-loop test can be used during full scale testing or when using complex simulation models as a time domain simulation to investigate rearward amplification. The results should be better reproducible and generic such that the results of different studies can be compared more easily.
- Investigate the mathematic relation between rearward amplification calculated in the frequency and time domain. With this relation the results of the two approaches can be compared more accurately.
- Perform road test with several vehicle combinations in order to validate the single track vehicle models used in this study.
- This study uses both linear vehicle and tyre models. The validity of the results should be investigated when the vehicle behaviour or tyre characteristics become non-linear for large

articulation angles, high loads and large tyre slip angles. This requires detailed tyre characteristics. Especially the non-linear part of the cornering stiffness to vertical load characteristic should be measured more accurately. Also check the validity of the kinematic coupling of a truck-full trailer combination.

- Finally, it is recommended to investigate the possibility to define the requirements on the dynamic behaviour of articulated vehicles in terms of the so-called string stability, which provides a more or less structured framework allowing for analysis of amplification of disturbances in interconnected system. Within this framework, one approach is to define disturbance transfer functions from one subsystem to another in the interconnected system and then determine the disturbance amplification by means of bounds on input-output norms.





---

## Bibliography

---

- [1] Road vehicles- heavy commercial combinations and articulated buses lateral stability test methods. ISO/FDIS 4791:1999(E).
- [2] [www.dafrucks.com](http://www.dafrucks.com).
- [3] [www.ecocombi.com](http://www.ecocombi.com).
- [4] ACEA. Official publication of the GSR (Regulation (EC) No 661/2009). Technical Regulations No 52, 2009. ACEA 20091118.
- [5] R. Andrzejewski and J. Awrejcewicz. *Nonlinear dynamics of a wheeled vehicle*. Springer, 2005.
- [6] J. Aurell and T. Wadman. Vehicle combinations based on the modular concept, background and analysis. Technical Report ISSN 0347-2485, Volvo Trucks, 2007.
- [7] I.J.M. Besselink. *Vehicle Dynamics*. Eindhoven University of Technology, Mechanical Engineering - Dynamics and Control, 2008. Lecture notes 4L150.
- [8] P. Christidis and G. Leduc. Longer and heavier vehicles for freight transport. Technical Report EUR 23933 EN - 2009, European Commission, Joint Research Centre, Institute for Prospective Technological Studies, 2009.
- [9] G. de Ceuster, T. Breemers, B. van Herbruggen, K. Verweij, I. Davydenko, M. Klingender, B. Jacob, H. Arki, and M. Bereni. Effects of adapting the rules on weights and dimensions of heavy commercial vehicles as established within Directive 96/53/EC. Technical Report TREN/G3/318/2007, Transport and Mobility Leuven, TNO, Laboratoire Central des Ponts et Chaussées, RWTH Aachen University, November 2008.
- [10] J.R. Ellis. *Vehicle Handling Dynamics*. Page Bros, 1994.
- [11] R.D. Ervin, P.S. Fancher, and T.D. Gillespie. An overview of the dynamic performance properties of long truck combinations. Technical Report UMTRI-84-26, The University of Michigan Transportation Research Institute, July 1984.

- [12] E. Esmailzadeh and B. Tabarrok. Directional response and yaw stability of articulated log hauling trucks. *SAE Technical Paper Series*, (2000-01-3478), 2000.
- [13] P. Fancher, C. Winkler, R. Ervin, and H. Zhang. Using braking to control the lateral motions of full trailers. In *The dynamics of vehicles on roads and on tracks: Supplement to Vehicle System Dynamics Volume 29*, pages 462–478, 1998.
- [14] P.S. Fancher. Directional dynamics considerations for multi-articulated, multi-axled heavy vehicles. In *Vehicle Dynamics related to braking and steering*, volume SP-801. SAE International, 1989.
- [15] P.S. Fancher and A. Mathew. A vehicle dynamics handbook for single-unit and articulated heavy trucks. Technical Report UMTRI-81-21, The University of Michigan Transportation Research Institute, May 1987.
- [16] A. Germanchev and P. Eady. Heavy vehicle benchmarking study. Technical Report VC74134-01, for Organisation for Economic Co-operation and Development, by ARRB Consulting Australia, March 2009.
- [17] A. Hac, D. Fulk, and H. Chen. Stability and control considerations of vehicle-trailer combination. *SAE Technical Paper Series*, (2008-01-1228), 2008.
- [18] F. Hecker, H. Schramm, C. Beyer, G. Holler, and M. Bennett. Heavy vehicle stability notification and assistance. *SAE Technical Paper Series*, (2000-01-3481), 2000.
- [19] R.B.J. Hoogvelt, C.W. Klootwijk, and P.A.J. Ruijs. Ontwerp testmethode dynamische kantelstabiliteit voor zwaar verkeer. Technical Report 00.OR.VD.028.1/RH, TNO Wegtransportmiddelen, 2000.
- [20] L.W.L. Houben. Analysis of truck steering behaviour using a multi-body model. Master's thesis, Eindhoven University of Technology, Department Mechanical Engineering, Dynamics and Control Group and DAF Trucks N.V., Technical Analysis Group, 2008. DCT 2008-343.
- [21] G. Isiklar. Simulation of complex articulated commercial vehicles for different driving manoeuvres. Master's thesis, Eindhoven University of Technology, Department Mechanical Engineering, Dynamics and Control Group, 2007. DCT 2007.122.
- [22] K. Klotter. *Technische Schwingungslehre, Zweiter Band*. Springer Verlag, zweite edition, 1981.
- [23] I. Knight, W. Newton, T. Barlow, I. McCrae, M. Dodd, G. Couper, H. Davies, A. Daly, B. McMahon, E. Cook, V. Ramdas, N. Taylor, A. McKinnon, and A. Palmer. Longer and or Longer and Heavier Goods Vehicles (LHVs) A study of the likely effects if permitted in the UK: Final report. Technical Report PPR 285, for the Department for Transport, Transport Technology and Standards Division UK, by TRL Limited, June 2008.
- [24] K. Langwieder, J. Gwehenberger, T. Hummel, and J. Bende. Benefit potential of ESP in real accident situations involving cars and trucks. Technical report, GDV, Institute for vehicle safety Munich, May 2003. 18<sup>th</sup> International Technical Conference on the Enhanced Safety of Vehicles.

- [25] R. E. Mansvelders. The dynamic behaviour and stability control of a truck/full-trailer combination. Master's thesis, Eindhoven University of Technology, Department Mechanical Engineering, Dynamics and Control Group and DAF Trucks N.V., Technical Analysis Group, 2006. DCT 2006.137.
- [26] M. Mitschke. *Dynamik der Kraftfahrzeuge, Band C, Fahrverhalten*. Springer Verlag, second edition, 1990.
- [27] S. Neele. Ecocombi's in de strijd tegen uitlaatemissies en files. In *Eco Design*, number 19, pages 6–8. Maart 2009.
- [28] H.B. Pacejka. *Tyre and vehicle dynamics*. Butterworth Heimann, 2006, second edition.
- [29] J.P. Pauwelussen, G. Anghelache, dr. Theodorescu, and A. Schmeitz. Yaw stability of articulated trucks. Leonardo DaVinci, module 10.
- [30] H.C. Pflug. Innovative truck-trailer concepts as a means of efficiency improvement. Efficiency in Road Transport 62nd International Motor Show CV, Hanover, September 30 2008.
- [31] M. Pinxteren. Brake and roll-over performance of longer heavier vehicle combinations. Master's thesis, Eindhoven University of Technology, Department Mechanical Engineering, Dynamics and Control Group, 2009. DCT 2009.063.
- [32] A. Renschler. Speech by Andreas Renschler, Board of Management DaimlerChrysler, Truck Group Chairman of the VDA Board Group Commercial Vehicles. given at the VDA Press Conference Commercial Vehicle Concepts for the Future EuroCombi, September 20 2006.
- [33] L. Segel, R. Ervin, and P. Fancher. *The mechanics of heavy-duty trucks and truck combinations*. The International Association for Vehicle Design, 1981.
- [34] H. Troger and K. Zeman. A nonlinear analysis of generic types of loss of stability of the steady state motion of a tractor-semitrailer. In *Vehicle System Dynamics*, volume 13, pages 161–172, 1984.
- [35] B. Veldpaus and R. Huisman. Lineaire laterale bandeigenschappen ten behoeve van FEM-simulaties. Internal report 51051/03-036, DAF Trucks N.V. Technical Analysis Group, 2004.
- [36] C.B. Winkler, D. Blower, R.D. Ervin, and R.M. Chalasani. *Rollover of heavy commercial vehicles*. Society of Automotive Engineers, Inc., 2000.



---

## Equations of Motion

---

In this appendix, equations of motion are derived which can be applied on all vehicles discussed in this report. Equations of motion are derived for a vehicle with two articulations, which is the maximum in the European Union. The corresponding masses, inertias and cornering stiffnesses have to be set to zero if vehicles with less articulations are considered.

The assumptions used in the vehicle modelling are discussed first. Then the equations of motion for a vehicle with single axles are derived. The generalisation to multiple axles is made after that.

### A.1 Assumptions for single track vehicle modelling

The following assumptions are used:

- Small articulation angles and tyre slip angles; linear equations of motion.
- The left and right tyres on an axle can be lumped into a single equivalent 'tyre'.
- No body roll; the centers of gravity of the units are in the ground plane.
- Centre point steering; no pneumatic or mechanical trail.
- Constant forward velocity.
- No aerodynamic forces work on the vehicle combination.

### A.2 Equations of motion with single axles

Figure A.1 shows the free body diagram of a single track vehicle model with two articulations.

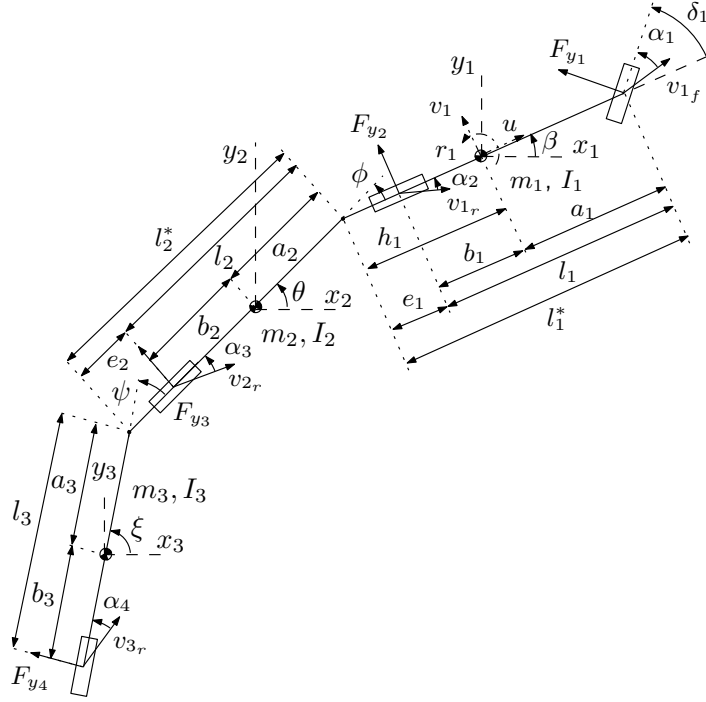


Figure A.1: Free body diagram vehicle with two articulations

Lagrange equations of motion are used:

$$\frac{d}{dt} \frac{\partial T}{\partial \dot{q}_i} - \frac{\partial T}{\partial q_i} + \frac{\partial U}{\partial q_i} = Q_i \quad i = 1 \dots n, \quad (\text{A.1})$$

with  $T$  the kinetic energy,  $U$  the potential energy,  $Q_i$  the generalised force,  $n$  the number of states and  $q_i$  the generalised coordinates.

A linear approach is used in this study. This means that the articulation angles and tyre slip angles are assumed to be small. The following relations apply:

$$\begin{aligned} x &= x_1 = x_2 = x_3 \\ y_2 &= y_1 - h_1\beta - a_2\theta \\ y_3 &= y_1 - h_1\beta - l_2^*\theta - a_3\xi. \end{aligned} \quad (\text{A.2})$$

The generalised coordinates are:

$$q = \begin{bmatrix} x & y_1 & \beta & \theta & \xi \end{bmatrix}^T. \quad (\text{A.3})$$

The kinetic energy can now be expressed as:

$$\begin{aligned} T &= \frac{1}{2}m_1(\dot{x}^2 + \dot{y}_1^2) + \frac{1}{2}m_2(\dot{x}^2 + \dot{y}_2^2) + \frac{1}{2}m_3(\dot{x}^2 + \dot{y}_3^2) + \frac{1}{2}I_1\dot{\beta}^2 + \frac{1}{2}I_2\dot{\theta}^2 + \frac{1}{2}I_3\dot{\xi}^2 \\ &= \frac{1}{2}(m_1 + m_2 + m_3)(\dot{x}^2) + \frac{1}{2}(m_2 + m_3)(h_1^2\dot{\beta}^2 - 2h_1\dot{y}_1\dot{\beta}) \\ &\quad + \frac{1}{2}m_2(a_2^2\dot{\theta}^2 - 2\dot{y}_1a_2\dot{\theta} + 2h_1\dot{\beta}a_2\dot{\theta}) + \frac{1}{2}m_3(l_2^{*2}\dot{\theta}^2 + a_3^2\dot{\xi}^2 - 2\dot{y}_1l_2^*\dot{\theta} - 2\dot{y}_1a_3\dot{\xi} \\ &\quad + 2h_1\dot{\beta}l_2^*\dot{\theta} + 2h_1\dot{\beta}a_3\dot{\xi} + 2l_2^*\dot{\theta}a_3\dot{\xi}) + \frac{1}{2}I_1\dot{\beta}^2 + \frac{1}{2}I_2\dot{\theta}^2 + \frac{1}{2}I_3\dot{\xi}^2. \end{aligned} \quad (\text{A.4})$$

This yields for the Lagrange terms:

$$\begin{aligned}
\frac{d}{dt} \frac{\partial T}{\partial \dot{x}} &= (m_1 + m_2 + m_3) \ddot{x} \\
\frac{d}{dt} \frac{\partial T}{\partial \dot{y}_1} &= (m_1 + m_2 + m_3) \ddot{y}_1 - (m_2 + m_3) h_1 \ddot{\beta} - m_2 a_2 \ddot{\theta} - m_3 (l_2^* \ddot{\theta} + a_3 \ddot{\xi}) \\
\frac{d}{dt} \frac{\partial T}{\partial \dot{\beta}} &= (m_2 + m_3) h_1 (h_1 \ddot{\beta} + \ddot{y}_1) + m_2 h_1 a_2 \ddot{\theta} + m_3 h_1 (l_2^* \ddot{\theta} + a_3 \ddot{\xi}) + I_1 \ddot{\beta} \\
\frac{d}{dt} \frac{\partial T}{\partial \dot{\theta}} &= m_2 a_2 (a_2 \ddot{\theta} - \ddot{y}_1 + h_1 \ddot{\beta}) + m_3 l_2^* (l_2^* \ddot{\theta} - \ddot{y}_1 + h_1 \ddot{\beta} + a_3 \ddot{\xi}) + I_2 \ddot{\theta} \\
\frac{d}{dt} \frac{\partial T}{\partial \dot{\xi}} &= m_3 a_3 (a_3 \ddot{\xi} - \ddot{y}_1 + h_1 \ddot{\beta} + l_2^* \ddot{\theta}) + I_3 \ddot{\xi} \\
\frac{\partial T}{\partial q_i} &= 0 \quad i = 1 \dots n \\
\frac{\partial U}{\partial q_i} &= 0 \quad i = 1 \dots n.
\end{aligned} \tag{A.5}$$

The generalised forces can be derived using virtual work:

$$\begin{aligned}
\Delta W &= (-F_{y_1} \delta_1 - F_{y_3} \phi - F_{y_4} \psi) \Delta x + \\
&\quad (F_{y_1}) \Delta(y_1 + a_1 \beta) + \\
&\quad (F_{y_2}) \Delta(y_1 - b_1 \beta) + \\
&\quad (F_{y_3}) \Delta(y_1 - h_1 \beta - l_2 \theta) + \\
&\quad (F_{y_4}) \Delta(y_1 - h_1 \beta - l_2^* \theta - l_3 \xi).
\end{aligned} \tag{A.6}$$

This yields for the generalised forces of each state:

$$\begin{aligned}
Q_x &= -F_{y_1} \delta_1 - F_{y_3} \phi - F_{y_4} \psi \\
Q_{y_1} &= F_{y_1} + F_{y_2} + F_{y_3} + F_{y_4} \\
Q_\beta &= a_1 F_{y_1} - b_1 F_{y_2} - h_1 F_{y_3} - h_1 F_{y_4} \\
Q_\theta &= -l_2 F_{y_3} - l_2^* F_{y_4} \\
Q_\xi &= -l_3 F_{y_4}.
\end{aligned} \tag{A.7}$$

The global coordinates used so far are expressed in vehicle speeds and local coordinates. The following relations are used:

$$\begin{aligned}
\dot{x} &= u - v_1 \beta \\
\dot{y}_1 &= v_1 + u \beta \\
\dot{\beta} &= r_1 \\
\theta &= \beta + \phi \\
\xi &= \theta + \psi \\
&= \beta + \phi + \psi.
\end{aligned} \tag{A.8}$$

The tyre forces are expressed in the local coordinates:

$$\begin{aligned}
F_{y1} &= -\frac{1}{u} C_1 (v_1 + a_1 r_1) + C_1 \delta_1 \\
F_{y2} &= -\frac{1}{u} C_2 (v_1 - b_1 r_1) \\
F_{y3} &= -\frac{1}{u} C_3 (v_1 - h_1 r_1 - l_2 \dot{\theta}) + C_3 \phi \\
F_{y4} &= -\frac{1}{u} C_4 (v_1 - h_1 r_1 - l_2^* \dot{\theta} - l_3 \dot{\xi}) + C_4 (\phi + \psi).
\end{aligned} \tag{A.9}$$

Finally, the equations of motion can be expressed using only local coordinates. The state vector is  $x = [v_1 \ r_1 \ \dot{\phi} \ \dot{\psi} \ \phi \ \psi]^T$ . The first equation describing the longitudinal dynamics is not considered as the forward speed  $u$  is assumed to be constant. The following abbreviations are used:

$$\begin{aligned}
C &= C_1 + C_2 \\
C_t &= C_4 + C_4 \\
Cs_1 &= a_1 C_1 - b_1 C_2 \\
Cq_1^2 &= a_1^2 C_1 + b_1^2 C_2.
\end{aligned} \tag{A.10}$$

The equations of motion read:

$$\left. \begin{aligned}
&\{m_1 + m_2 + m_3\} (\dot{v}_1 + ur_1) - \{m_2(h_1 + a_2) + m_3(h_1 + l_2^* + a_3)\} \dot{r}_1 \\
&\quad - \frac{1}{u} [\{C + C_t\} v_1 + \{Cs_1 - C_3(h_1 + l_2) - C_4(h_1 + l_2^* + l_3)\} r_1 \\
&\quad - \{C_3 l_2 + C_4(l_2^* + l_3)\} \dot{\phi} - C_4 l_3 \dot{\psi} - C_t u \phi - C_4 u \psi] + C_1 \delta_1 \\
&-h \{m_2 + m_3\} (\dot{v}_1 + ur_1) + \{I_1 + m_2 h_1 (h_1 + a_2) + m_3 h_1 (h_1 + l_2^* + a_3)\} \dot{r}_1 \\
&\quad + \{m_2 h_1 a_2 + m_3 h_1 (l_2^* + a_3)\} \ddot{\phi} + m_3 h_1 a_3 \ddot{\psi} = \\
&\quad -\frac{1}{u} [\{Cs_1 - C_t h_1\} v_1 + \{Cq_1^2 + C_3 h_1 (h_1 + l_2) + C_4 h_1 (h_1 + l_2^* + l_3)\} r_1 \\
&\quad + \{C_3 h_1 l_2 + C_4 h_1 (l_2^* + l_3)\} \dot{\phi} + C_4 h_1 l_3 \dot{\psi} + C_t h_1 u \phi + C_4 h_1 u \psi] + C_1 a_1 \delta_1 \\
&- \{m_2 a_2 + m_3 l_2^*\} (\dot{v}_1 + ur_1) + \{I_2 + m_2 a_2 (h_1 + a_2) + m_3 l_2^* (h_1 + l_2^* + a_3)\} \dot{r}_1 \\
&\quad + \{I_2 + m_2 a_2^2 + m_3 l_2^* (l_2^* + a_3)\} \ddot{\phi} + m_3 a_3 l_2^* \ddot{\psi} = \\
&\quad -\frac{1}{u} [-\{C_3 l_2 + C_4 l_2^*\} v_1 + \{C_3 l_2 (h_1 + l_2) + C_4 l_2^* (h_1 + l_2^* + l_3)\} r_1 \\
&\quad + \{C_3 l_2^2 + C_4 l_2^* (l_2^* + l_3)\} \dot{\phi} + C_4 l_3 l_2^* \dot{\psi} + \{C_3 l_2 + C_4 l_2^*\} u \phi + C_4 l_2^* u \psi] \\
&-m_3 a_3 (\dot{v}_1 + ur_1) + \{I_3 + m_3 a_3 (h_1 + l_2^* + a_3)\} \dot{r}_1 + \{I_3 + m_3 a_3 (l_2^* + a_3)\} \ddot{\phi} \\
&\quad + \{I_3 + m_3 a_3^2\} \ddot{\psi} = -\frac{1}{u} [-C_4 l_3 v_1 + C_4 l_3 \{h_1 + l_2^* + l_3\} r_1 \\
&\quad + C_4 l_3 \{l_2^* + l_3\} \dot{\phi} + C_4 l_3^2 \dot{\psi} + C_4 l_3 u \phi + C_4 l_3 u \psi]
\end{aligned} \right\}. \tag{A.11}$$

For a vehicle combination with one articulation, use;  $C_4 = 0$ ,  $m_3 = 0$ ,  $I_3 = 0$ . The state vector is  $x = [v_1 \ r_1 \ \dot{\phi} \ \dot{\psi}]^T$ . For a single vehicle, use;  $C_3 = C_4 = 0$ ,  $m_2 = m_3 = 0$ ,  $I_2 = I_3 = 0$ . The state vector is;  $x = [v_1 \ r_1]^T$ .

### A.3 Equations of motion with multiple axles

An introduction to modelling multiple axles has been made in section 5.1 (page 69). The generalisation for  $n$  axles per group is made in this appendix.



The  $i^{th}$  axle group has  $n_i$  axles. Figure A.2 illustrates these parameters for Ecocombi D.

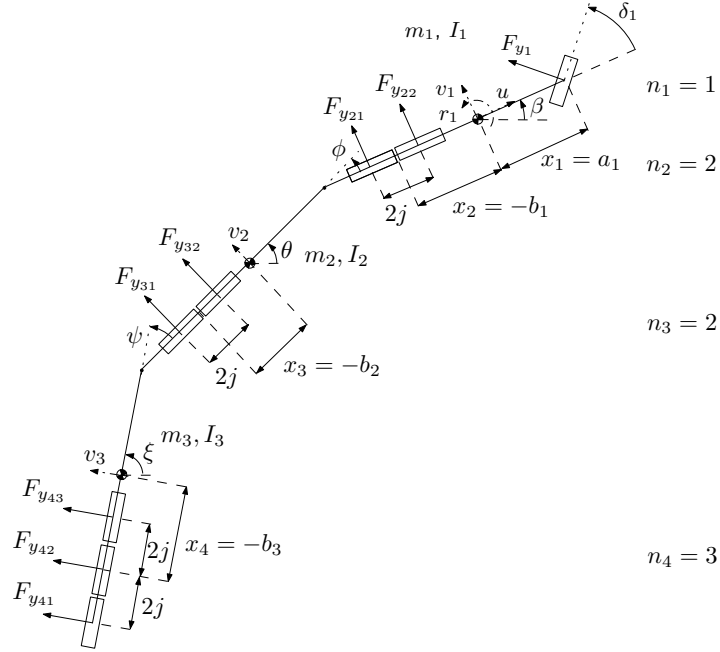


Figure A.2: Free body diagram of Ecocombi D with multiple axles

Furthermore, the following abbreviations are used:

$$\begin{aligned} F_{yin} &= -\frac{1}{u}C_i(v^* + x_i r^*) \\ F_{yij} &= -\frac{1}{u}C_i j r^*, \end{aligned} \tag{A.12}$$

where  $r^*$  and  $v^*$  are the yaw gain and lateral velocity of the articulation the axle group is on. Table A.1 lists  $i$ ,  $x$ ,  $r^*$  and  $v^*$  for the axle groups used in this study.

Axle group	$i$	$x_i$	$r^*$	$v^*$
Front axle towing vehicle	1	$a_1$	$r_1$	$v_1$
Rear axle towing vehicle	2	$-b_1$	$r_1$	$v_1$
Trailer axle first articulation	3	$-b_2$	$r_2$	$v_2$
Trailer axle second articulation	4	$-b_3$	$r_3$	$v_3$

Table A.1: Abbreviations for the axle groups

The yaw gains and lateral velocities relate as follows:

$$\left. \begin{aligned} r_2 &= \dot{\theta} = r_1 + \dot{\phi} \\ r_3 &= \dot{\xi} = r_2 + \dot{\psi} \\ v_2 &= v_1 - h_1 r_1 - a_2 r_2 - u \dot{\phi} \\ v_3 &= v_2 - h_2 r_2 - a_3 r_3 - u \dot{\psi} \end{aligned} \right\}. \quad (\text{A.13})$$

When multiple axles are applied, both the sum of the tyre forces (lateral equilibrium equation) and the sum of the tyre forces times their distance to the centre of gravity (moment equilibrium equation) change. Table A.2 shows an overview of the force and moment contributions for the two equations for single axles, tandem axles  $n = 2$ , triple axle  $n = 3$  and groups of four axles  $n = 4$ .

$n_i$	Tyre forces	Sum tyre forces	Moment contribution
1	$F_{y_{i1}} = F_{y_{in}}$	$F_{y_{in}}$	$x_i F_{y_{in}}$
2	$F_{y_{i1}} = F_{y_{in}} - F_{y_{ij}}$ $F_{y_{i2}} = F_{y_{in}} + F_{y_{ij}}$	$2F_{y_{in}}$	$(x_i - j)F_{y_{i1}} + (x_i + j)F_{y_{i2}}$ $= 2x_i F_{y_{in}} + (2 \cdot 1^2)j F_{y_{ij}}$ $= 2x_i F_{y_{in}} + 2j F_{y_{ij}}$
3	$F_{y_{i1}} = F_{y_{in}} - 2F_{y_{ij}}$ $F_{y_{i2}} = F_{y_{in}}$ $F_{y_{i3}} = F_{y_{in}} + 2F_{y_{ij}}$	$3F_{y_{in}}$	$(x_i - 2j)F_{y_{i1}} + x_i F_{y_{i2}} + (x_i + 2j)F_{y_{i3}}$ $= 3x_i F_{y_{in}} + (2 \cdot 2^2)j F_{y_{ij}}$ $= 3x_i F_{y_{in}} + 8j F_{y_{ij}}$
4	$F_{y_{i1}} = F_{y_{in}} - 3F_{y_{ij}}$ $F_{y_{i2}} = F_{y_{in}} - F_{y_{ij}}$ $F_{y_{i3}} = F_{y_{in}} + F_{y_{ij}}$ $F_{y_{i4}} = F_{y_{in}} + 3F_{y_{ij}}$	$4F_{y_{in}}$	$(x_i - 3j)F_{y_{i1}} + (x_i - j)F_{y_{i2}} + (x_i + j)F_{y_{i3}} + (x_i + 3j)F_{y_{i4}}$ $= 4x_i F_{y_{in}} + (2 \cdot 3^2 + 2 \cdot 1^2)j F_{y_{ij}}$ $= 4x_i F_{y_{in}} + 20j F_{y_{ij}}$

Table A.2: Force and moment contributions for multiple axles

In general, the total force and moment contributions of the  $i^{th}$  axle group consisting of  $n_i$  axles at distance  $x_i$  from the centre of gravity is:

$$\begin{aligned} \text{total force contribution:} & \quad n_i F_{y_{in}} \\ \text{total moment contribution:} & \quad n_i x_i F_{y_{in}} + \text{fact}_i j F_{y_{ij}}, \end{aligned} \quad (\text{A.14})$$

with,

$$\text{fact}_i = 2 \sum_{ii=1}^{\lceil \frac{n_i}{2} \rceil} \{n_i - (2ii - 1)\}^2, \quad (\text{A.15})$$

where  $\lceil \frac{n_i}{2} \rceil$  means that the fraction  $\frac{n_i}{2}$  should be ceiled to the next integer.

The equations of motion of a general vehicle combination with two articulations can now be expressed using the lateral velocities and yaw gains of each articulation individually as:

$$\left. \begin{aligned} m_1(\dot{v}_1 + ur_1) &= \sum_{i=1}^2 n_i F_{y_{in}} + C_1 \delta_1 \\ I_1 \dot{r}_1 &= \sum_{i=1}^2 [n_i x_i F_{y_{in}} + \text{fact}_i j F_{y_{ij}}] + C_1 a_1 \delta_1 \\ m_2(\dot{v}_2 + ur_2) &= n_3 F_{y_{3n}} \\ I_2 \dot{r}_2 &= n_3 x_3 F_{y_{3n}} + \text{fact}_3 j F_{y_{3j}} \\ m_3(\dot{v}_3 + ur_3) &= n_4 F_{y_{4n}} \\ I_3 \dot{r}_3 &= n_4 x_4 F_{y_{4n}} + \text{fact}_4 j F_{y_{4j}} \end{aligned} \right\}. \quad (\text{A.16})$$

Note that the tyre forces are expressed as function of the lateral velocity and yaw rate of the same articulation the axle group is on, in contrast to the equations derived in (A.11). The steering of the first axle is added to the equations of motion. Furthermore, the equations in (A.13) should be added to link the yaw moments and lateral velocities of the units. Again, the respective mass, inertia and tyre stiffnesses should be set to zero if vehicles with less articulations are considered.



---

## Vehicle and Tyre Parameters

---

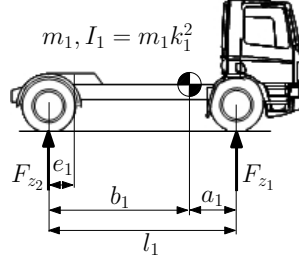
This appendix gives an overview of the tyre and vehicle parameters used in the simulations.

### Tyres

Symbol	Description	Unit	Value
$f$	normalised cornering stiffness	1/rad	5.73
$j$	half distance between two axles in an axle group	m	0.7

Table B.1: Tyre parameters

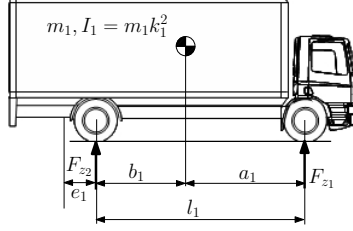
## Tractor



Symbol	Description	Unit	Value
$l_1$	wheelbase	m	3.6
$F_{z_1}$	front axle load	N	50620
$F_{z_2}$	rear axle load	N	22455
$m_1$	mass	kg	7449
$a_1$	distance front axle to cog	m	1.10
$b_1$	distance rear axle to cog	m	2.49
$k_1$	radius of gyration	m	1.89

Table B.2: Tractor parameter, based on DAF FT XF105 Super Space Cab [2]

## Truck

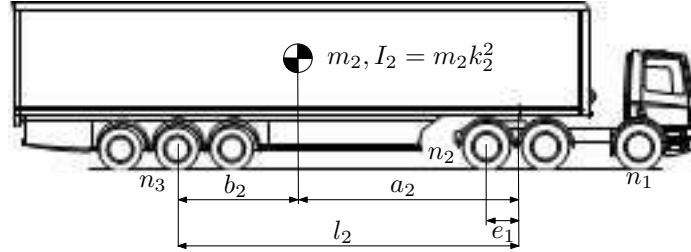


Symbol	Description	Unit	Value
$l_1$	wheelbase	m	5
$F_{z_1}$	front axle load unladen	N	51659
$F_{z_2}$	rear axle load unladen	N	22524
$m_u$	mass unladen	kg	7562
$m_l$	load	kg	7438
$m_1$	total mass	kg	15000
$a_1$	distance front axle to cog laden	m	2.5
$b_1$	distance rear axle to cog laden	m	2.5
$k_1$	radius of gyration laden	m	1.44

Table B.3: Truck parameter, based on DAF FA XF105 Super Space Cab [2]

### Tractor-semitrailer

For tractor parameters, see above.



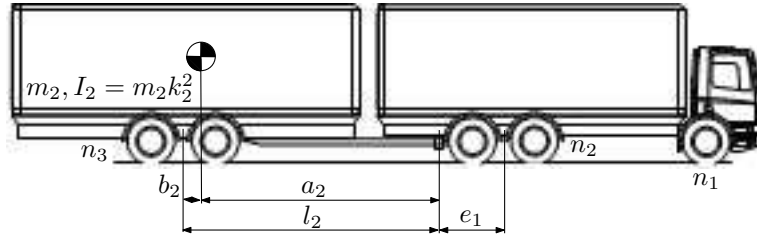
Symbol	Description	Unit	Value
$l_2$	wheelbase trailer	m	8.13
$a_2$	distance hitch point to cog trailer	m	4.98
$b_2$	distance cog trailer to trailer axle	m	3.15
$k_2$	radius of gyration	m	4.05
$m_2$	trailer mass	kg	32551
$e_1$	distance rear axle towing vehicle to coupling point	m	-0.68
$n_1$	Number of axles front axle group	-	1
$n_2$	Number of axles rear axle group	-	2
$n_3$	Number of axles trailer axle group	-	3

Table B.4: Semitrailer parameters



### Truck-centre axle trailer

For truck parameters, see above.

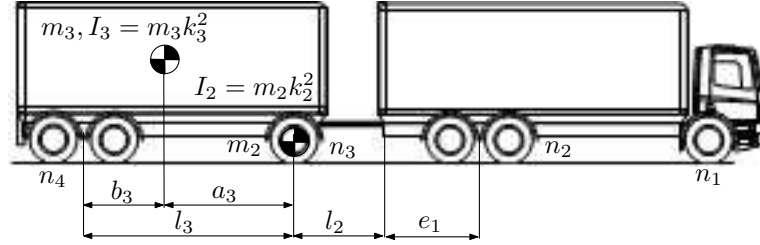


Symbol	Description	Unit	Value
$l_2$	wheelbase trailer	m	7
$a_2$	distance hitch point to cog trailer	m	7
$b_2$	distance cog trailer to trailer axle	m	0
$k_2$	radius of gyration	m	2.41
$m_2$	trailer mass	kg	25000
$e_1$	distance rear axle towing vehicle to coupling point	m	0.5
$n_1$	Number of axles front axle group	-	1
$n_2$	Number of axles rear axle group	-	2
$n_3$	Number of axles trailer axle group	-	2

Table B.5: Centre axle trailer parameters

### Truck-full trailer

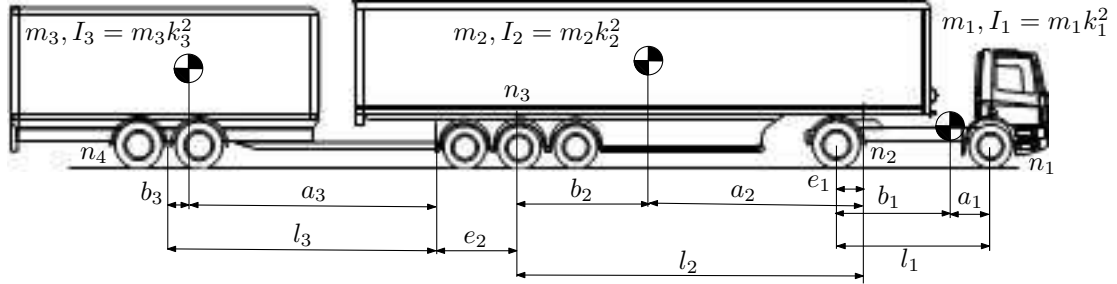
For truck parameters, see above.



Symbol	Description	Unit	Value
$l_3$	wheelbase trailer	m	5
$a_3$	distance front axle trailer to cog trailer	m	2.5
$b_3$	distance cog trailer to trailer rear axle	m	2.5
$k_3$	radius of gyration trailer	m	1.44
$m_3$	trailer mass	kg	25000
$e_1$	distance rear axle towing vehicle to coupling point	m	2
$e_2$	Mechanical trail front axle trailer	m	0
$l_2$	Drawbar length	m	3
$m_2$	Steering dolly mass	kg	0
$k_2$	Steering dolly radius of gyration	m	0
$n_1$	Number of axles front axle group	-	1
$n_2$	Number of axles rear axle group	-	2
$n_3$	Number of axles trailer front axle group	-	1
$n_4$	Number of axles trailer rear axle group	-	2

Table B.6: Full trailer parameters

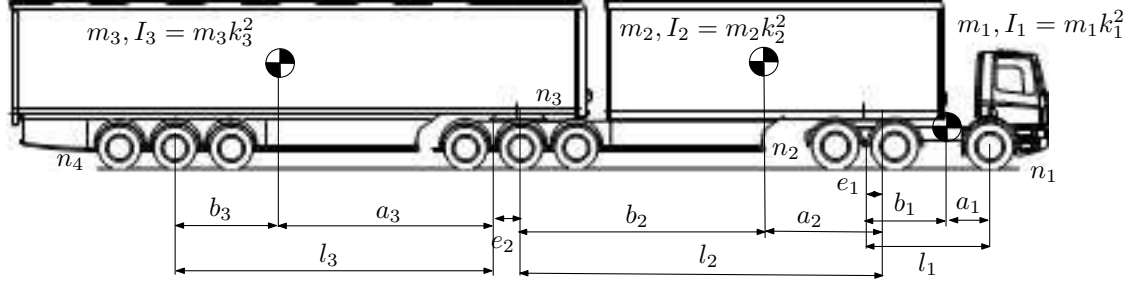
## Ecocombi A



Symbol	Description	Unit	Value
$l_1$	wheelbase towing vehicle	m	3.8
$a_1$	distance front axle towing vehicle to cog towing vehicle	m	1.17
$b_1$	distance cog towing vehicle to towing vehicle rear axle	m	2.63
$m_1$	towing vehicle mass	kg	7469
$k_1$	radius of gyration towing vehicle	m	1.89
$e_1$	distance rear axle towing vehicle to first coupling point	m	-0.74
$n_1$	number of axles front towing vehicle axle group	-	1
$n_2$	number of axles rear towing vehicle axle group	-	2
$l_2$	wheelbase first trailer	m	8.48
$a_2$	distance hitch point first trailer to cog first trailer	m	5.20
$b_2$	distance cog first trailer to first trailer axle	m	3.27
$m_2$	first trailer mass	kg	33353
$k_2$	radius of gyration first trailer	m	3.93
$e_2$	distance rear axle first trailer to second coupling point	m	2.53
$n_3$	number of axles first trailer axle group	-	3
$l_3$	wheelbase second trailer	m	5.97
$a_3$	distance hitch point second trailer to cog second trailer	m	5.91
$b_3$	distance cog second trailer to second trailer axle	m	0.1
$m_3$	second trailer mass	kg	19178
$k_3$	radius of gyration second trailer	m	2.26
$n_4$	number of axles second trailer axle group	-	2

Table B.7: Ecocombi A parameters, based on [31]

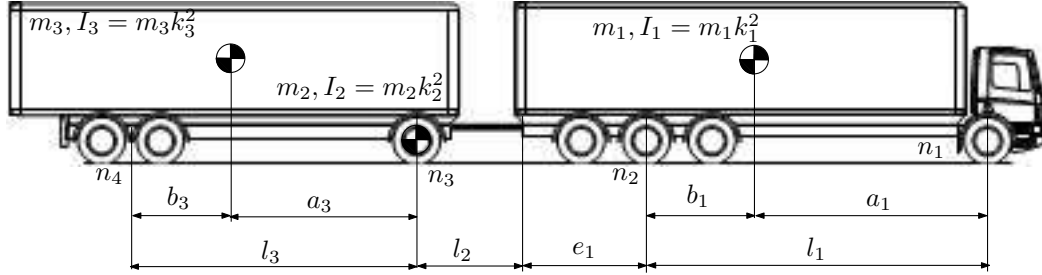
## Ecocombi B



Symbol	Description	Unit	Value
$l_1$	wheelbase towing vehicle	m	3.8
$a_1$	distance front axle towing vehicle to cog towing vehicle	m	1.17
$b_1$	distance cog towing vehicle to towing vehicle rear axle	m	2.63
$m_1$	towing vehicle mass	kg	7469
$k_1$	radius of gyration towing vehicle	m	1.89
$e_1$	distance rear axle towing vehicle to first coupling point	m	-0.74
$n_1$	number of axles front towing vehicle axle group	-	1
$n_2$	number of axles rear towing vehicle axle group	-	2
$l_2$	wheelbase first trailer	m	8.48
$a_2$	distance hitch point first trailer to cog first trailer	m	2.31
$b_2$	distance cog first trailer to first trailer axle	m	6.17
$m_2$	first trailer mass	kg	19178
$k_2$	radius of gyration first trailer	m	2.26
$e_2$	distance rear axle first trailer to second coupling point	m	0.32
$n_3$	number of axles first trailer axle group	-	3
$l_3$	wheelbase second trailer	m	8.48
$a_3$	distance hitch point second trailer to cog second trailer	m	5.2
$b_3$	distance cog second trailer to second trailer axle	m	3.28
$m_3$	second trailer mass	kg	33353
$k_3$	radius of gyration second trailer	m	3.93
$n_4$	number of axles second trailer axle group	-	3

Table B.8: Ecocombi B parameters, based on [31]

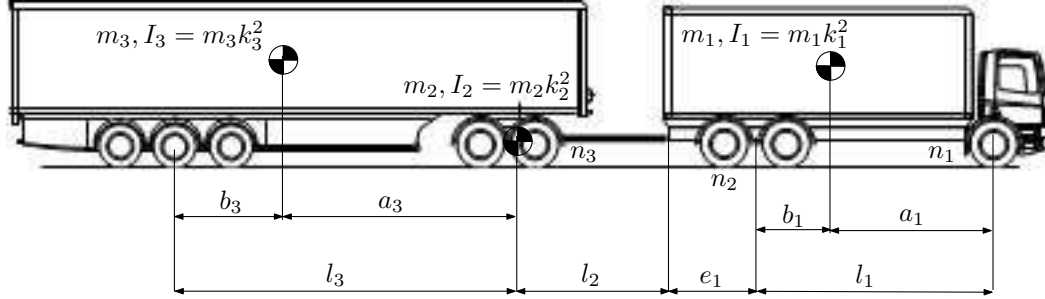
## Ecocombi C



Symbol	Description	Unit	Value
$l_1$	wheelbase towing vehicle	m	6.5
$a_1$	distance front axle towing vehicle to cog towing vehicle	m	4.98
$b_1$	distance cog towing vehicle to towing vehicle rear axle	m	1.52
$m_1$	towing vehicle mass	kg	33448
$k_1$	radius of gyration towing vehicle	m	3.07
$e_1$	distance rear axle towing vehicle to first coupling point	m	3.5
$n_1$	number of axles front towing vehicle axle group	-	1
$n_2$	number of axles rear towing vehicle axle group	-	3
$l_2$	wheelbase first trailer	m	2.7
$a_2$	distance hitch point first trailer to cog first trailer	m	2.7
$b_2$	distance cog first trailer to first trailer axle	m	0
$m_2$	first trailer mass	kg	0
$k_2$	radius of gyration first trailer	m	0
$e_2$	distance rear axle first trailer to second coupling point	m	0
$n_3$	number of axles first trailer axle group	-	1
$l_3$	wheelbase second trailer	m	5.7
$a_3$	distance hitch point second trailer to cog second trailer	m	3.8
$b_3$	distance cog second trailer to second trailer axle	m	1.9
$m_3$	second trailer mass	kg	26552
$k_3$	radius of gyration second trailer	m	2.89
$n_4$	number of axles second trailer axle group	-	2

Table B.9: Ecocombi C parameters, based on [31]

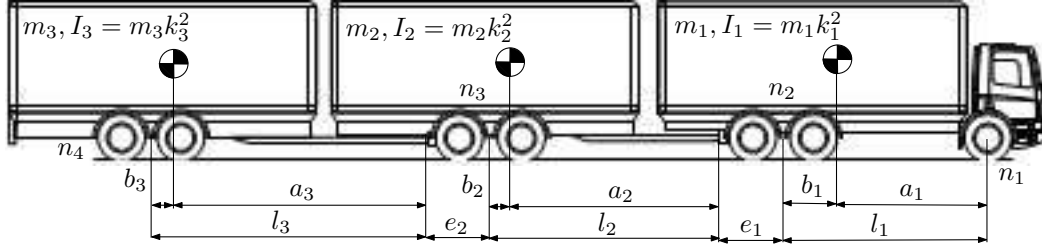
## Ecocombi D



Symbol	Description	Unit	Value
$l_1$	wheelbase towing vehicle	m	5.7
$a_1$	distance front axle towing vehicle to cog towing vehicle	m	4.01
$b_1$	distance cog towing vehicle to towing vehicle rear axle	m	1.69
$m_1$	towing vehicle mass	kg	26706
$k_1$	radius of gyration towing vehicle	m	2.59
$e_1$	distance rear axle towing vehicle to first coupling point	m	2.65
$n_1$	number of axles front towing vehicle axle group	-	1
$n_2$	number of axles rear towing vehicle axle group	-	2
$l_2$	wheelbase first trailer	m	3.5
$a_2$	distance hitch point first trailer to cog first trailer	m	3.5
$b_2$	distance cog first trailer to first trailer axle	m	0
$m_2$	first trailer mass	kg	0
$k_2$	radius of gyration first trailer	m	0
$e_2$	distance rear axle first trailer to second coupling point	m	0
$n_3$	number of axles first trailer axle group	-	2
$l_3$	wheelbase second trailer	m	8.48
$a_3$	distance hitch point second trailer to cog second trailer	m	5.2
$b_3$	distance cog second trailer to second trailer axle	m	3.28
$m_3$	second trailer mass	kg	33294
$k_3$	radius of gyration second trailer	m	3.93
$n_4$	number of axles second trailer axle group	-	3

Table B.10: Ecocombi D parameters, based on [31]

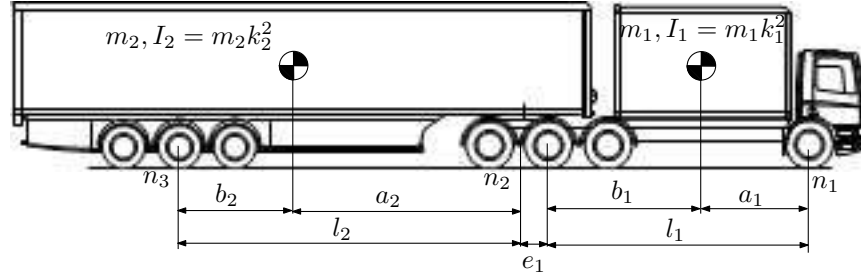
## Ecocombi E



Symbol	Description	Unit	Value
$l_1$	wheelbase towing vehicle	m	5.7
$a_1$	distance front axle towing vehicle to cog towing vehicle	m	4.03
$b_1$	distance cog towing vehicle to towing vehicle rear axle	m	1.67
$m_1$	towing vehicle mass	kg	27258
$k_1$	radius of gyration towing vehicle	m	2.59
$e_1$	distance rear axle towing vehicle to first coupling point	m	2.12
$n_1$	number of axles front towing vehicle axle group	-	1
$n_2$	number of axles rear towing vehicle axle group	-	2
$l_2$	wheelbase first trailer	m	5.31
$a_2$	distance hitch point first trailer to cog first trailer	m	5.25
$b_2$	distance cog first trailer to first trailer axle	m	0.06
$m_2$	first trailer mass	kg	16371
$k_2$	radius of gyration first trailer	m	1.88
$e_2$	distance rear axle first trailer to second coupling point	m	2.19
$n_3$	number of axles first trailer axle group	-	2
$l_3$	wheelbase second trailer	m	5.31
$a_3$	distance hitch point second trailer to cog second trailer	m	5.25
$b_3$	distance cog second trailer to second trailer axle	m	0.06
$m_3$	second trailer mass	kg	16371
$k_3$	radius of gyration second trailer	m	1.88
$n_4$	number of axles second trailer axle group	-	2

Table B.11: Ecocombi E parameters, based on [31]

## Ecocombi F

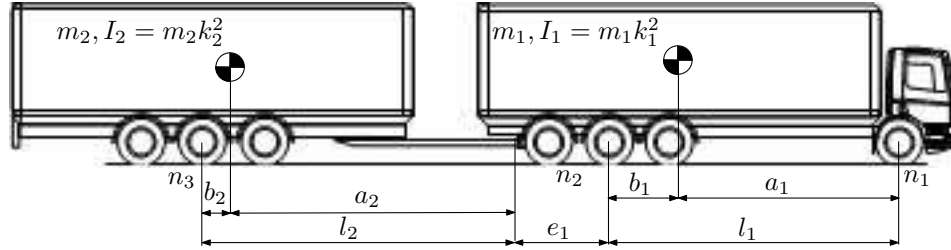


Symbol	Description	Unit	Value
$l_1$	wheelbase towing vehicle	m	6.65
$a_1$	distance front axle towing vehicle to cog towing vehicle	m	3.02
$b_1$	distance cog towing vehicle to towing vehicle rear axle	m	3.63
$m_1$	towing vehicle mass	kg	23330
$k_1$	radius of gyration towing vehicle	m	1.87
$e_1$	distance rear axle towing vehicle to first coupling point	m	1.75
$n_1$	number of axles front towing vehicle axle group	-	1
$n_2$	number of axles rear towing vehicle axle group	-	3
$l_2$	wheelbase first trailer	m	8.48
$a_2$	distance hitch point first trailer to cog first trailer	m	5.2
$b_2$	distance cog first trailer to first trailer axle	m	3.28
$m_2$	first trailer mass	kg	36670
$k_2$	radius of gyration first trailer	m	3.93
$n_3$	number of axles first trailer axle group	-	3

Table B.12: Ecocombi F parameters, based on [31]



## Ecocombi G



Symbol	Description	Unit	Value
$l_1$	wheelbase towing vehicle	m	6.5
$a_1$	distance front axle towing vehicle to cog towing vehicle	m	4.98
$b_1$	distance cog towing vehicle to towing vehicle rear axle	m	1.52
$m_1$	towing vehicle mass	kg	33448
$k_1$	radius of gyration towing vehicle	m	3.07
$e_1$	distance rear axle towing vehicle to first coupling point	m	3.1
$n_1$	number of axles front towing vehicle axle group	-	1
$n_2$	number of axles rear towing vehicle axle group	-	3
$l_2$	wheelbase first trailer	m	7.05
$a_2$	distance hitch point first trailer to cog first trailer	m	7
$b_2$	distance cog first trailer to first trailer axle	m	0.05
$m_2$	first trailer mass	kg	26552
$k_2$	radius of gyration first trailer	m	2.89
$n_3$	number of axles first trailer axle group	-	3

Table B.13: Ecocombi G parameters, based on [31]